NOAA Technical Memorandum ERL PMEL-32

DRIFT CHARACTERISTICS OF NORTHEASTERN BERING SEA ICE DURING 1980

C. H. Pease
S. A. Salo

Pacific Marine Environmental Laboratory
Seattle, Washington
July 1981

UNITED STATES
DEPARTMENT OF COMMERCE
Malcolm Baldrige,
Secretary

NATIONAL OCEANIC AND
ATMOSPHERIC ADMINISTRATION
John V. Byrne,
Administrator

Environmental Research
Laboratories
Joseph O. Fletcher,
Acting Director

NOTICE

The Environmental Research Laboratories do not approve, recommend, or endorse any proprietary product or proprietary material mentioned in this publication. No reference shall be made to the Environmental Research Laboratories or to this publication furnished by the Environmental Research Laboratories in any advertising or sales promotion which would indicate or imply that the Environmental Research Laboratories approve, recommend, or endorse any proprietary product or proprietary material mentioned herein, or which has as its purpose an intent to be used or purchased because of this Environmental Research Laboratories publication.

CONTENTS

TABLES

FIGURES

FRONTISPIECE. Alouette II helicopter (belonging to Evergreen Helicopters of Alaska, Inc.), idling at floe site one. The helicopter was equipped with skiis, exterior equipment baskets, and rotor with a clutch.

DRIFT CHARACTERISTICS OF NORTHEASTERN BERING SEA ICE DURING 1980*

by

C.H. Pease and S.A. Salo

Pacific Marine Environmental Laboratory
3711 15th Avenue Northeast
Seattle, Washington 98105

ABSTRACT. An ice drift experiment was conducted in the northeastern Bering Sea for eight days during late February and early March 1980. Current, meteorological, and ice floe data from two floe sites were collected serially and compared to regional observations. The floe initially drifted eastward because of the dominant eastward current and generally opposite the weak northeasterly wind. After a day, the floe abruptly changed drift direction toward the northwest concomitant with a reversal in current direction. This event preceded the local change in wind direction which accompanied the passage of a low-pressure center over the eastern Bering Sea. During this storm, northward currents and southeasterly winds caused the floe to accelerate toward the Bering Strait. After the storm, the winds dominated the floe drift and the currents relative to the ice were weak.

During and after the passage of the storm, a major shearline in the pack ice was observed from Sledge Island toward the southeast to within 75 km of the Yukon River Delta, indicating that ice in Norton Sound was cut off from the main drift stream. The ice floes were characteristically a meter thick with a few centimeters of snow, gaining 15 cm of snow during the storm. Ice concentrations averaged 9-10 tenths and the pack was generally comprised of big to vast floes, although new-to-young ice was observed in the Nome polynya before the storm, along the shear zone, and in a number of leads.

A vector representation of the relative velocity fields is presented with a discussion of the forcing terms on the floe drift. The analysis of rotation angles of the wind and current to the floe drift and the relative speeds suggest that the current has a very strong influence on ice drift in this region.

*Contribution No. 540 from the NOAA/ERL Pacific Marine Environmental Laboratory.

1. INTRODUCTION

During the last week of February and the first week of March 1980, an experiment was conducted on the ice in the northeastern Bering Sea. The experiment site was accessed by helicopter (frontispiece) from Nome, Alaska, when weather permitted (Fig. 1). Measurements of wind velocity, current velocity, floe position, and floe rotation were made primarily to estimate air stress and water stress on the first-year sea ice (Fig. 2). Secondary purposes of the experiment included obtaining case studies of floe drift, under-ice currents, and wind variations between coastal stations and the ice. This memorandum presents the field data from the drifting site, compares these observations with regional analyses, and discusses the drift site data within the context of the current and wind forcing. The paper concludes with a summary of the results and a discussion of the ice drift scenario.

The ice station was first occupied late on 28 February (GMT) 1980 at approximately 64° 15'N, 166° 30'W (Fig. 3). The station drifted toward the east for about a day and then abruptly changed drift direction toward the northwest on 1 March. By 3 March (GMT) we decided that the station soon would be out of helicopter range of Nome, so we moved the instrument array to a new floe about 40 km southeast of the old floe site. The timing of the move was fortunate because a low-pressure center entered the area that evening and prevented helicopter operations for several days. It was imperative to have kept the site in flight range since all the instruments were self-recording. Figure 3 shows that the tendency for the ice to drift toward the northwest continued throughout the remainder of the experiment.

2. METEOROLOGICAL CONDITIONS

2.1 Regional Weather Observations

Appendix A details twice-daily sea level pressure (SLP) fields and approximate surface wind conditions for 14 February to 16 March 1980. The pressures were digitized from 00 GMT and 12 GMT Alaska Region NWS surface analyses. Surface winds were estimated from these pressures by

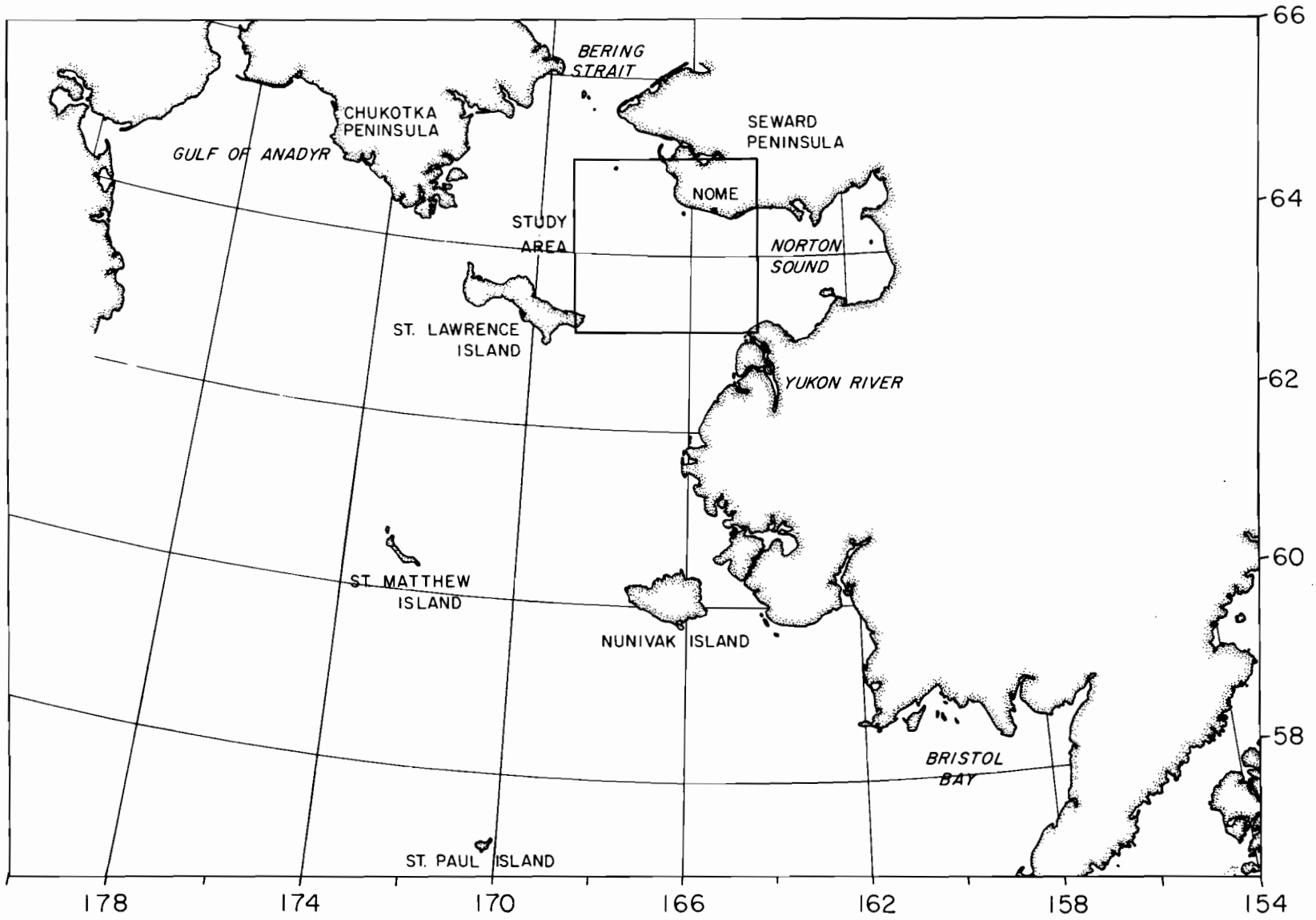

Figure 1. Study area in the northeastern Bering Sea during late February, early March 1980.

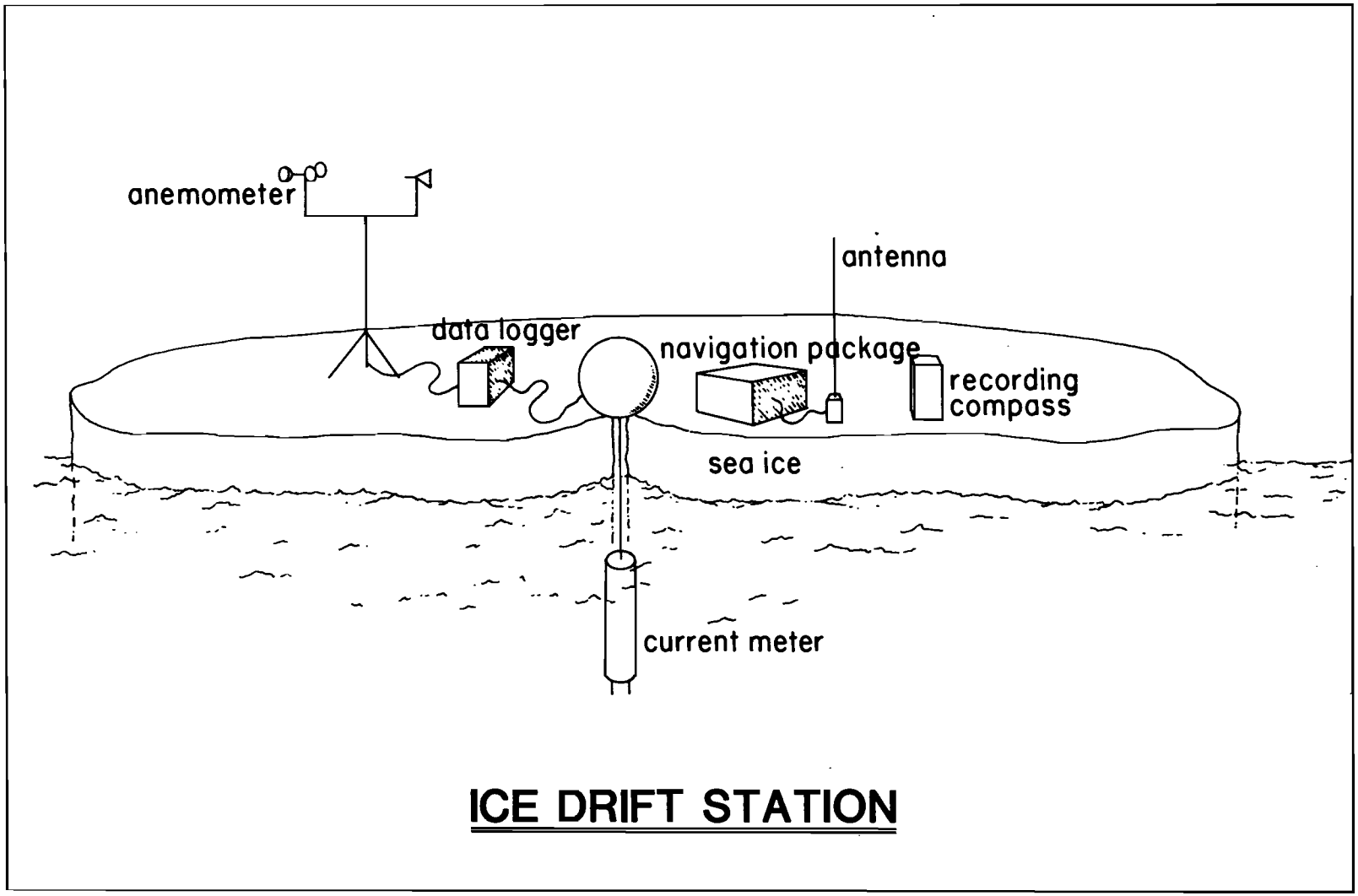

Figure 2. Schematic diagram of the ice drift station occupied during the 1980 experiment.

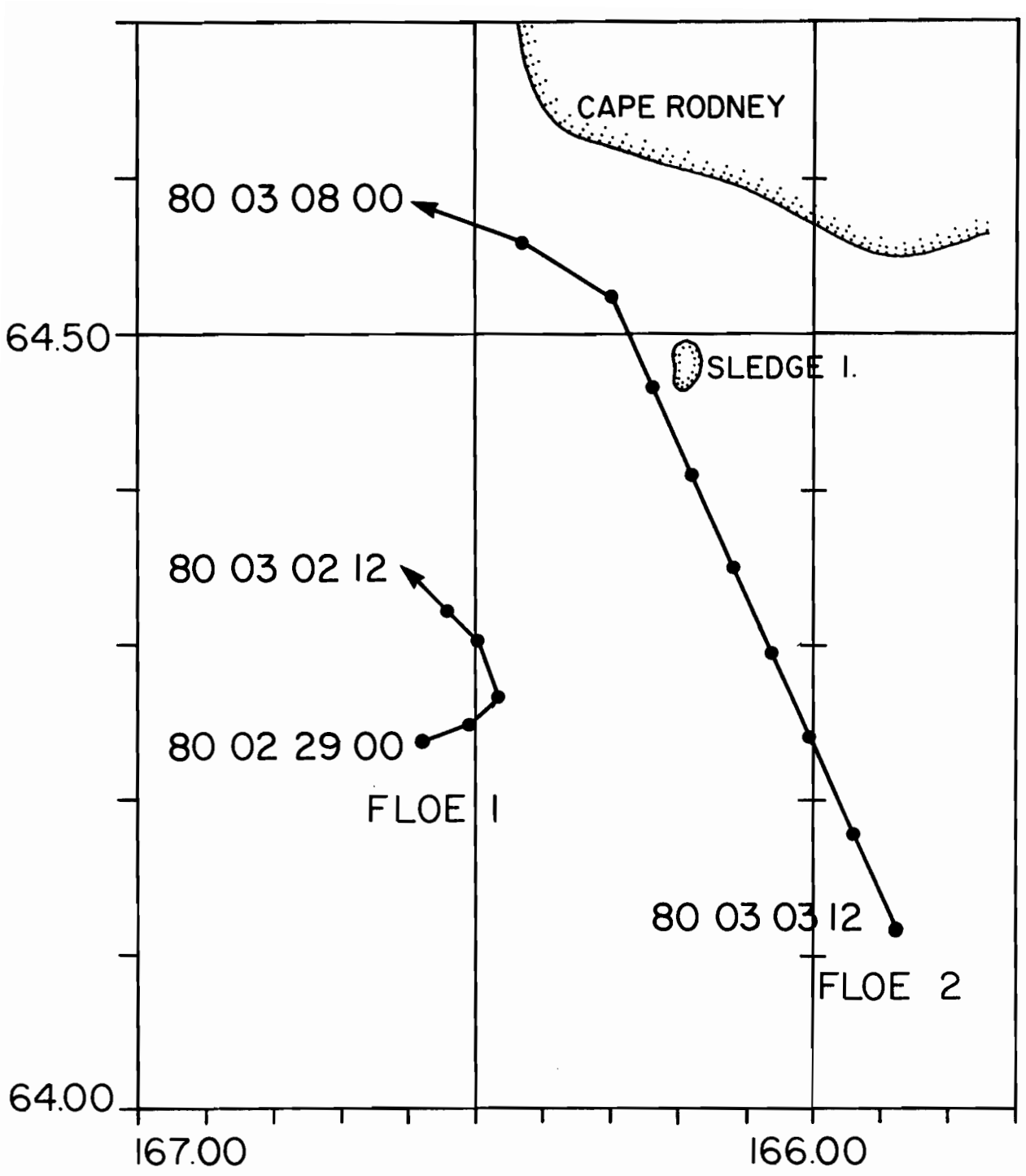

Figure 3. Smoothed plot of ice drift for the two floes occupied during the experiment. The GMT date and time information are given in year, month, day, and hour with time marks every 12 hours.

calculating gradient winds, reducing the gradient wind speeds by 20%, and rotating the vectors 30° toward the left using METLIB, a program for evaluating boundary layer winds (Overland, et al., 1980). Appendix B reports twice-daily surface air temperature (SAT) fields analyzed and digitized for the same period from station reports included on the Alaska Region NWS surface charts. The contoured SAT plots were also constructed using METLIB.

Throughout most of the month the surface winds in the experiment region were from the northeastern quadrant reflecting the climatological winter pattern of the Aleutian low- and Siberian high-pressure systems (Overland, 1981). Exceptions to this wind direction occurred on 14-15 February and 4-7 March related to the passage of low-pressure centers to the west of the region and on 24-26 February related to the passage of a high-pressure center to the east of the region. Strong easterlies developed in Norton Sound and the northern Bering Sea as the early March low approached, partially accounting for the change in ice drift observed on 29 February and 1 March.

The SATs were warmest (0 to 5°C) in mid-February and the first week in March and were associated with southerly winds during the two low-pressure events. In contrast the SATs were coldest (-15 to -25°C) during periods of intense northeasterly winds centered around 20-21 February and 13-14 March. Thus our field observations were made entirely during the relatively warm period associated with the passage of the early March low.

The NWS meteorological station at Nome is shadowed by the Kiglaik Mountains to the north and northeast. Consequently northerly to northeasterly winds are reduced at Nome compared to winds away from land over Norton Sound and the northern Bering Sea. Another effect is that the mountains seem to steer southerly and southeasterly winds to a more easterly direction. Figure 4 shows the wind time series for Nome, and Figure 5 compares this to the average observed winds from the monthly summaries of local climatological data for Nome (National Climate Center, NOAA, Federal Building, Asheville, North Carolina 28801) with METLIB predicted winds for Nome from 00 GMT on 14 February through 12 GMT on 16 March. Observed winds tended to be rotated clockwise

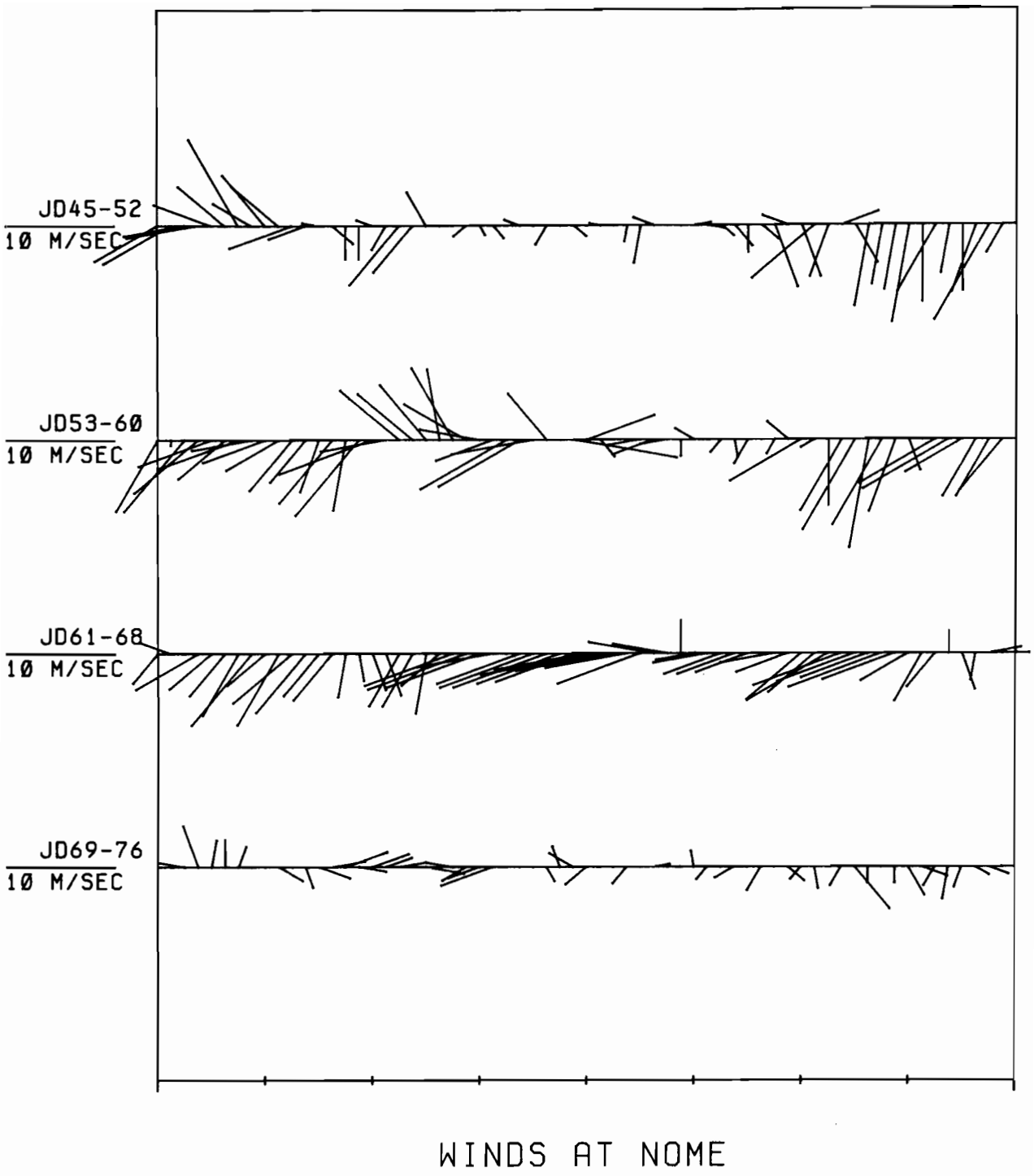

Figure 4. Three-hourly observed winds at Nome from 00 GMT on 14 February (JD45) 1980 to 21 GMT on 16 March (JD76) 1980. Speed is scaled at left and direction follows oceanographic convention. Time ticks are every 24 hours.

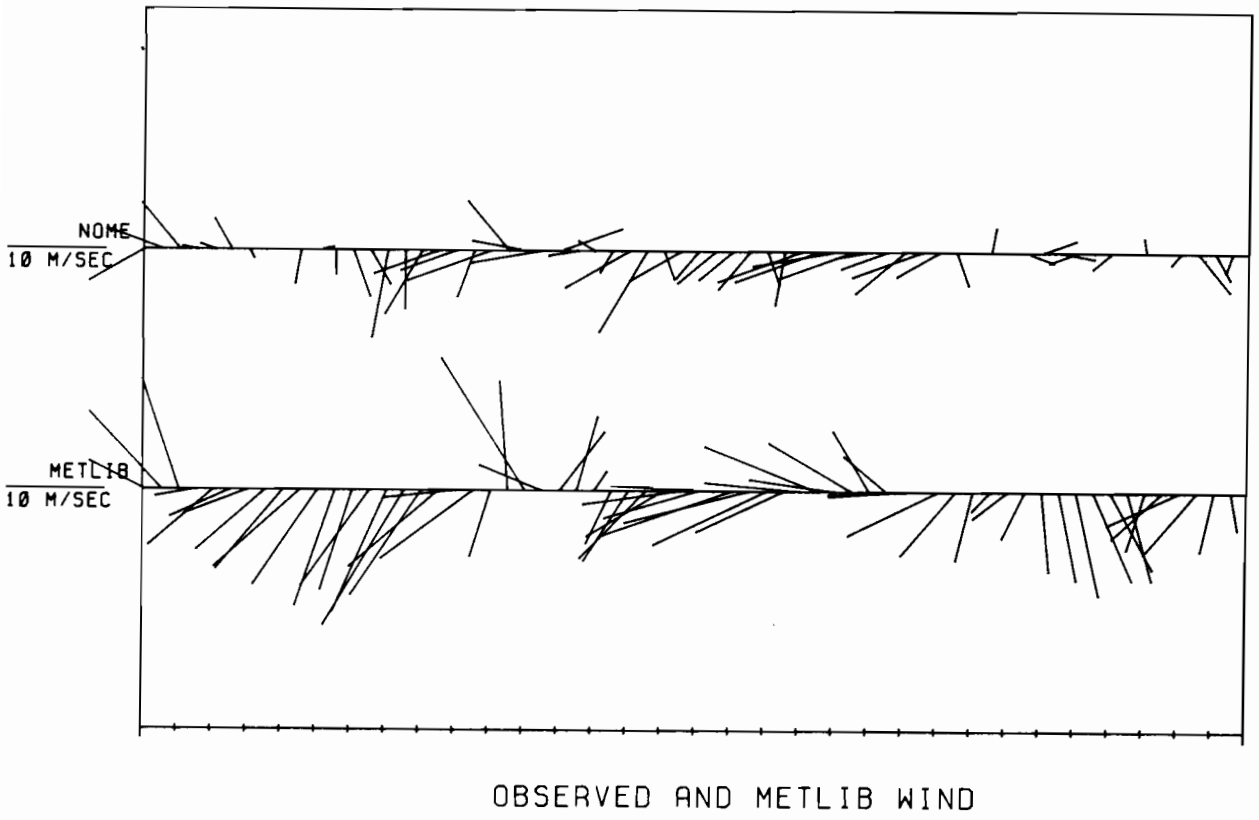

Figure 5. Comparison of six-hourly averaged winds at Nome with METLIB-calculated winds for Nome from 00 GMT on 14 February (JD45) 1980 to 12 GMT on 16 March (JD76) 1980. Speed is scaled at left and direction follows oceanographic convention. Averages are centered on the stated times.

(anticyclonically) by 14° and reduced in magnitude by 5 m s^{-1} from their METLIB counterparts. This is equivalent to a ratio of the observed wind with the gradient wind of 0.41 (S.D. = 0.26). The largest reduction in wind speed occurred during northerly to northeasterly winds and the greatest turning occurred during southeasterly winds. This suggests that Nome wind observations are probably not representative for regions away from the same orographic influence.

2.2 Wind Measurements on the Ice

Wind was measured over the ice every ten minutes with an Aanderaa anemometer affixed to a three-meter mast and recorded on magnetic tape in a data logger (Fig. 6). Hourly block averages of this data are shown in Figure 7, beginning with 2230 GMT on 28 February and ending with 2130 GMT on 7 March. These one-hour average winds are compared with METLIB winds at the floe site every twelve hours in Figure 8 from 00 GMT on 29 February to 12 GMT on 7 March. The METLIB wind speeds were only 0.5 m s^{-1} greater than and rotated on the average 7° clockwise (anticyclonically) from the observed winds. This is equivalent to a ratio of the observed wind with the gradient wind of 0.76 (S.D. = 0.40). This suggests that METLIB winds calculated from the Alaska Region NWS analysis give a reasonable representation of winds over western Norton Sound and the northern Bering Sea. A further comparison between observed winds at Nome and observed winds on the ice every three hours from 21 GMT on 28 February to 21 GMT on 7 March (Fig. 9) verifies that Nome winds are not representative of winds over the open pack ice in this region. The direction shift during the latter two-thirds of the observation period is particularly noticeable and further supports the idea that the mountains deflect southeast winds toward the east.

3. OCEANOGRAPHIC CONDITIONS

3.1 Regional Current Patterns

Few direct observations of currents during winter have been made in the study area. The regional current has been inferred by continuity from winter observations north of the Bering Strait, in western Norton

Figure 6. Anemometer with data logger at the first floe site. Cups and vane are 3 m above the surface. Note that helicopter skis, equipment, and footsteps have only penetrated the upper centimeters of the snow. (Photo by D. L. Bell.)

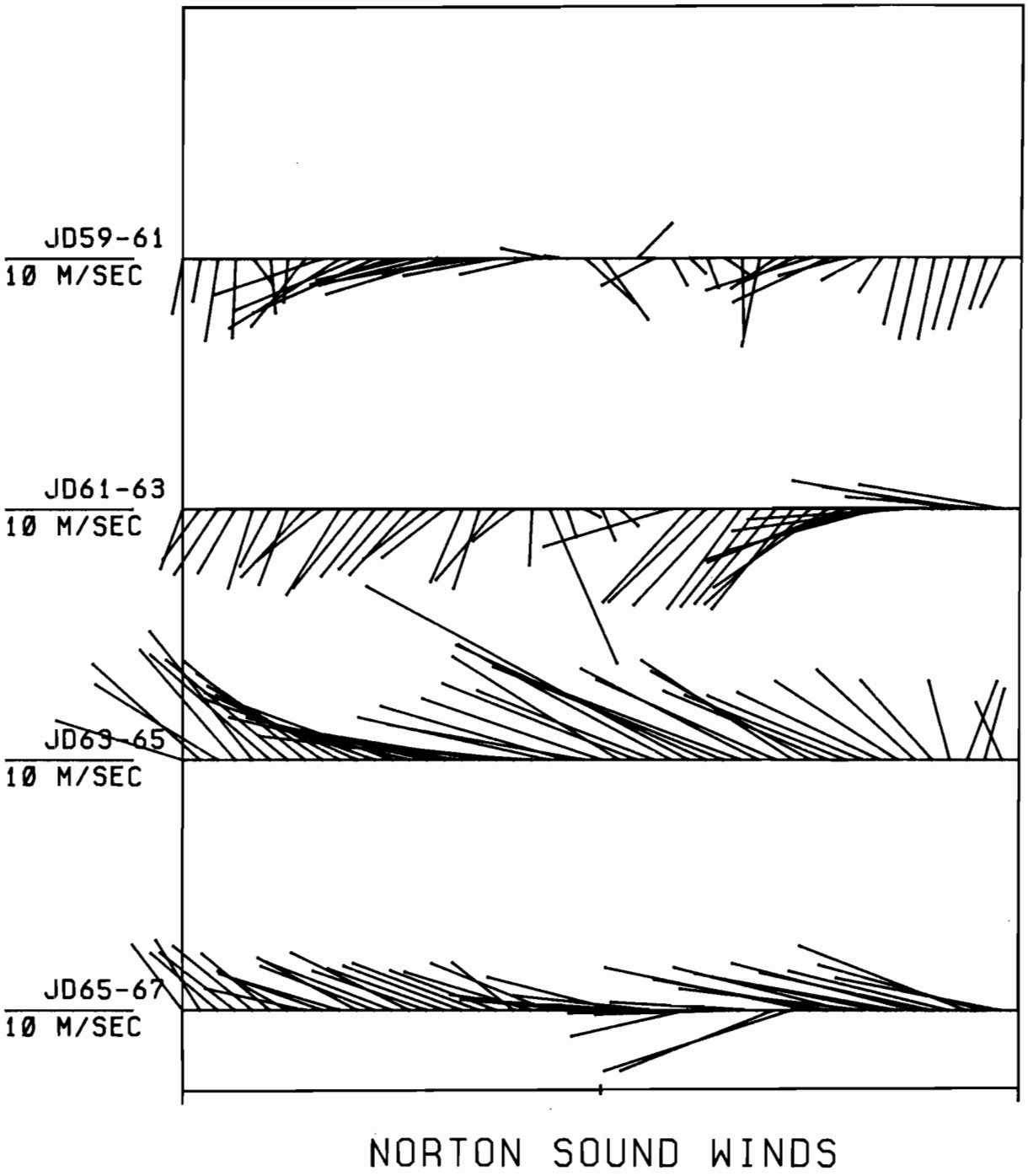

Figure 7. Hourly block-averaged observed winds at the ice from 2230 GMT 28 February (JD59) 1980 to 2130 GMT on 7 March (JD67) 1980. Speed is scaled at left and direction follows oceanographic convention. There were no observations at 2330 GMT on 2 March (JD62) and 0030 GMT on 3 March (JD63) while we moved gear to the second floe site.

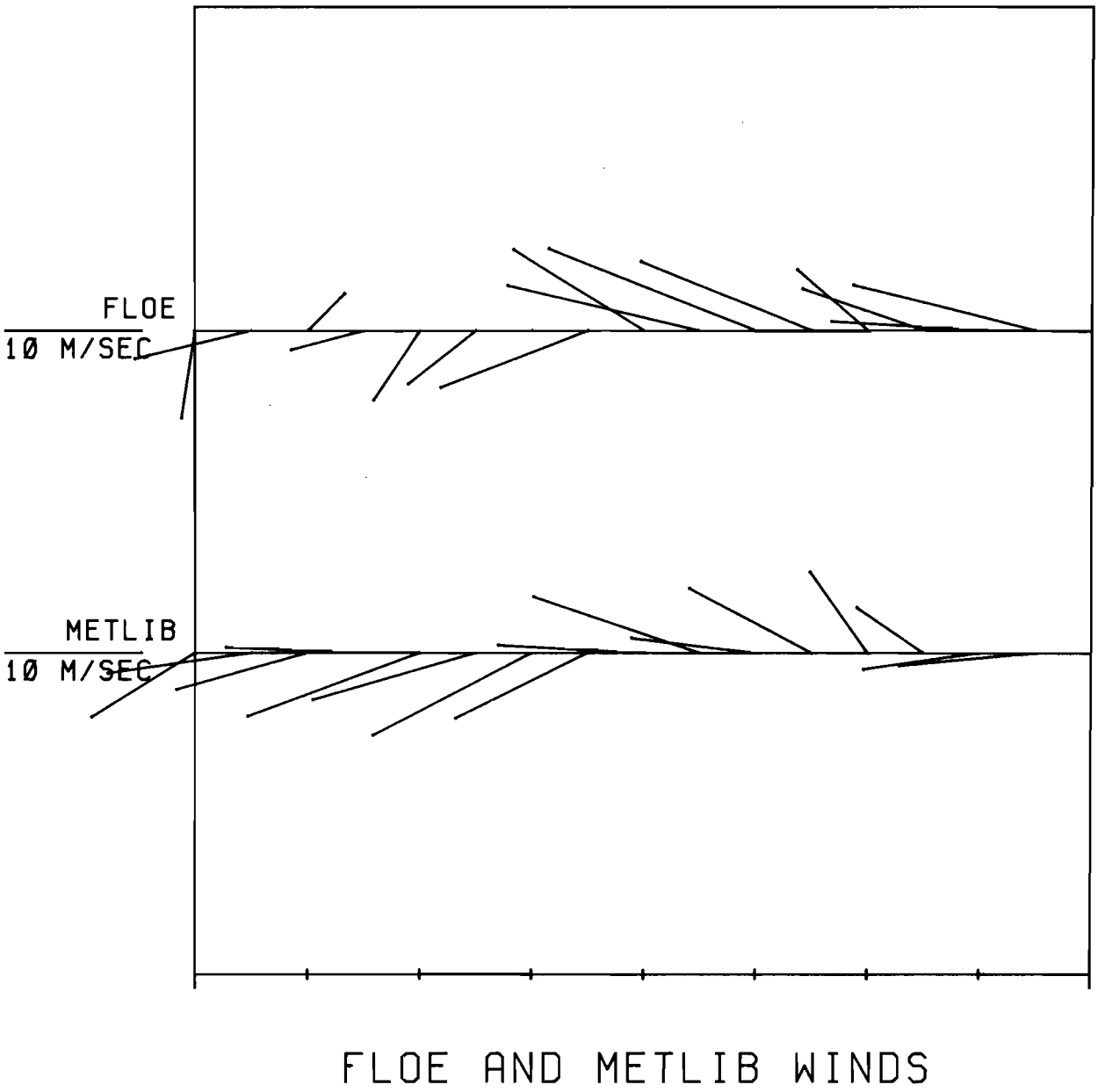

Figure 8. Comparison of hourly averaged winds at the floes with METLIB-calculated winds from 00 GMT on 29 February (JD60) 1980 to 12 GMT on 7 March (JD67) 1980. No wind observation was made on the floe at 00 GMT on 3 March (JD63). Speed is scaled at left and direction follows oceanographic convention.

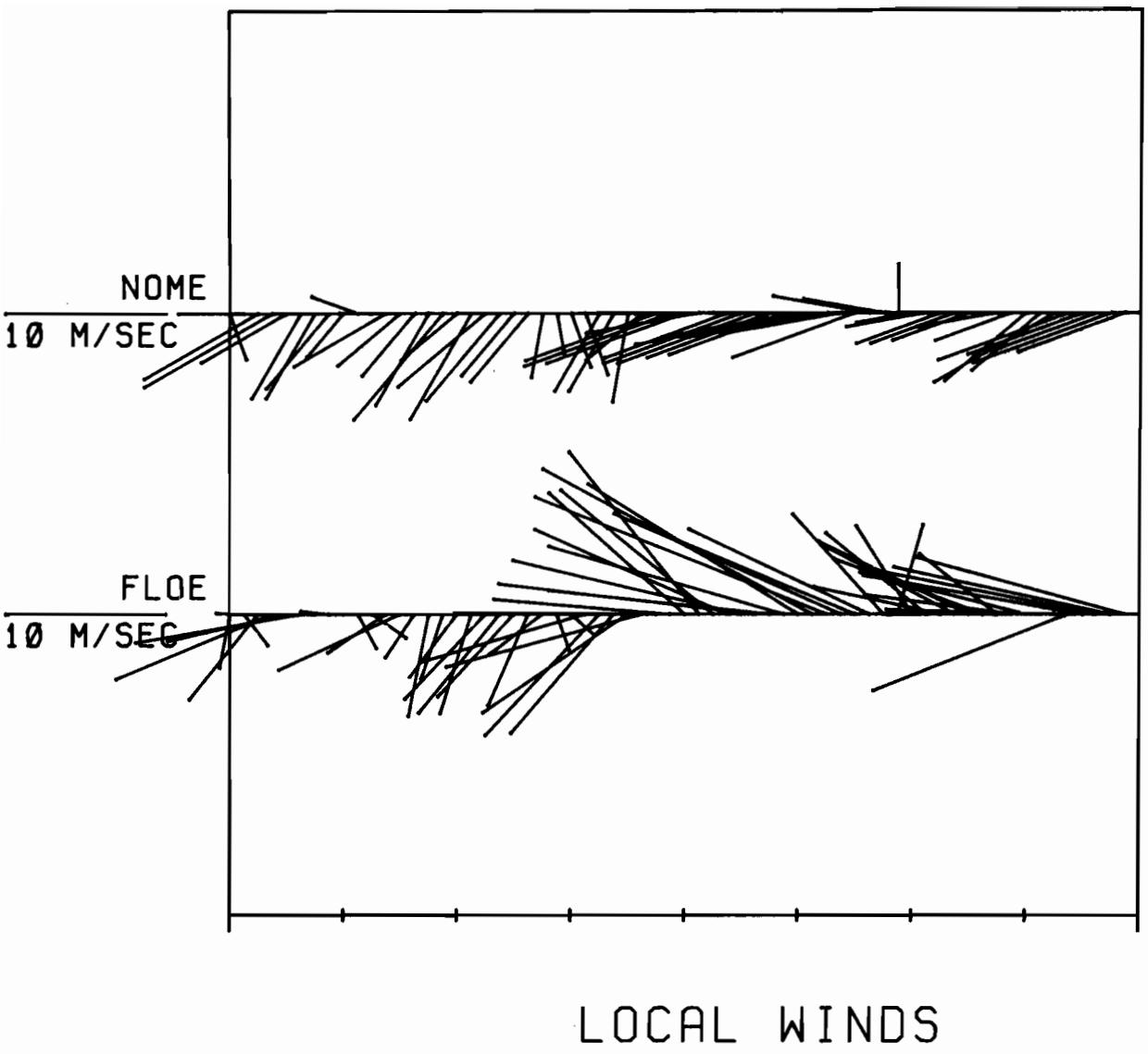

Figure 9. Comparison of three-hourly observed winds at Nome with corresponding observed winds on the ice from 2100 GMT on 28 February (JD59) to 1980 to 2100 GMT on 7 March (JD67) 1980. Speed is scaled at left and direction follows oceanographic convention.

Sound, and between St. Lawrence Island and Yukon Delta region (Coachman and Aagaard, 1981; Muench, et al. 1981; and Coachman, et al. 1975). The average winter current is northward to northwestward roughly paralleling the bathymetry but is punctuated by occasional reversals of approximately a week duration related to the large-scale meteorological forcing and subsequent sea surface elevation differences between the Bering and Chukchi Seas (Coachman and Aagaard, 1981).

According to Pearson, et al. (1981), the dominant tidal current component in Norton Sound is the diurnal (K1) component, but the tidal currents are strongly a function of position (Table 1). By comparison, the M2 tidal current component is weak in Norton Sound, and the S2 tidal component is weak throughout the Bering Sea (Table 1). In the northern Sound the K1 current ellipse is extremely elongated on the east-west axis, but away from the coast the ellipse broadens and the major axis is oriented toward northwest-southeast. West of Sledge Island the K1 component decreases in importance. Pearson, et al. (1981) found that although tidal current speeds of 20-30 cm s^{-1} may occur within Norton Sound, tidal current speeds just west of the sound are considerably weaker. Further, the presence of ice may decrease the speed of the tidal currents and shift the phases and ellipse orientations (Pearson, et al., 1981).

3.2 Current Observations Under the Ice

An internally recording Model RCM-4 Aanderaa current meter was suspended two meters below the sea surface through a hole drilled in the ice. The current meter compass was calibrated to ±2.0° magnetic in March 1978 (NW Regional Calibration Center, 300 - 120th Ave. N.E., Bellevue, WA 98005). The drafts of the ice floes were each about 90 cm, placing the rotor of the meter at about 1.1 m below the bottom of the ice and the center of the 40-cm-high vane at about 1.3 m below the bottom of the ice. The sampling rate on the current meter was two minutes. This data was processed in accordance with techniques described by Charnell and Krancus (1976). Hour averages of these measurements are presented in Figure 10. The mean relative current including data from both floes was 4.8 cm s^{-1} directed towards 059 degrees (true).

Table 1. Tidal current ellipse representation for selected stations within the experimental region (adapted from Pearson, et al., 1981).

Station	Water Depth	Meter Depth	Lat N deg	Lat N min	Long W deg	Long W min	Yr	JD	O_1 major H	O_1 major G	O_1 major D	O_1 min H	O_1 min R	K_1 major H	K_1 major G	K_1 major D	K_1 min H	K_1 min R	N_2 major H	N_2 major G	N_2 major D	N_2 min H	N_2 min R	M_2 major H	M_2 major G	M_2 major D	M_2 min H	M_2 min R
LD3	37	33	64	00	168	00	78	204	1.9	342	63	0.1	C	4.0	24	73	1.7	C	1.3	39	103	1.1	A	4.9	78	322	3.5	A
LD4	20	16	64	47	166	50	78	205	3.9	144	194	1.6	C	7.5	222	309	0.9	C	2.7	358	17	0.4	C	6.8	74	356	4.0	A
NC20	19	5	64	00	165	29	77	189	18.5	315	70	3.0	C	33.0	22	70	5.7	C	2.0	244	126	0.5	A	7.5	303	155	0.9	A
NC14	32	21	64	22	165	22	76	234	14.5	327	93	0.4	C	27.7	27	94	0.9	C	1.9	167	90	0.5	C	3.3	182	85	0.5	C

[1] Amplitudes H are cm/sec, phases G are referred to Greenwich, and direction D of major axis is compass degrees. C refers to clockwise rotation, A to anticlockwise. To obtain phase and direction of minor axis, add 90° to major axis direction; then add 90° to major axis phase if rotation is clockwise, or subtract 90° if anticlockwise.

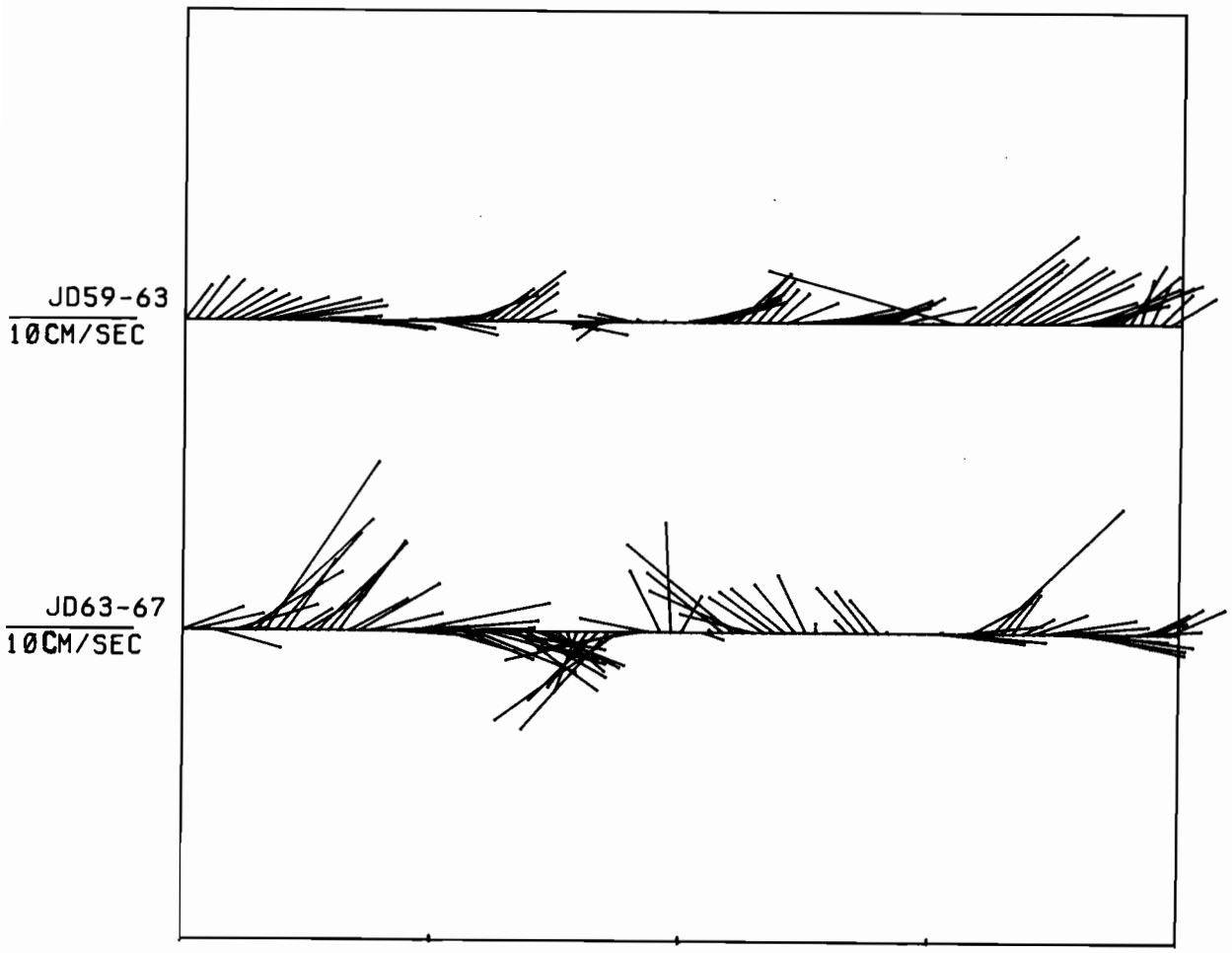

Figure 10. Hourly block-averaged observed currents relative to the ice from 2230 GMT on 28 February (JD59) 1980 to 2130 GMT on 7 March (JD67) 1980. Speed is scaled at left. There were no observations from 2030 GMT on 2 March (JD62) to 0030 GMT on 3 March (JD63).

An estimate of absolute current was desired to indicate the overall importance of the current to the lateral stress on the ice. Floe velocities calculated from floe drift data described in Sec. 4.2 were vector-added to the observed relative current. Hour averages of this estimate of the absolute current are presented in Figure 11. The mean absolute current including data from both floes was 12.2 cm s^{-1} directed toward 358 degrees (true). Although the absolute current was generally uniformly northward there was an episode of floe reversal during the first day of the experiment. Thus the easterly drift of ice during the first day of the experiment was strongly controlled by the current.

A current meter (deployed by R.B. Tripp and K. Aagaard of the Department of Oceanography at the University of Washington) about 3 m from the bottom in 20.7 m of water was located near King Island (about 50 km northwest of our most northerly floe position). Figure 12 shows the hourly vector-averaged current recorded at this mooring for a two-week period spanning our observations. Comparison of absolute current estimates to these observations suggests that the southward current at the beginning of the experiment was real and that the rest of the period was correctly identified as generally northward. The average northward component of the velocity from King Island was 12.8 cm s^{-1}, and the estimated northward component from the floe was 11.5 cm s^{-1}. Also, the average eastward component near King Island was -4.4 cm s^{-1}, while the estimate from the floe was -2.0 cm s^{-1}.

4. ICE CONDITIONS AND DRIFT

4.1 Regional Ice Observations

A glossary of ice terms used in this section is given in Appendix C. Analysis of sea ice conditions for the Bering Sea by the Navy-NOAA Joint Ice Center (*Eastern-Western Arctic Sea Ice Analysis 1980*) using infrared images from NOAA-6 and TYROS-N polar-orbiting satellites indicates that the region was 9 to 10 tenths covered with first-year and young ice throughout the experiment (Fig. 13a,b,c). In addition, visual photographs were made by ice observers from the Naval Polar Oceanography Center on two ice reconnaissance flights by Navy P3

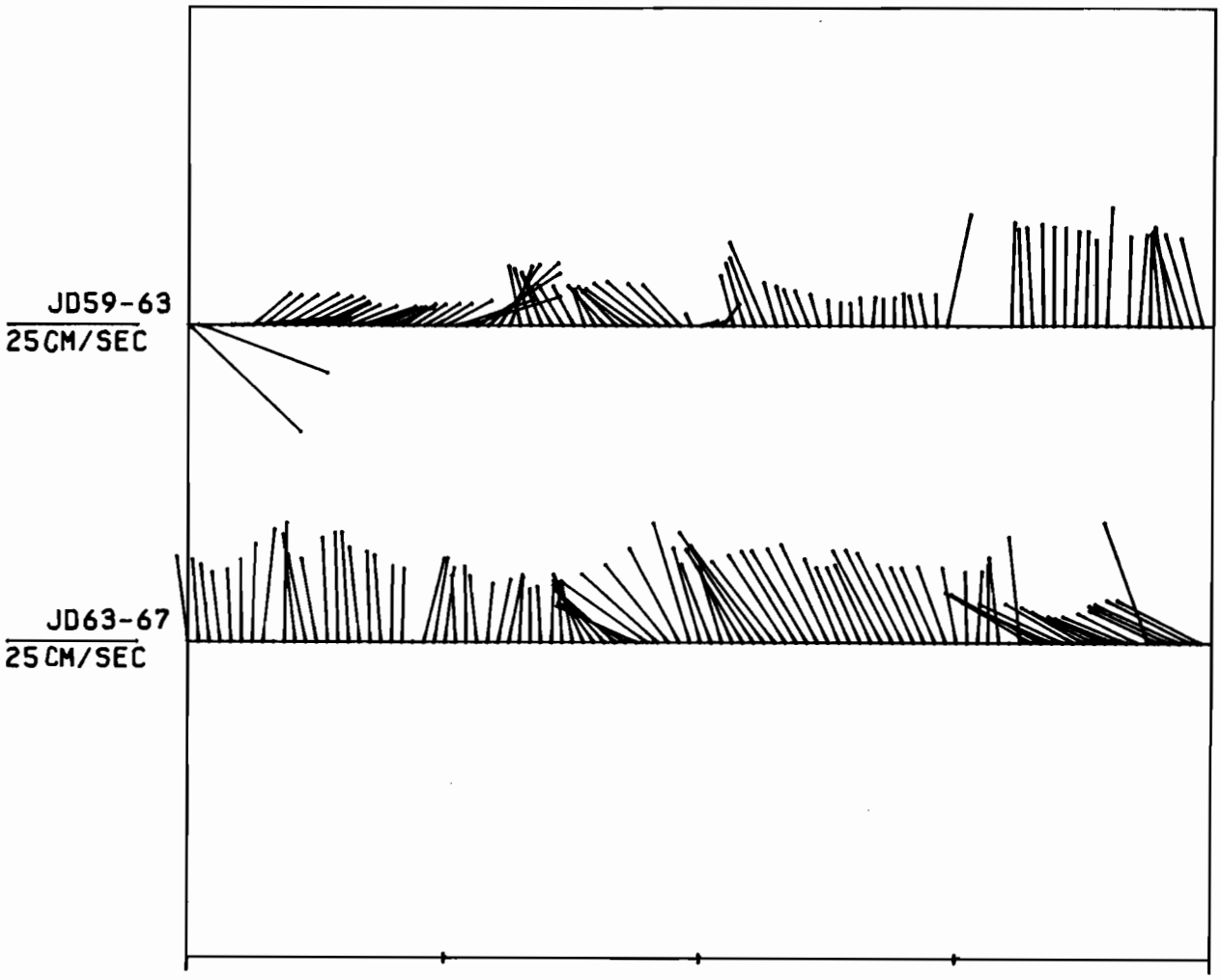

Figure 11. Hourly absolute currents calculated from observed relative currents and ice drift velocities from 2230 GMT on 28 February (JD59) 1980 to 2130 GMT on 7 March (JD67) 1980. Note scale change from previous figure.

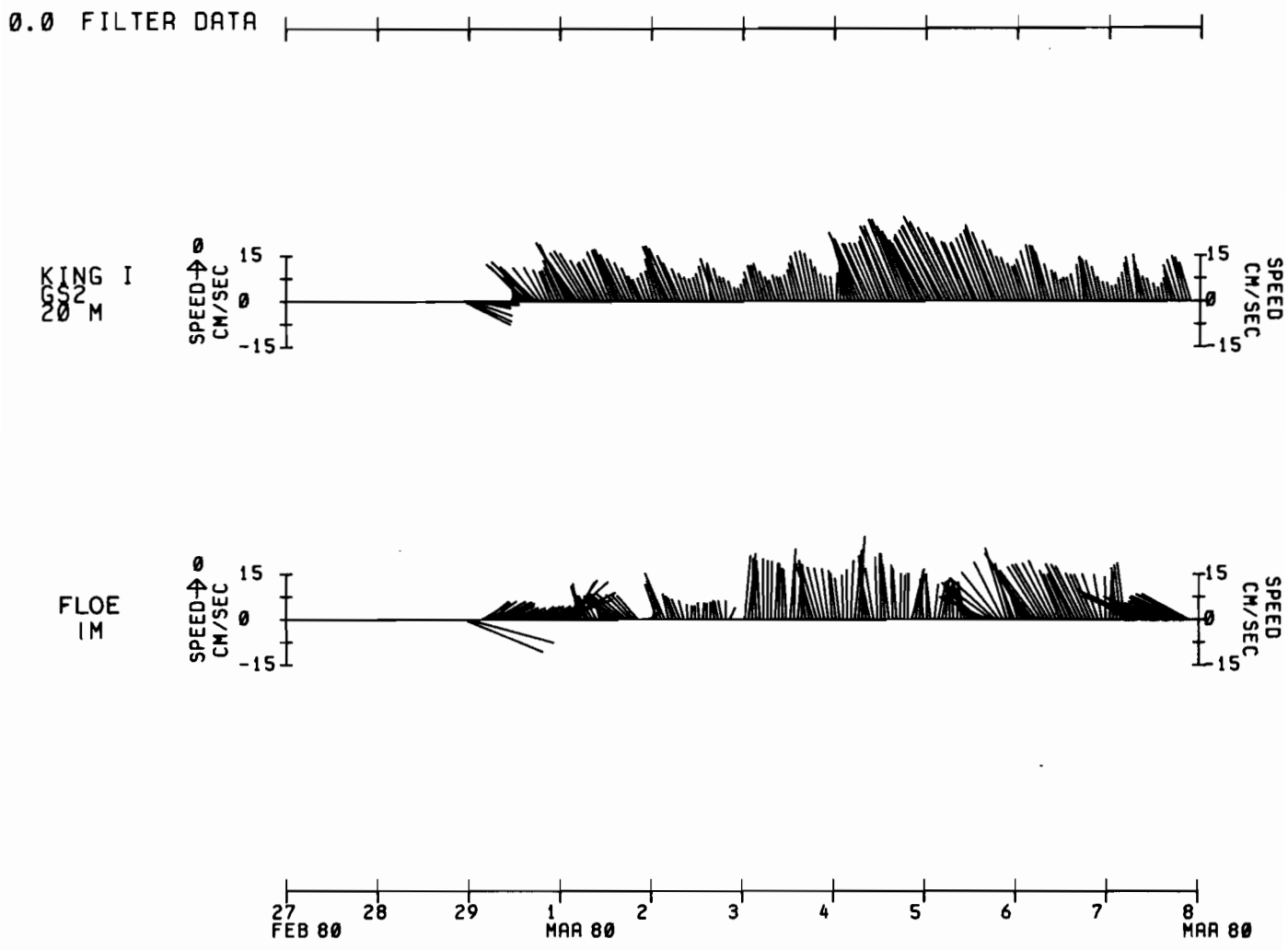

Figure 12. Comparison of average currents from a bottom-moored current meter near King Island (50 km northwest of the most northerly floe position) with the absolute current calculated from the experiment data. The King Island record begins with 26 February (JD57) and continues through 10 March (JD70).

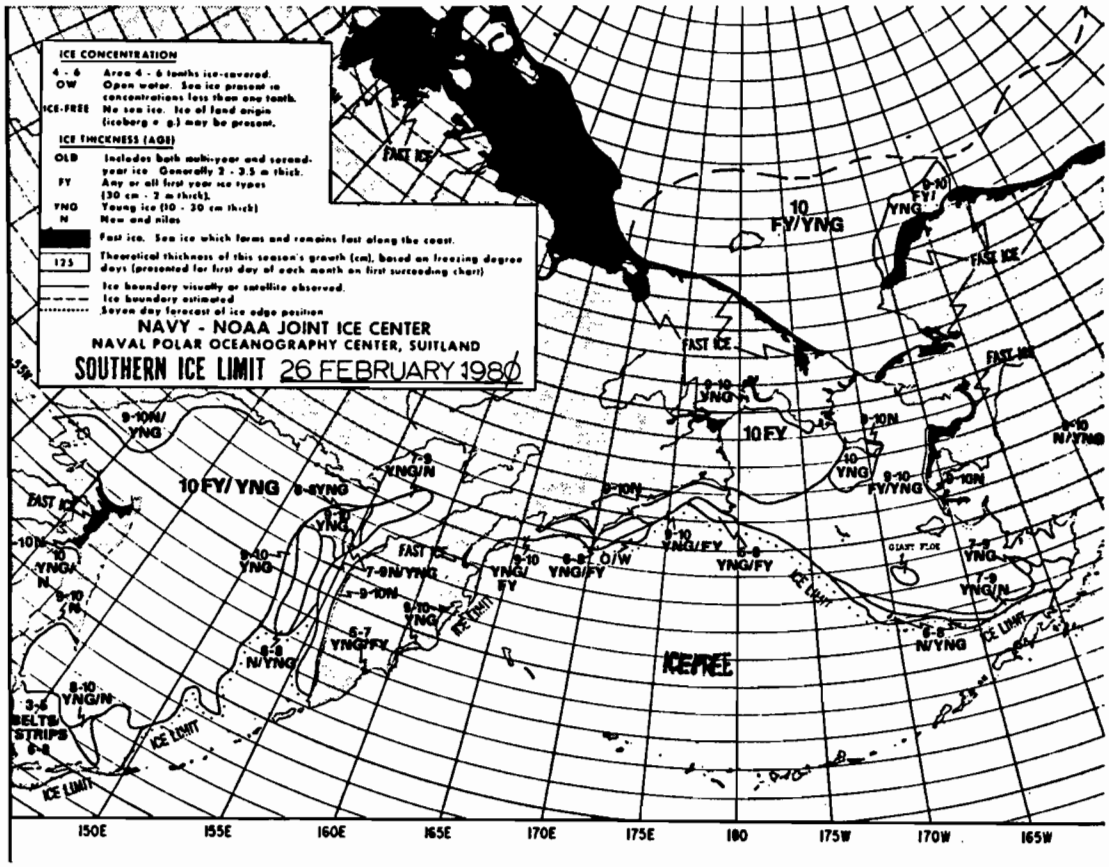

Figure 13a. Analysis of sea ice conditions for 26 February 1980 for the Bering Sea by the Navy-NOAA Joint Ice Center.

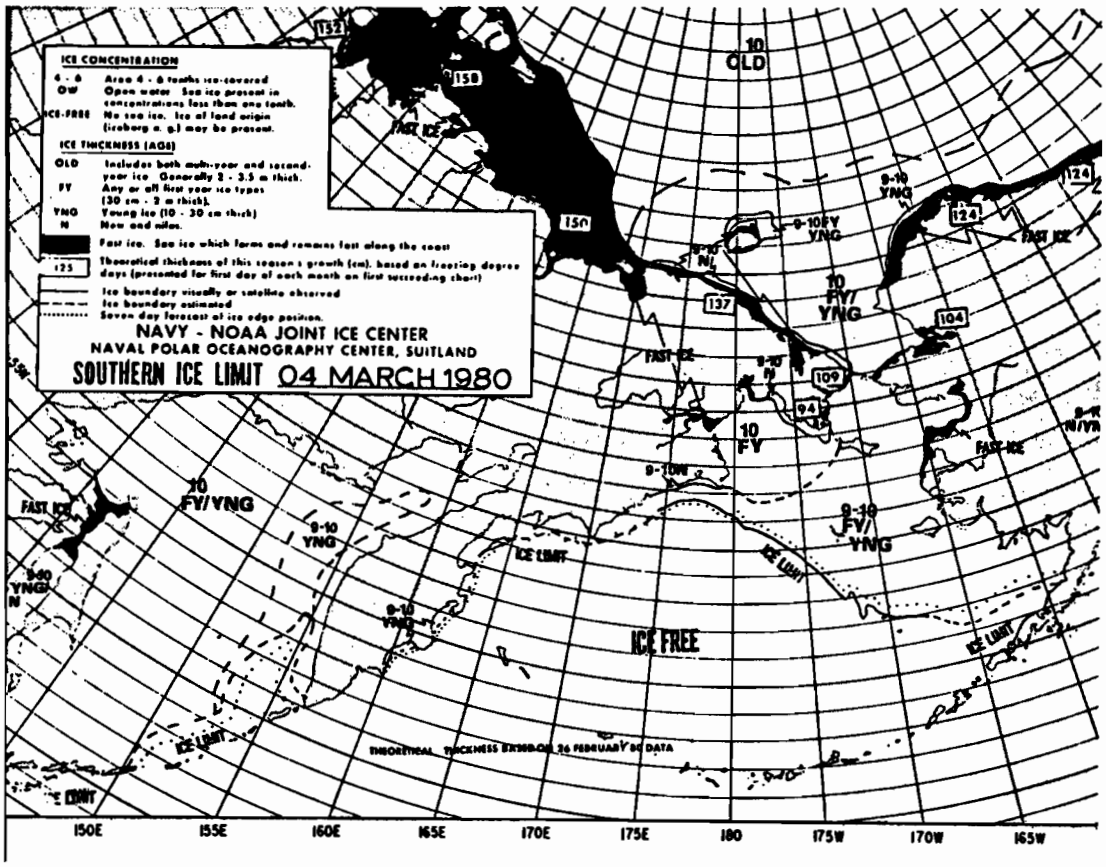

Figure 13b. Analysis of sea ice conditions for 4 March 1980 for the Bering Sea by the Navy-NOAA Joint Ice Center.

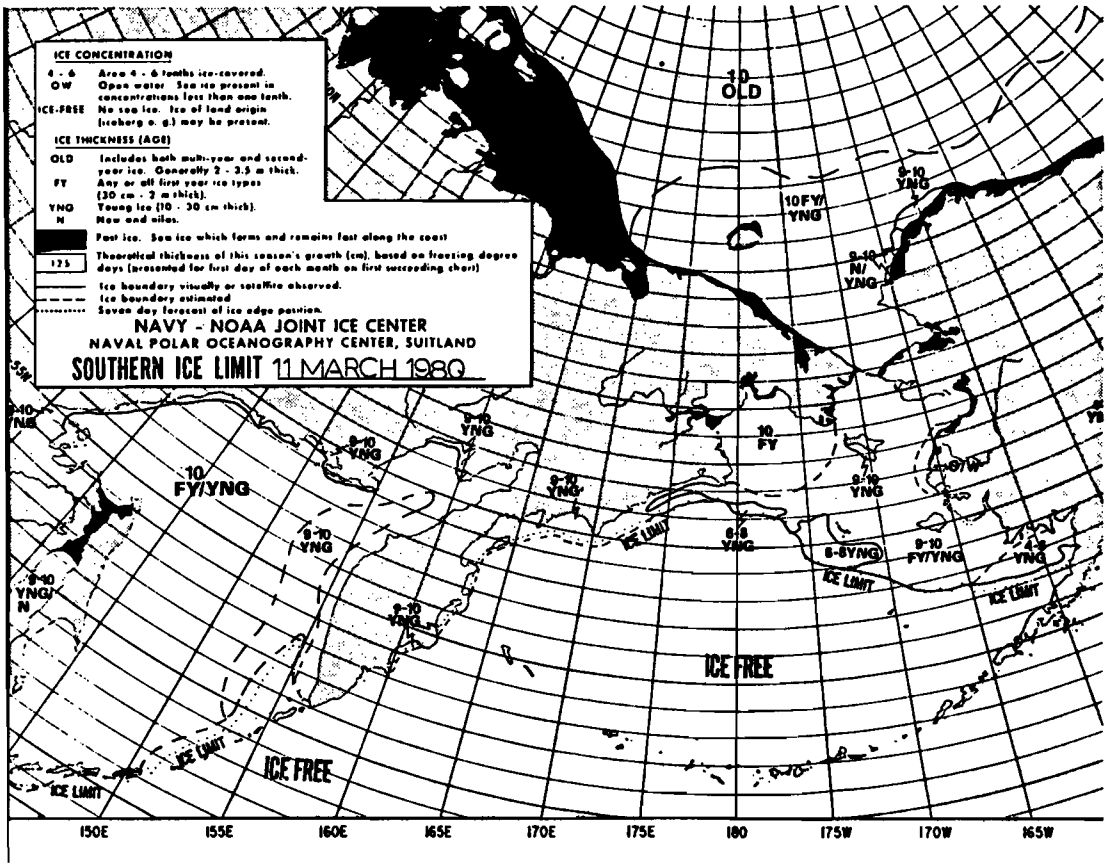

Figure 13c. Analysis of sea ice conditions for 11 March 1980 for the Bering Sea by the Navy-NOAA Joint Ice Center.

aircraft on 28-29 March and 6-7 March 1980 (Fig. 14). The northern portions of these flights overlapped our helicopter reconnaissance flights. Figure 15 illustrates ice conditions common to both aircraft in the overlapping observation area during the last two days in February. Big (0.5- to 2-km diameter) and vast (2- to 10-km diameter) floes were interspersed with leads containing open water through nilas. New ice was actively growing in open areas and finger rafting of nilas was prevalent during local dynamic events (Fig. 16). A major polynya existed along the Seward Peninsula from Cape Nome to Sledge Island such that there was only about 2 km of fast ice, approximately 5 km of open water through nilas, and then pack ice (Fig. 17).

Coring of floes in the region suggested that the ambient first-year ice had fairly uniform thicknesses of 0.9 to 1.0 m, plus a more variable snow cover of a few cm to about 20 cm. The snow-ice interface was well defined although the snow was metamorphosed to more rounded grains and firn (LaChapelle, 1969) and compacted by the wind into small-scale sastrugi. Surface snow features varied in appearance from large grit sandpaper to capillary waves and small drifts. The snow was dense enough so that the helicopter skis only penetrated about one centimeter (Frontispiece). No hoar crystals in the snow nor rime on the equipment were observed during the experiment.

With the arrival of the low-pressure system and subsequent shift in the current, ice drift, and wind the polynya near Nome closed. Precipitation from the storm varied somewhat with location but 10 cm of snow in 3 days was typical. Snow on the new ice was typically flooded (Fig. 17). This was noted by the Navy ice observers during their flight on 6-7 March and during our helicopter reconnaissance bracketing the same period. Also the Navy ice observers recorded a major lead parallel to the coast and 75 km distant from the Yukon Delta south to Cape Romanzof, and we observed a flaw zone (resulting from shear) parallel to the coast and only 2 km distant from south of Sledge Island to west of Cape Wooley (Fig. 18). These observations suggest that the fast ice system around the Yukon Delta remained intact during the storm and that little ice from Norton Sound was contributed to the northward movement of the pack toward the Bering Strait. Ice in Norton Sound was temporarily cut

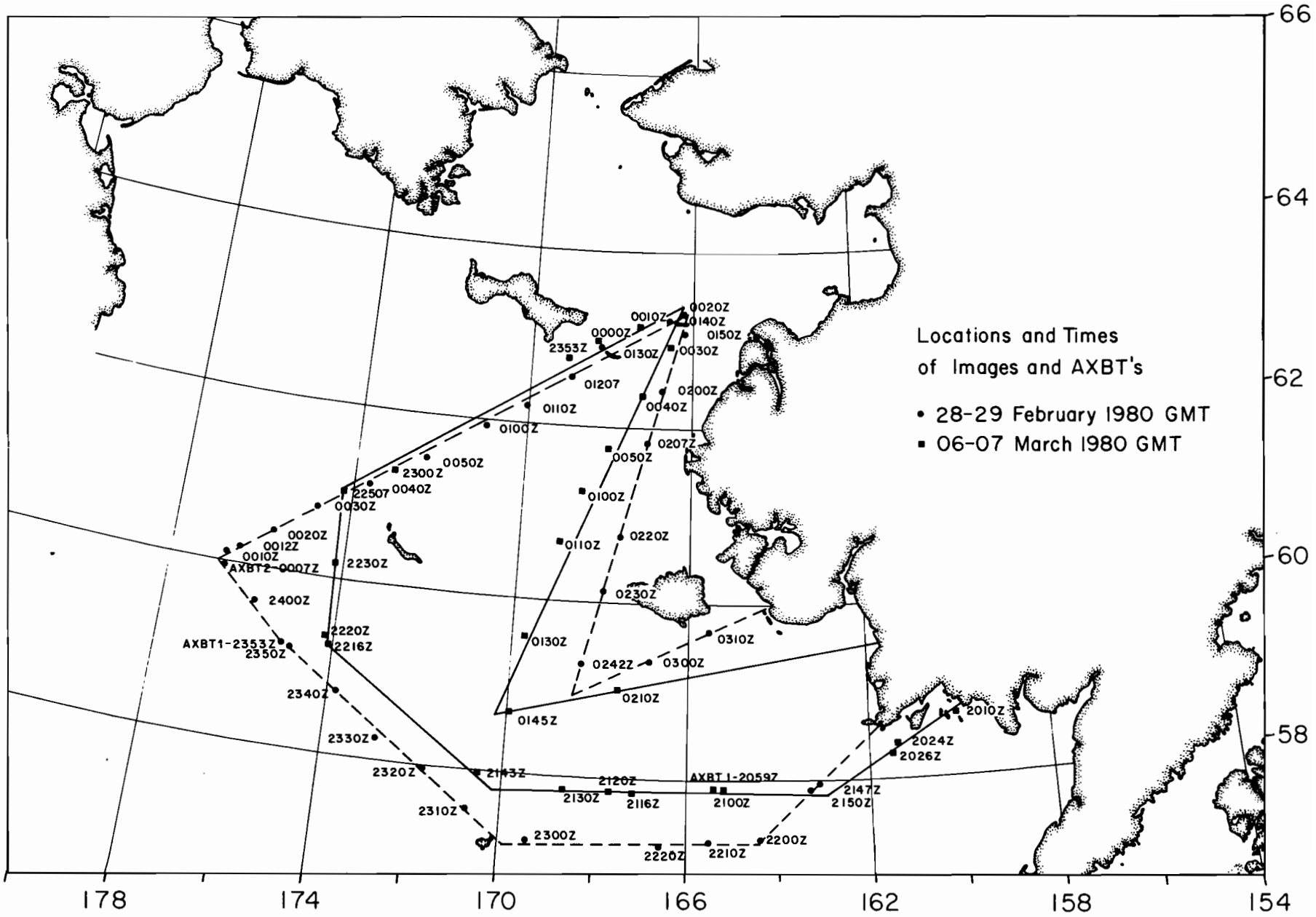

Figure 14. Tracks for ice reconnaissance flights by Navy P3 aircraft on 28-29 March and 6-7 March 1980.

Figure 15. Typical ice conditions in the study area during the last week of February 1980. Floe sizes ranged from a few tens of meters to a kilometer in diameter. Open water was generally 10% or less. Seward Peninsula in the background. (Photo by D. L. Bell.)

Figure 16. Rafting of nilas in a polynya near Nome. Black strip was open water. Scale of photo is about 1 km on a side.

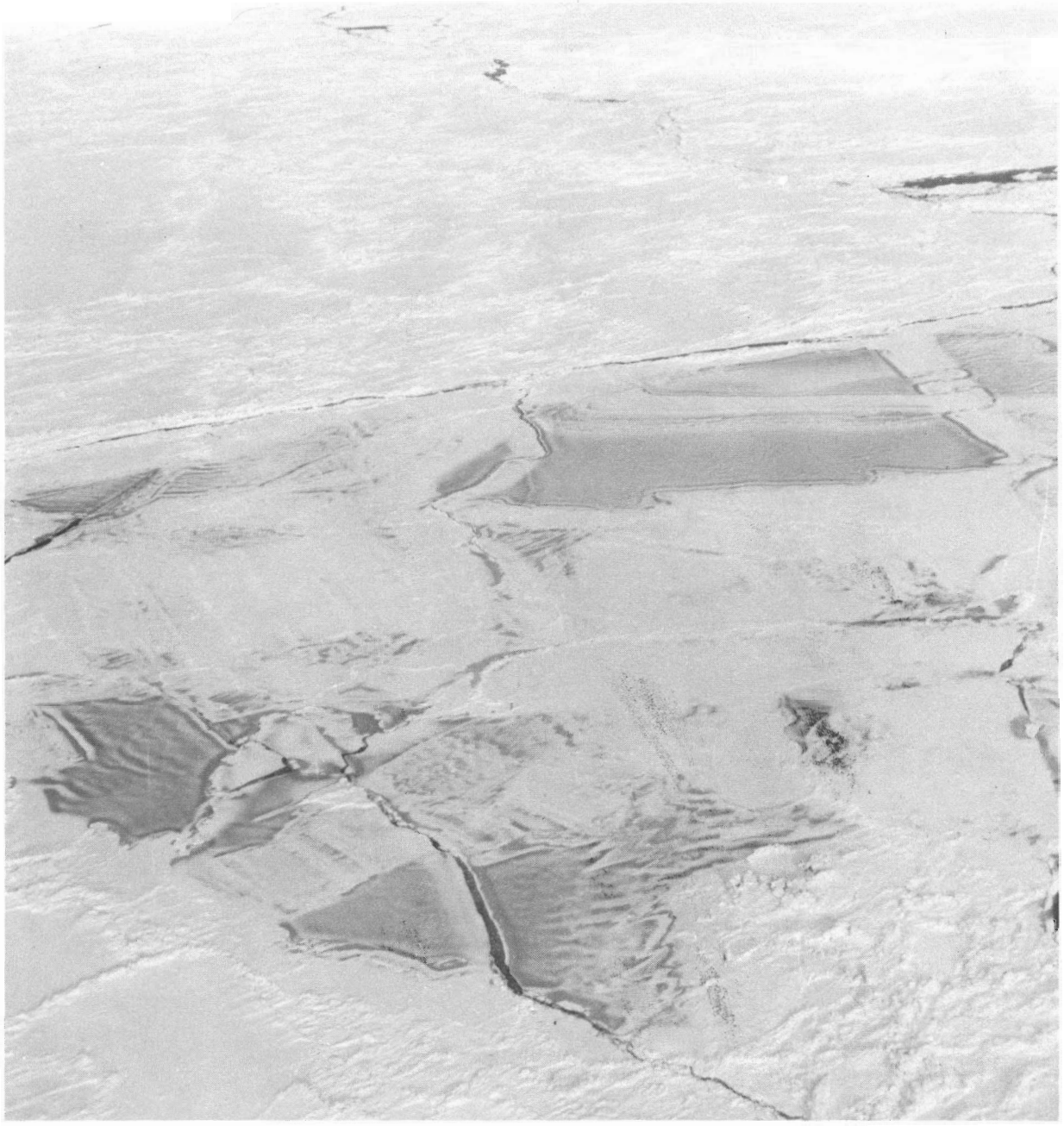

Figure 17. Flooded snow on new ice after the storm on about 6 March 1980. Scale of photo is about 2 km on a side. (Photo by D. L. Bell.)

Figure 18. Flaw or shear line in the pack tending northwest (lower left) to southeast (lower right) from Sledge Island on about 5 March 1980. (Photo by D. L. Bell.)

from the main body of the pack ice by a shear from the region off the Yukon Delta to the vicinity of Sledge Island and beyond. The flaw zone actually extended far enough into western Norton Sound and was sufficiently well defined that we were able to use it to estimate the direction of pack ice drift in the area to help recover our ice station at the end of the experiment.

4.2 Measured Ice Drift

Floe position was measured with a Digital Marine North Star 6000 Automatic Loran-C Receiver with a drift resolution calibrated to 20 meters. The observations were recorded on paper tape by a thermo-mechanical printer through a general-purpose interface for the first day and thereafter were recorded by hand in log books during daylight hours when weather permitted. The power for the printer was converted from DC to AC by a static inverter which failed because of voltage irregularities. The receiver itself operated on DC and was not affected by the failure. Observations were made every ten minutes while we were on site. A twelve-hour smooth plot of these results is given in Figure 3 (Sec. 1).

Missing observations were filled in by linear interpolation and velocities calculated by center-differencing. Two-hour, block-averaged drift velocities are shown in Figure 19. These are compared to the relative current and wind measurements and demonstrate the limited number of floe position observations. Note particularly the lack of observations for four days during the storm when we could not fly or could not find the floe. A maximum in floe speed would have been expected to occur coincident with the maximum in wind speed during the storm, unlike the smoothed floe speed imposed by our interpolation procedure.

Possibly a more constructive comparison of the relative current, wind, and floe drift is made with 35-hour running-filtered data (Fig. 20). This filter removes tidal influences and other high-frequency noise so the comparison is less sensitive to the interpolation present in the floe velocity. Note that the ice did not move downwind during the first three days of the experiment, rather its drift was primarily controlled by the current stress. The wind on the southern pack shifted to southerly before the local wind shift was felt, so there

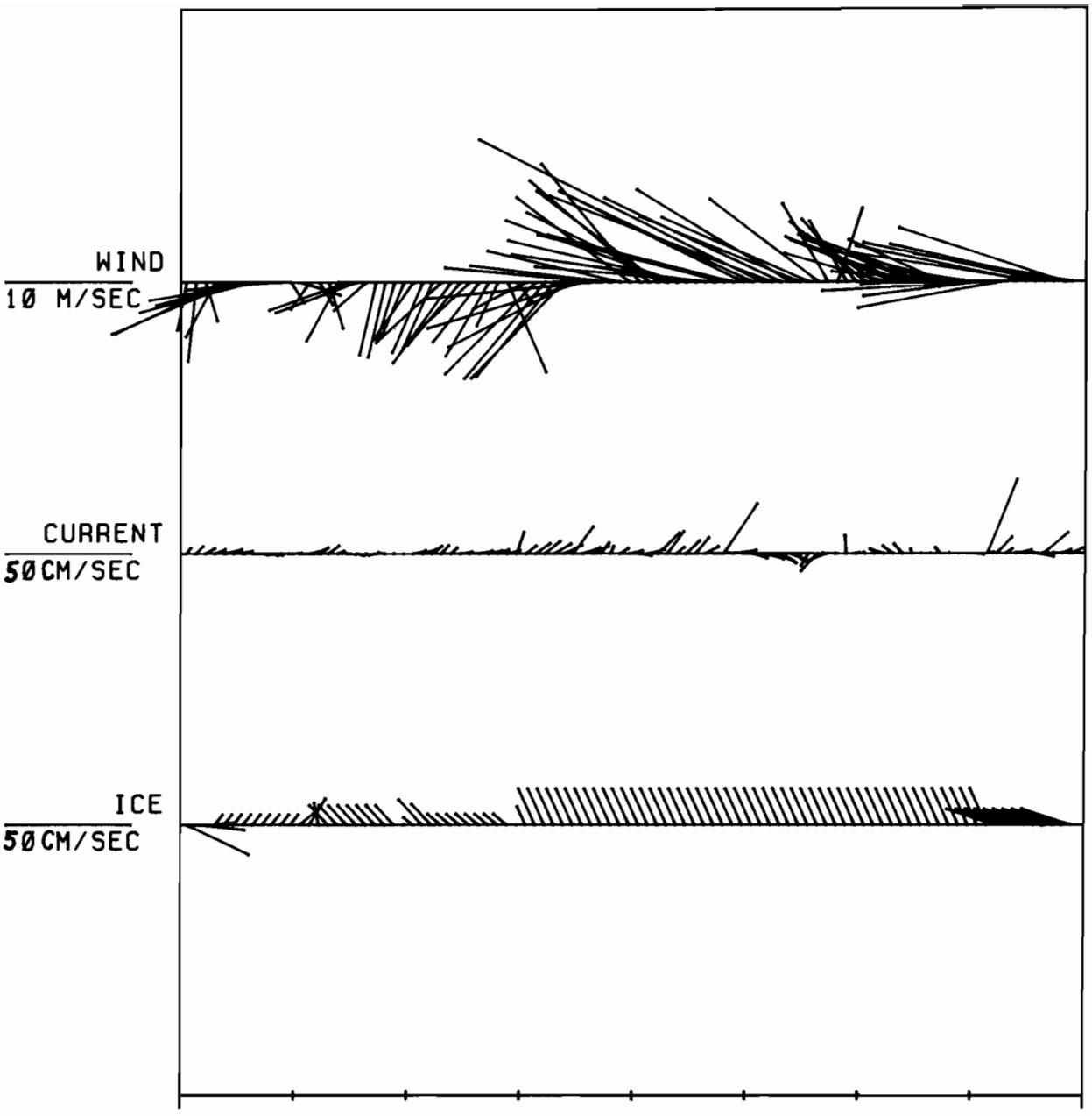

Figure 19. Two-hourly block-averaged winds, relative currents, and ice drift velocities from 2230 GMT on 28 February (JD59) 1980 to 2130 GMT on 7 March (JD67) 1980. Speed is scaled at left.

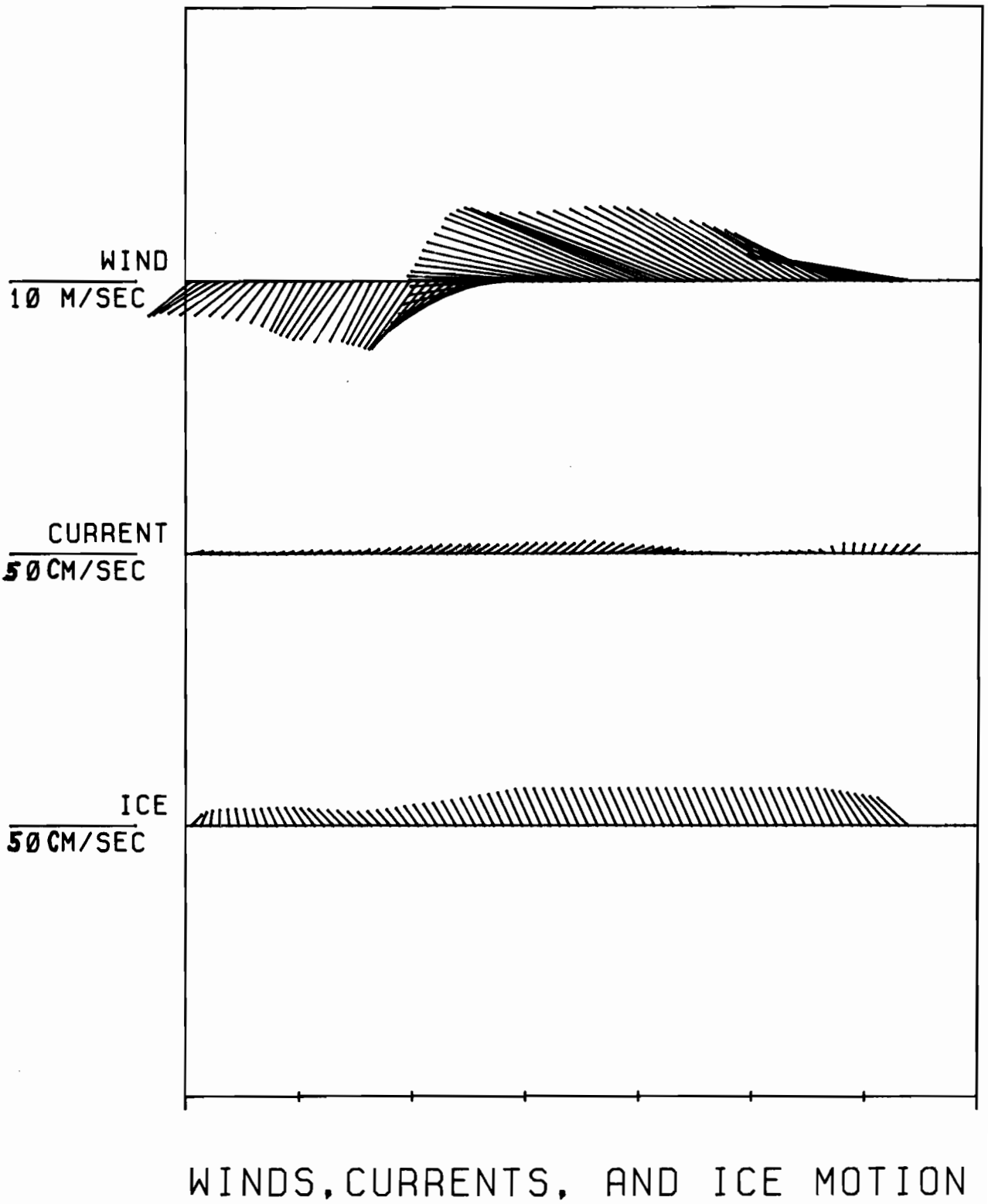

Figure 20. Two-hourly representation of 35-hour running-averaged winds, relative currents, and ice drift velocities. The beginning of the time series is equivalent to 15 GMT on 29 February (JD60).

was some possibility of internal stress. Once the local wind shifted to easterly and then southeasterly, the wind and current and any ice stress were acting more in consonance so that the floe accelerated.

To demonstrate the importance of the current on the drift in this region, Figure 21 shows two-hour block-averages of absolute current and ice drift. Although the absolute current estimates are themselves partial sums of our interpolated floe drift, they were verified independently (Sec. 3) and thus indicate the local importance of stress caused by the current as compared with stress caused by the wind during certain synoptic situations.

Rotation was also measured on the floe with an internally recording Model RCM-4 Aanderaa current meter with the rotor secured. The current meter's compass was calibrated to ±3.4° magnetic in March 1978 (NW Regional Calibration Center). The rotation of the floes was gradual with a net clockwise movement of 24° in 3 days for the first floe and 13° in 5 days for the second floe. The rotation rate was verified by sighting along the anemometer cross-arm with a hand compass on each visit. The rotation was probably caused by shear between ice motion (or current) to the west and the fast ice (or slower current) along the coast to the east during the northward to northwestward floe drift. Both floes were fairly rectangular in shape, and local ice concentrations were similar for each, but the first floe was larger in diameter with respect to its neighbors than the second floe. Thus the first floe may have had a higher rotation rate because of its rotational inertia.

5. DRIFT ANALYSIS

The angles of floe drift with the wind and current give an indication of the importance of one fluid over the other as the driving force. If the angle between the wind and floe drift is small and between the current and floe drift is large then the wind is dominating. Or, equivalently, if the angle between the current and floe drift is small then the current is dominating.

The turning angles between the wind and ice drift, α, and between relative current and ice drift, β, were calculated from the approp-

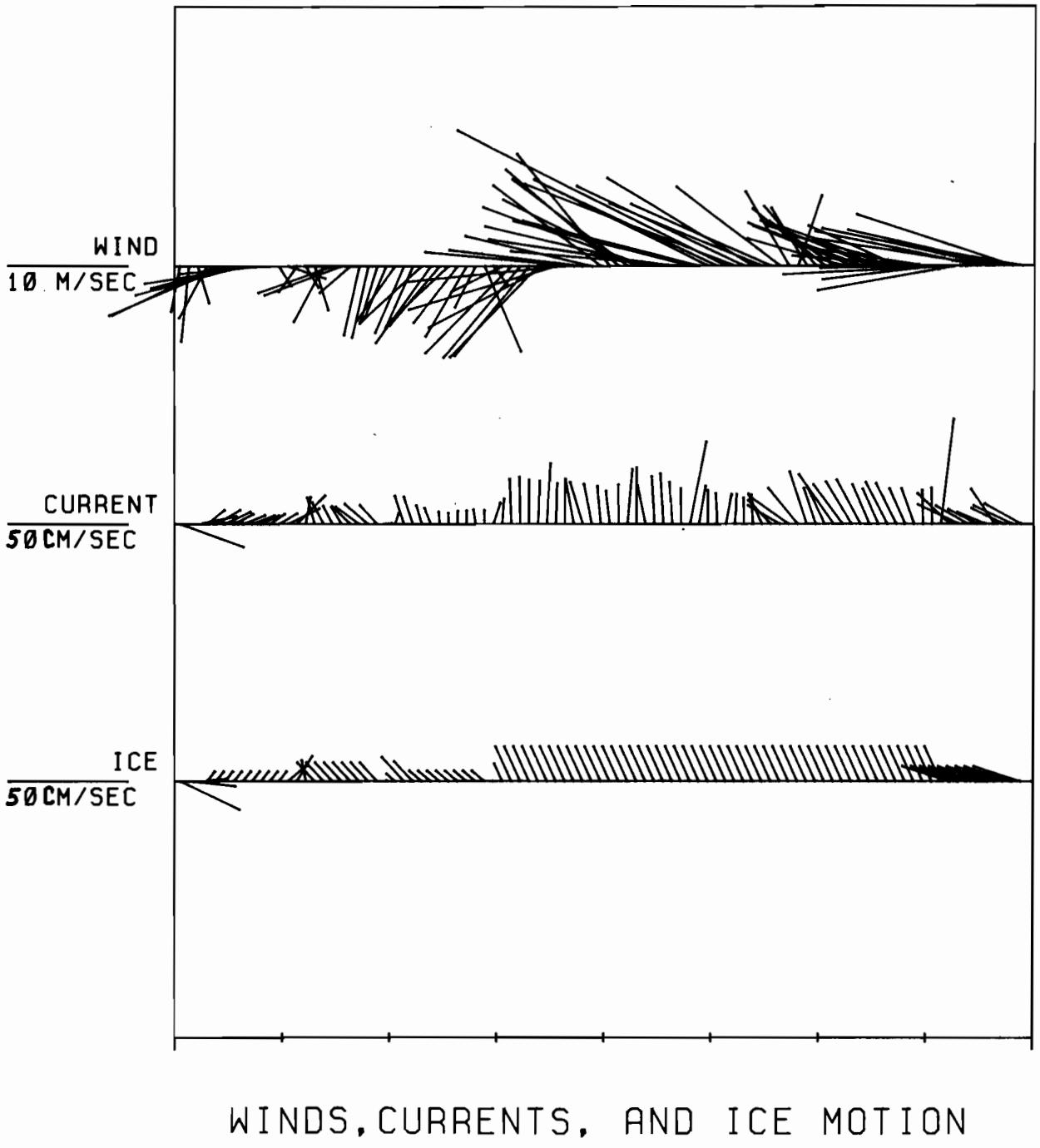

Figure 21. Two-hourly block-averaged winds, calculated absolute currents, and ice drift velocities from 2230 GMT on 28 February (JD59) 1980 to 2130 GMT on 7 March (JD67) 1980.

riate vectors by:

$$\alpha = \arctan \frac{V_a U_i - U_a V_i}{U_a U_i + V_a V_i} \qquad 1$$

$$\beta = \arctan \frac{V_w U_i - U_w V_i}{U_w U_i + V_w V_i} . \qquad 2$$

where U_a, V_a and U_w, V_w are the measured relative wind and current and U_i, V_i, the analyzed ice velocity.

The rotation angles of the wind and current to the floe drift direction, calculated according to Eqs. 1 and 2, are given in Figure 22. The 3-m wind direction shifted from just opposite the floe drift direction to the vicinity of 40° to the left of the floe drift direction in the latter half of the experiment. This indicates that control by the wind on the ice was very weak during the current reversal at the beginning of the experiment, but that the wind became more dominant during the storm. The relative current direction shifted from about 30° to the right of the floe drift direction during the current reversal in strait to roughly 100° of the floe drift direction during most of the first two-thirds of the experiment. The relative current direction then dropped off to 180°, and, later in the experiment, completed a circle in less than two days.

The magnitude of the relative velocities of the wind and current are given in Figure 23. This shows that the relative current was larger than the relative wind at the beginning of the experiment when approximately scaled by density. Also the relative current velocity dropped off to near zero during the circling event. Although there is some symmetry in the shapes of these velocity curves, there are many inflection points which are not consonant. Symmetry of shifts would imply drag of an instrument through its fluid as a result of being towed by the dominant fluid. Asymmetric shifts would imply that the fluids are acting independently. We observed some of each condition.

Figure 24(a-j) shows a representative selection of the smoothed vector relationships (relative wind, current, and ice drift) with their

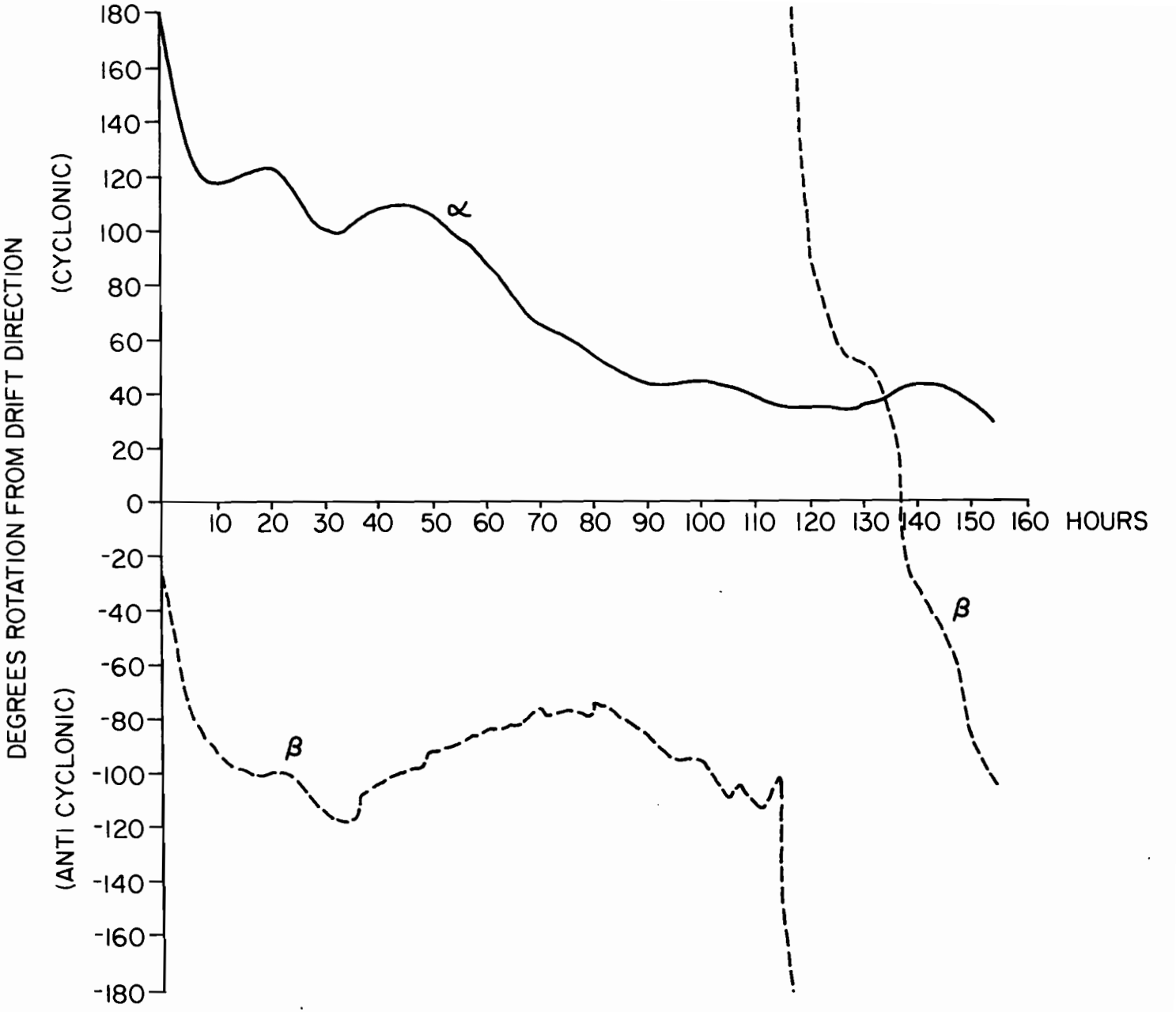

Figure 22. Rotation angles of the wind (α) and the current (β) to the floe drift direction.

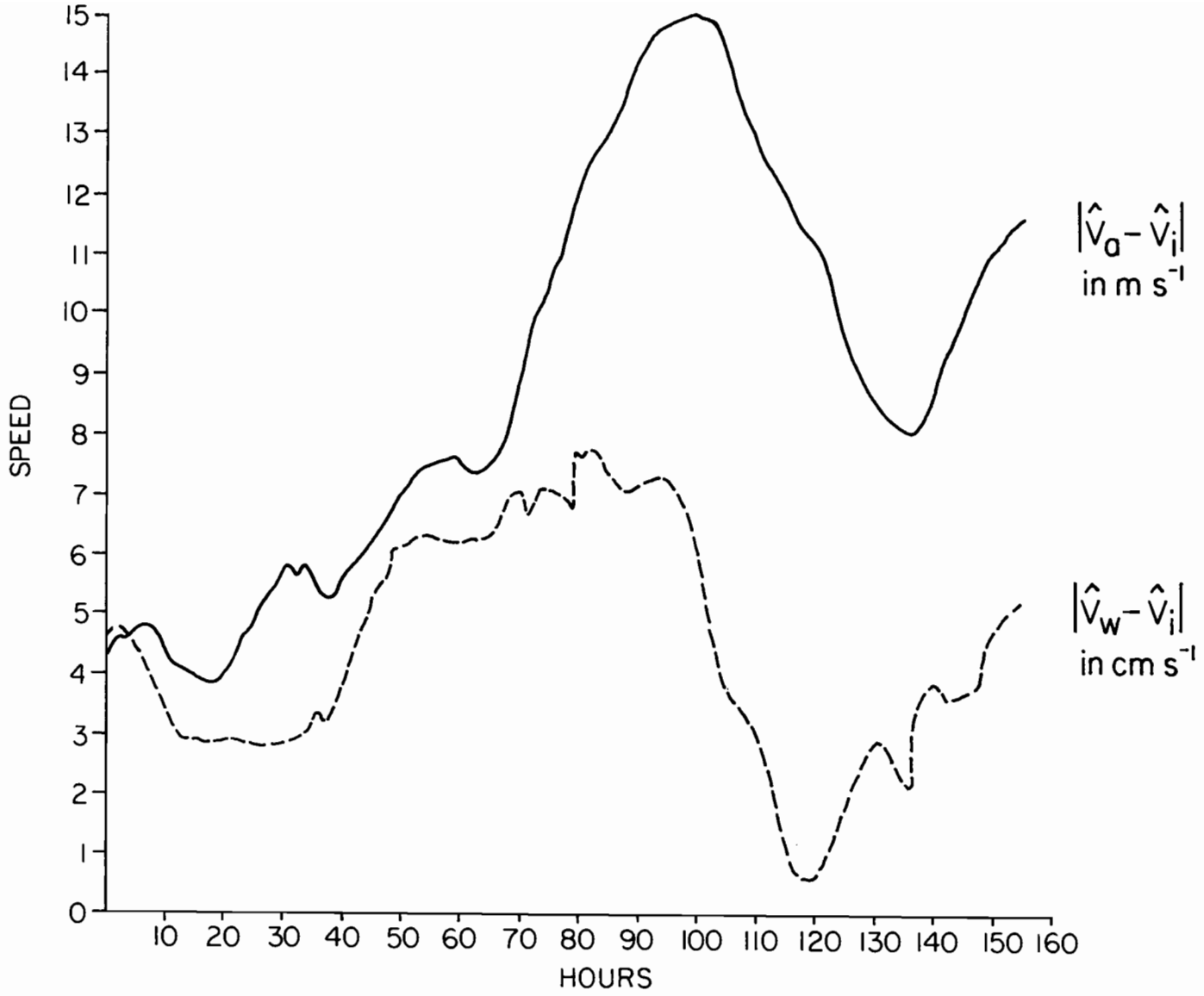

Figure 23. Relative wind ($|\hat{V}_a - \hat{V}_i|$) and current ($|\hat{V}_w - \hat{V}_i|$) speeds. Note that the difference in units is approximately equivalent to scaling by density.

rotation angles for every twelve hours during the experiment. The hour numbers on these vector plots refer to the elapsed hours axis in Figures 22 and 23. Of particular interest is the rotation in the relative current discussed above and further demonstrated in Figure 24(k). Also note that the ice drift only averaged 1.5% of the wind speed for all the cases and there was a tendency for the higher winds to have the lowest ice drift to wind velocity ratio (Fig. 24 (e and f)).

6. SUMMARY

6.1 Winds at Nome were not representative of winds over the ice in western Norton Sound and the Bering Strait. The mountains behind Nome reduced the speed of northerly winds and deflected southeasterly winds to a more easterly direction.

6.2 Comparisons of METLIB surface winds calculated from NWS Alaska Region surface pressure analyses with observed winds over the ice were highly favorable. Comparisons of METLIB winds with observed winds at Nome were unfavorable because of the orography.

6.3 The strong currents in the Bering Strait influenced the ice drift and, at the beginning of the experiment, dominated the ice stress balance in the study region.

6.4 During and after the storm, the ice supported a major shear zone from Sledge Island to within 75 km of the Yukon River Delta. The ice west of this line moved northwestward and ice east of this line seemed to move very little.

6.5 Several distinct events in the floe drift could be discerned from the turning angles between the ice drift and the wind and current and from the relative speeds, including the current-dominated regime early in the experiment, the coupling of the wind and current at the onset of the storm, and a period of extremely weak current. The ice drift for the experiment averaged only 1.5% of the wind speed. A summary of meteorological, oceanic, and floe drift events on the synoptic scale are included in Table 2.

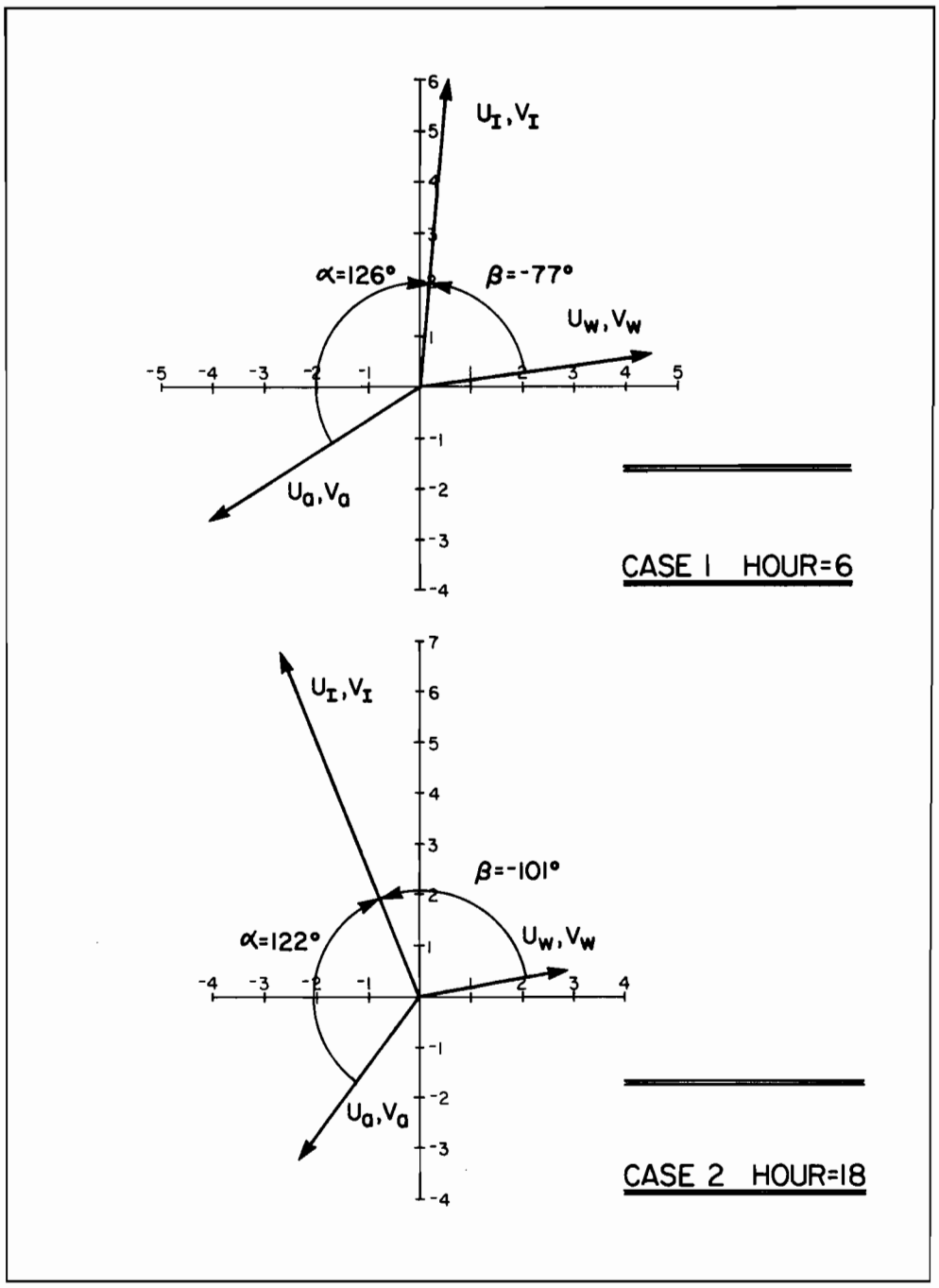

Figure 24a. Vector representation of relative wind (m s^{-1}), current (cm s^{-1}) and ice drift velocity (cm s^{-1}). The hour number refers to elapsed hours in figures 23-26.

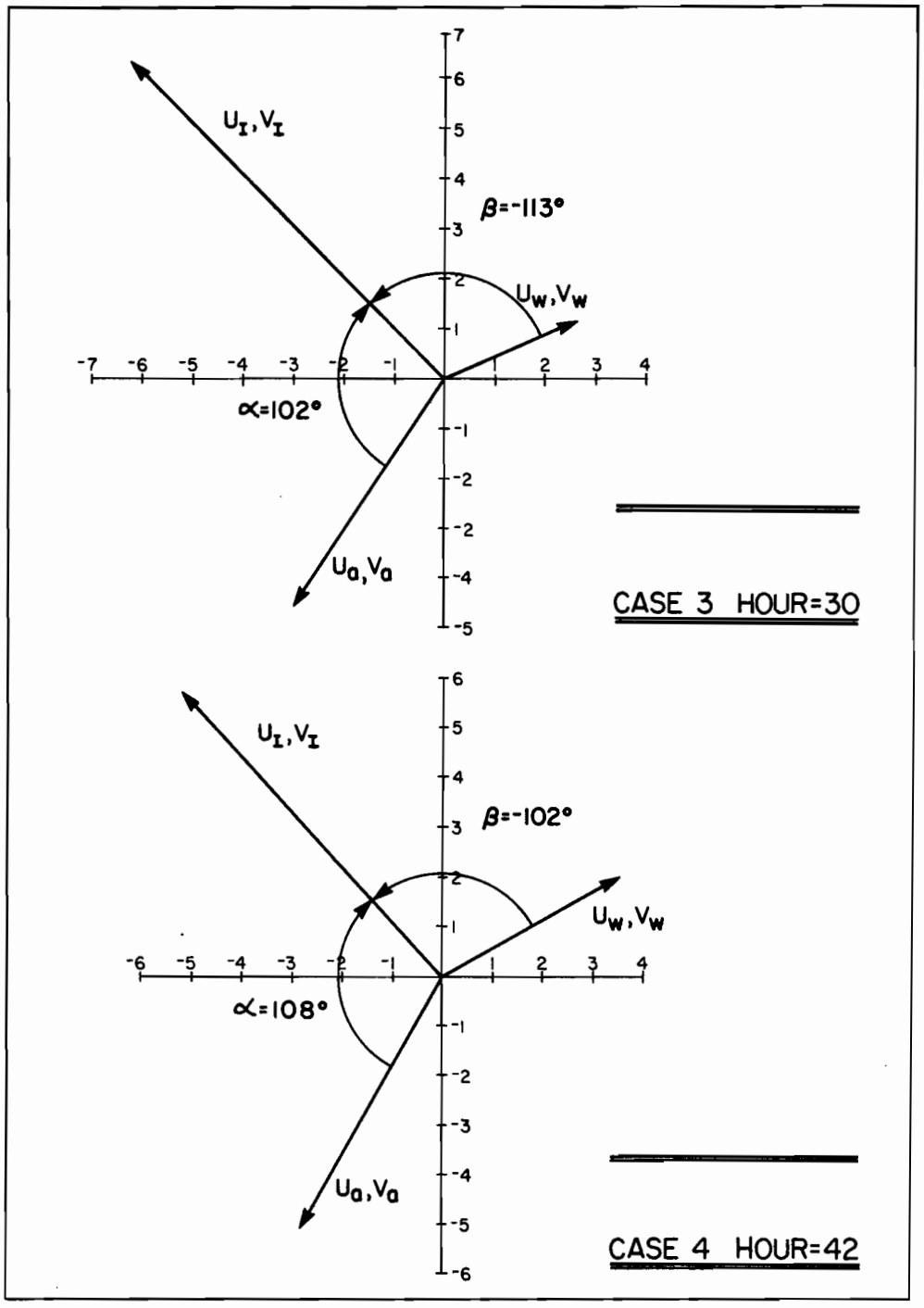

Figure 24b. Same as in Fig. 24a.

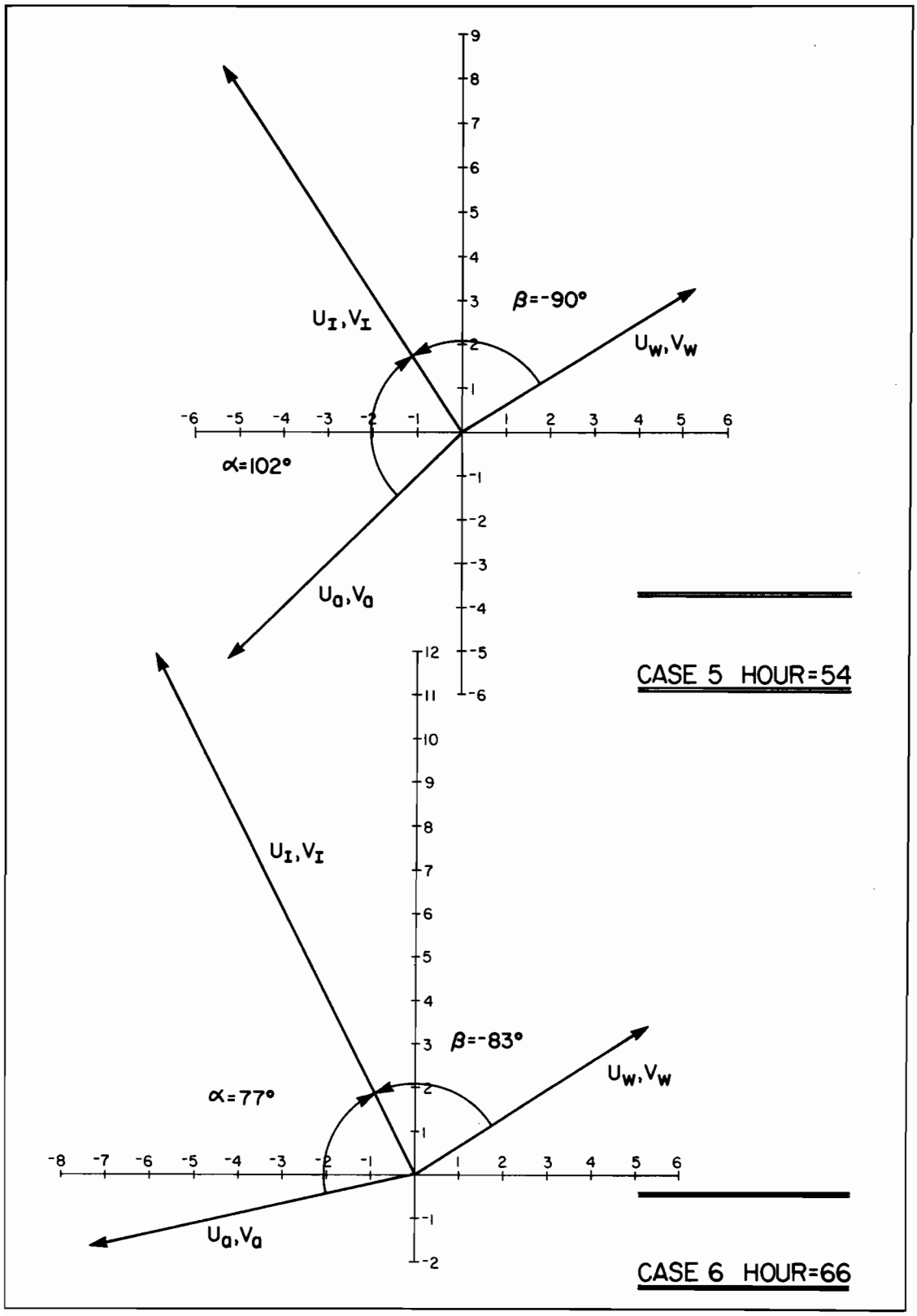

Figure 24c. Same as in Fig. 24a.

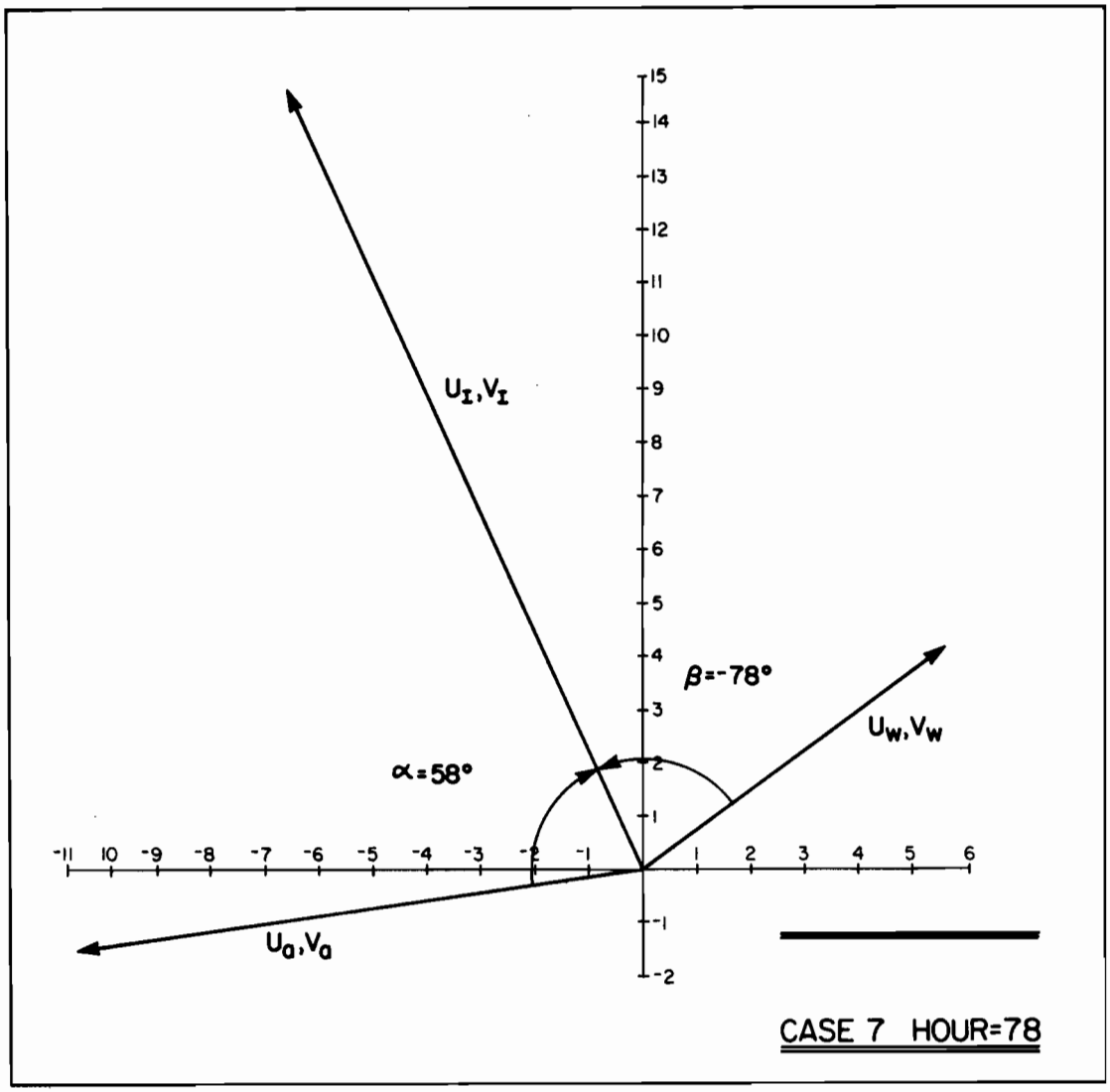

Figure 24d. Same as in Fig. 24a.

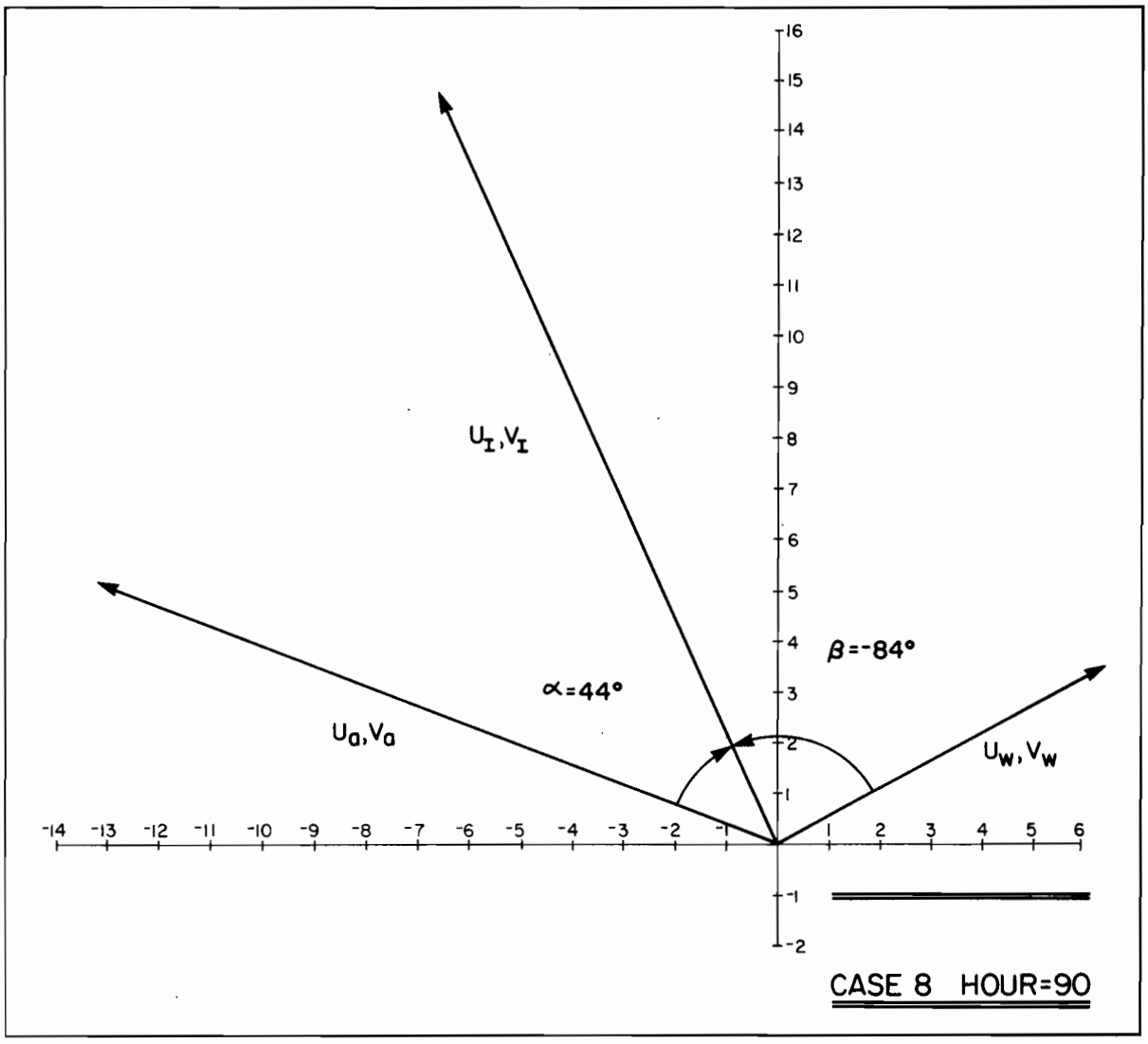

Figure 24e. Same as in 24a.

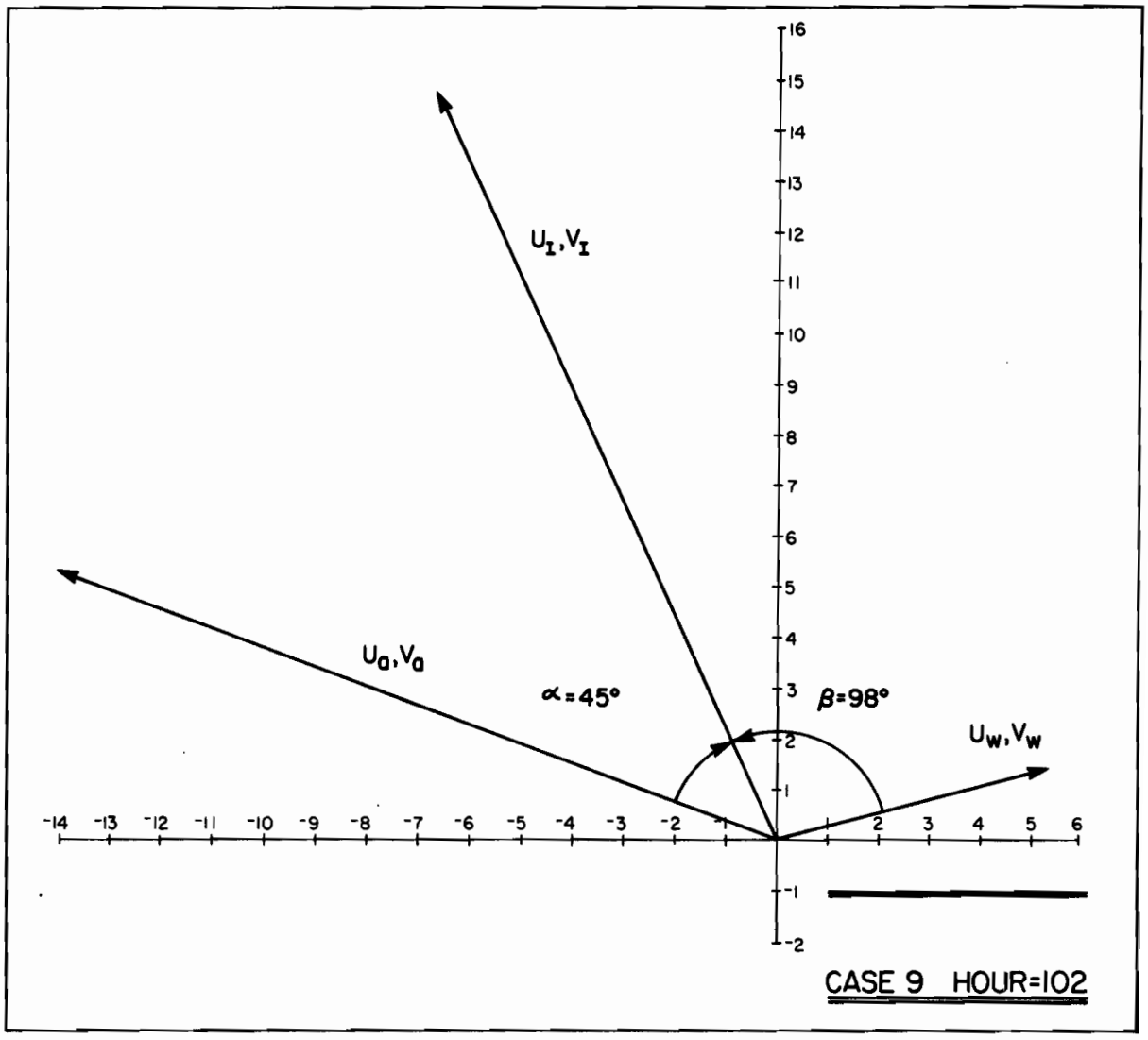

Figure 24f. Same as in Fig. 24a.

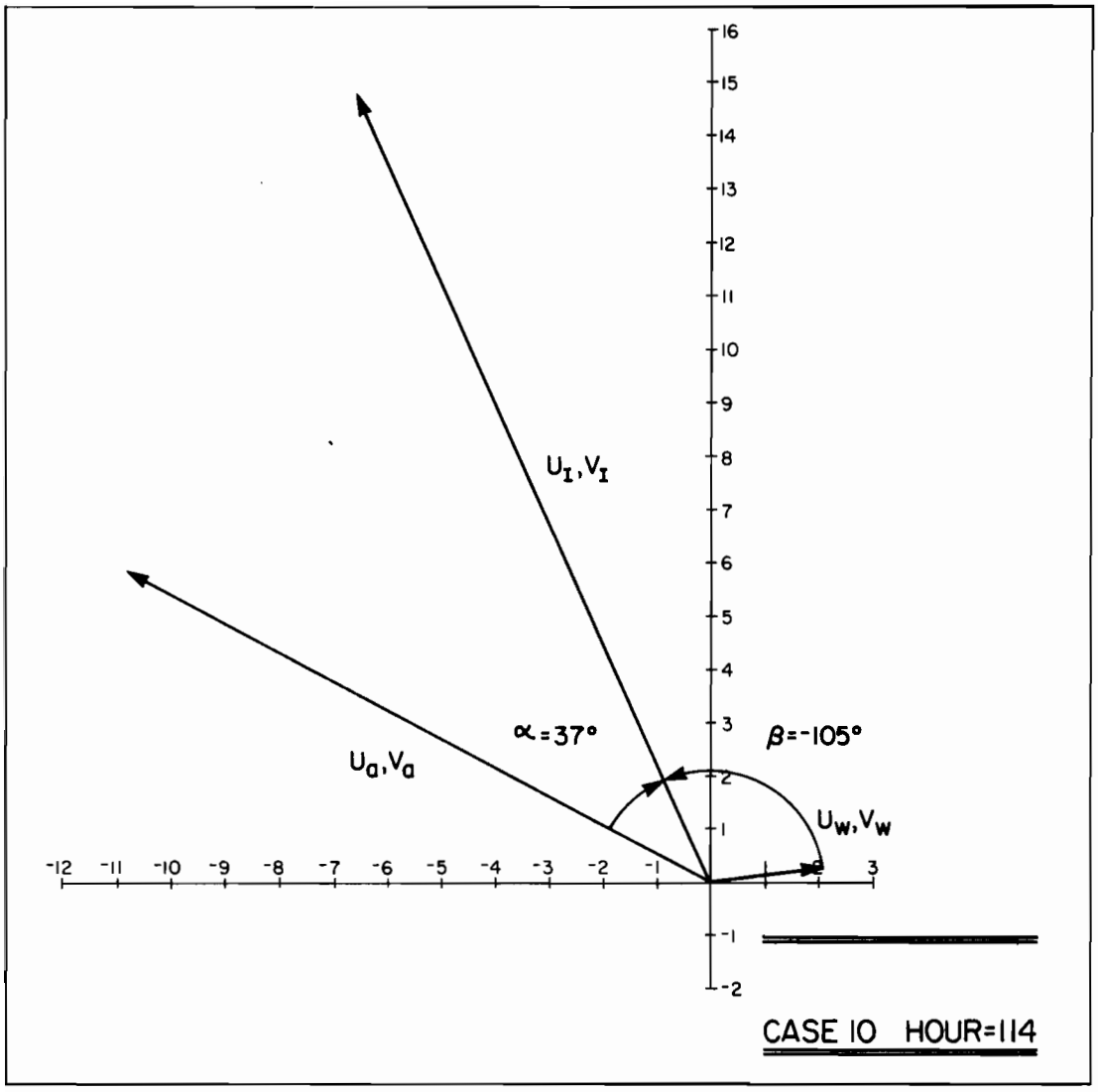

Figure 24g. Same as in Fig. 24a.

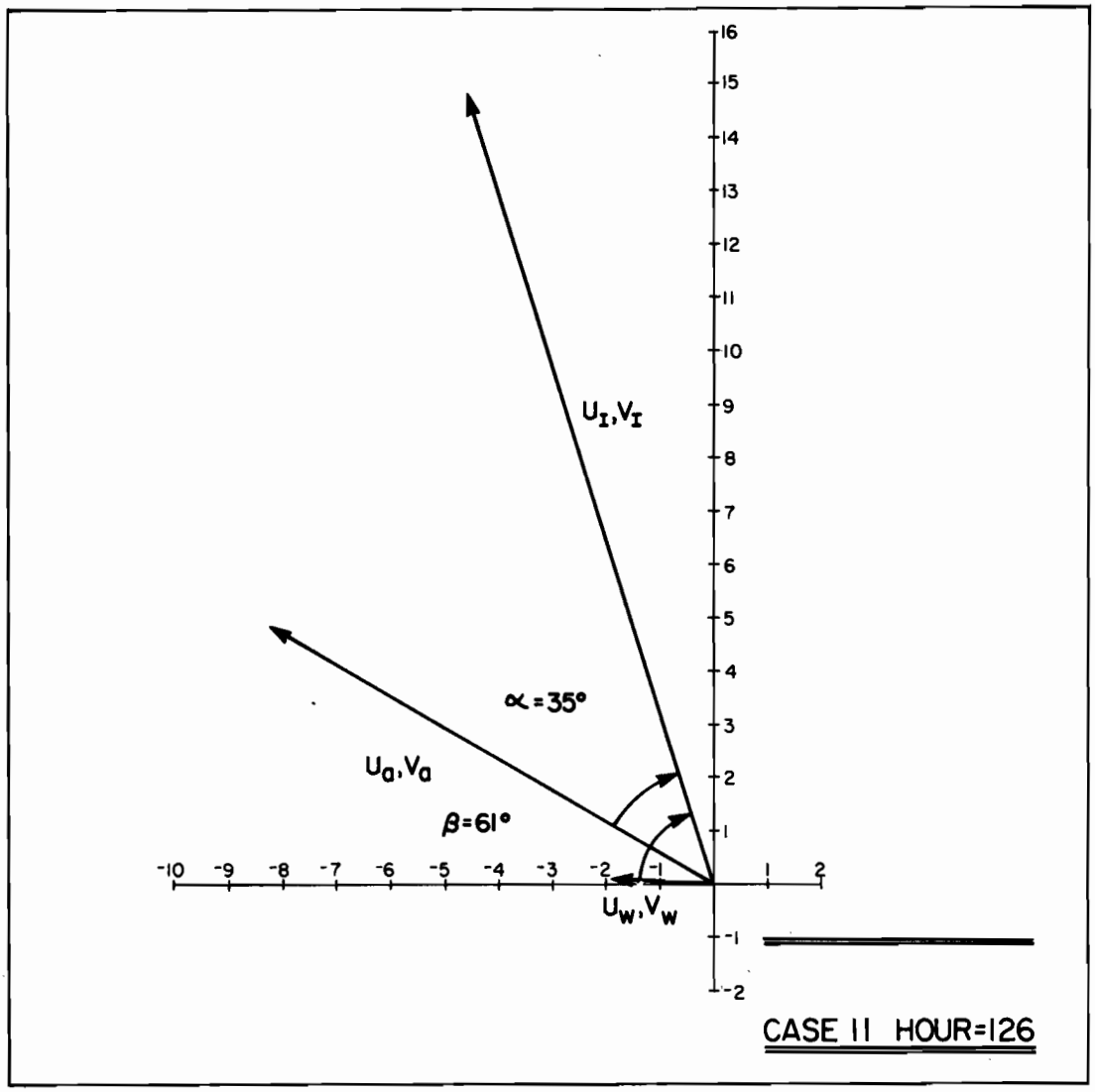

Figure 24h. Same as in Fig. 24a.

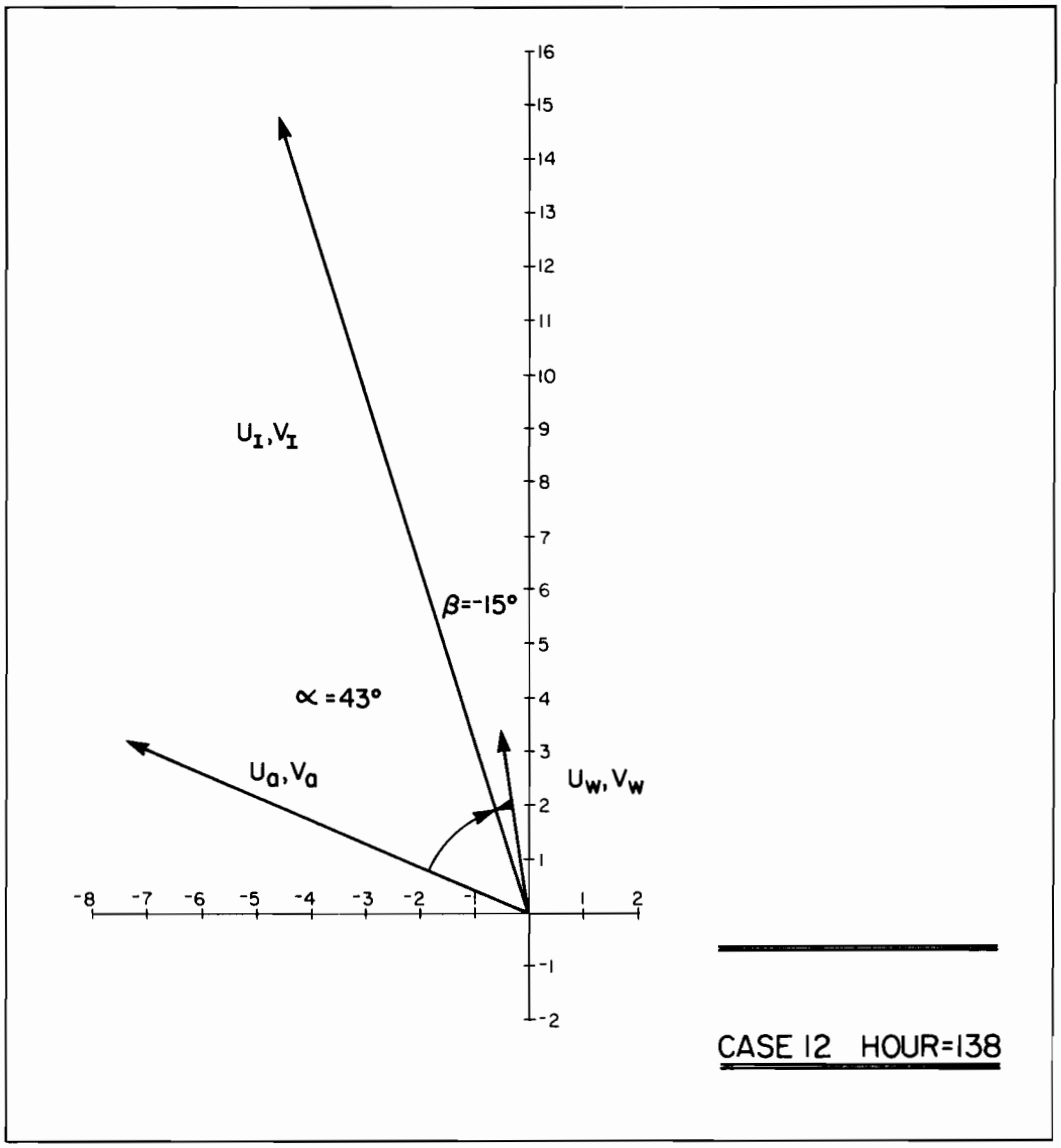

Figure 24i. Same as in Fig. 24a.

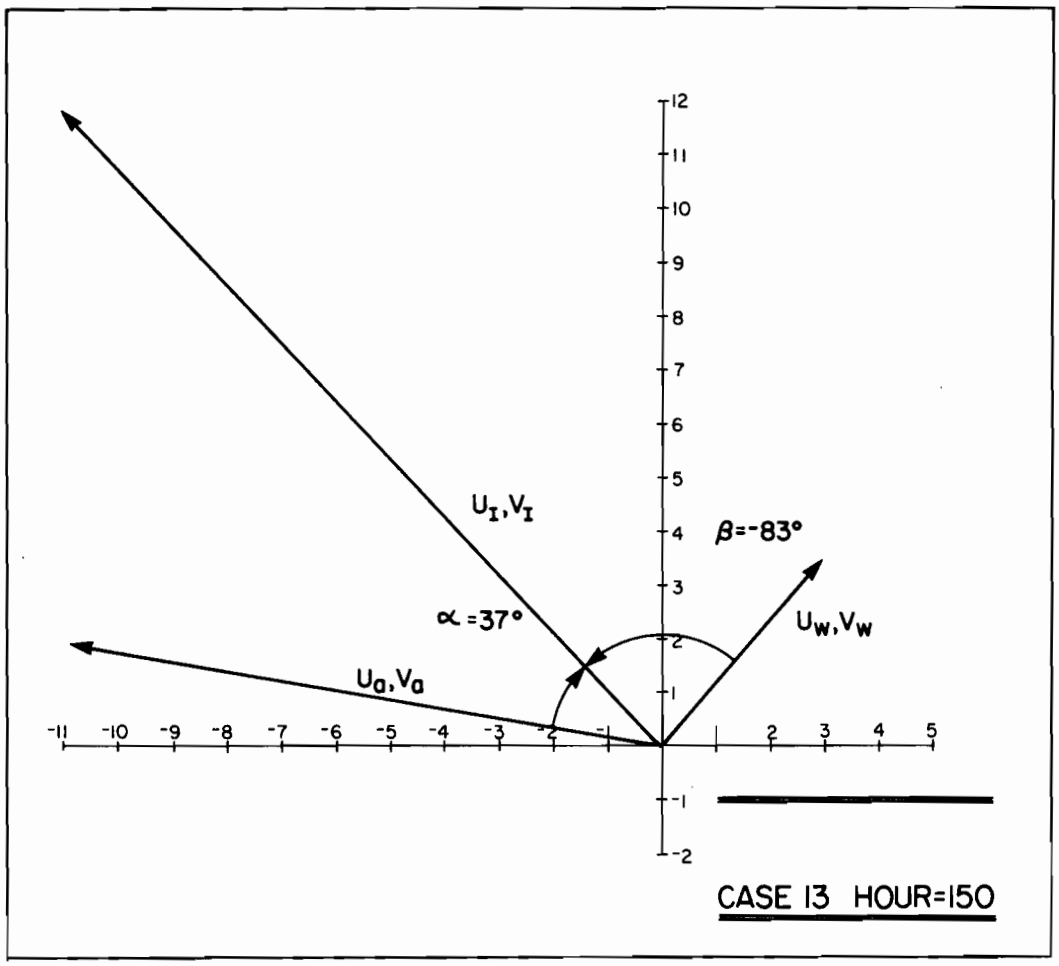

Figure 24j. Same as in Fig. 24a.

Table 2. Summary of synoptic events related to the condition and movement of pack ice.

Period	Wind Direction[1]	Current Direction[2]	Air Temperature[3]	Ice Drift Direction[4]
14-15 Feb	S-SE		0 to 5	
20-22 Feb	N-NE	S-SE	-20 to -15	
24-26 Feb	SW-SE	N-NW	-15 to -10	
28-29 Feb	E-NE	S-SE	-10 to -5	E-SE
5-7 Mar	E-SE	N-NW	-5 to 0	N-NW
13-14 Mar	NW-NE	S-SE	-20 to -15	

[1] Direction is given in meteorological convention and inferred from Appendix A.

[2] Direction is given in oceanographic convention from the King Island current meter record.

[3] Temperature is given in °C and inferred from Appendix B.

[4] Direction is given in oceanic convention and interpreted from Figure 19.

7. ACKNOWLEDGEMENTS

This memorandum is a contribution to the Marine Services Project at the Pacific Marine Environmental Laboratory. It was supported in part by the Bureau of Land Management through an interagency agreement with the National Oceanic and Atmospheric Administration, under which a multiyear program is being conducted to respond to the need for petroleum development on the Alaskan Continental Shelf, and is managed by the Outer Continental Shelf Environmental Assessment Program (OCSEAP).

David L. Bell provided invaluable engineering technical support throughout the experiment. Rudy (Shep) Shepkey, our pilot from Evergreen International believed us when we said it was safe to land on the ice, especially after he kindly helped chip ice out of the hydrographic hole. Bruce D. Webster, sea ice forecaster from NWS Fairbanks, procured electronics parts and made field observations for a few days. Seymour (Bud) Krepky, Meteorologist-in-Charge at NWS Nome, arranged lodging and gave other valuable logistics support. His staff made every effort to provide tailored forecasts for our operations. Delbert Barr, meteorologist at NWS Nome, guided local equipment procurement.

Much of the equipment used in the experiment was borrowed from other researchers. The Coastal Physics Group under Glenn Cannon at PMEL lent the current meters used for the oceanographic and ice rotation observations. Seelye Martin from the Department of Oceanography, University of Washington (UW), lent an ice auger and chisels. Thomas Grenfell, Department of Atmospheric Sciences, UW, lent the static inverter. Also Richard Tripp and his associates from the Department of Oceanography, UW, lent a locator beacon and generously provided bottom-moored current meter data for comparison to our through-the-ice measurements.

The National Weather Service Forecast Office in Anchorage supplied the surface analyses, and the National Climate Center in Nashville supplied climatological data. Lt.(jg) Mark Diunizio and Robert H. Davis flew the Navy ice reconnaissance for the Navy-NOAA Joint Ice Center within the Navy Polar Oceanography Center under the leadership of Commander James C. Langemo.

James D. Schumacher, James E. Overland, and Carl A. Pearson gave helpful advice on the physics. Sally A. Schoenberg analyzed and digitized some of the surface air temperature fields. Peter LaNore assisted with the computing.

8. REFERENCES

Charnell, R.L. and G. Krancus (1976): A Processing System for Aanderaa Current Meter Data. NOAA Technical Memorandum ERL PMEL-6, 50 pp.

Coachman, L.K. and K. Aagaard (1981): Reevaluation of water transports in the vicinity of Bering Strait. Chapter 7 in The Eastern Bering Sea Shelf: Oceanography and Resources, Vol. 1 (ed. by D.W. Hood and J.A. Calder), Gov't Printing Office, Washington, D.C., 95-110.

Coachman, L.K., K. Aagaard, and R.B. Tripp (1975): Bering Strait: The Regional Physical Oceanography. University of Washington Press, Seattle, 172 pp.

LaChapelle, E.R. (1969): Field Guide to Snow Crystals. University of Washington Press, Seattle, 101 pp.

Muench, R.D., R.B. Tripp, and J.D. Cline (1981): Circulation and hydrography of Norton Sound. Chapter 6 in The Eastern Bering Sea Shelf: Oceanography and Resources, Vol. 1 (ed. by D.W. Hood and J.A. Calder), Gov't Printing Office, Washington, D.C., 77-94.

Naval Polar Oceanography Center (1981): Eastern-Western Arctic Sea Ice Analysis 1980. Naval Polar Oceanography Center, Suitland, Maryland, 104 pp. + end papers.

Overland, J.E. (1981): Marine Climatology of the Bering Sea. Chapter 2 in The Eastern Bering Sea Shelf: Oceanography and Resources, Vol. 1 (ed. by D.W. Hood and J.A. Calder), Gov't Printing Office, Washington, D.C., 15-22.

Overland, J.E., R.A. Brown, and C.D. Mobley (1980): METLIB - A Program Library for Calculating and Plotting Marine Boundary Layer Wind Fields. NOAA Technical Memorandum ERL PMEL-20, 82 pp.

Pearson, C.A. (1981): Guide to R2D2 - Rapid Retrieval Data Display. NOAA Technical Memorandum ERL PMEL-29, 147 pp.

Pearson, C.A., H.O. Mofjeld, and R.B. Tripp (1981): Tides of the eastern Bering Sea shelf. Chapter 8 in The Eastern Bering Sea Shelf: Oceanography and Resources, Vol. 1 (ed. by D.W. Hood and J.A. Calder), Gov't Printing office, Washington, D.C., 111-130.

World Meteorological Organization (1970): WMO Sea Ice Nomenclature. WMO No. 259, 147 pp. + 52 pp. in supplements.

APPENDICES

APPENDIX A

SURFACE WINDS CALCULATED FROM ALASKA REGION NWS SEA LEVEL PRESSURE ANALYSES

Ultimately we will need a data source for wind data other than direct on-ice measurement for ice advection modelling. One possible source is wind estimates calculated from surface pressure fields. To test the validity of this source we obtained copies of the Alaska Region NWS surface pressure analyses and hand digitized pressures onto a grid compatible with National Meteorological Center's (NMC) Primitive Equation (PE) grid (Overland, et al. 1980). We chose the Alaska Region NWS analysis because we felt that the analysis is based on more surface observations than the NMC analysis because of cut-off times for NMC products. A program library for calculating and plotting marine boundary layer wind fields called METLIB (Overland, et al. 1980) was used to calculate gradient winds which were rotated counterclockwise (cyclonically) 30° and reduced in speed by 20% to mimic surface wind conditions.

The following vector wind plots represent the approximate surface wind conditions for 00Z and 12Z from 14 February through 16 March 1980, including the experiment period. Point comparisons of these winds with observed winds are made in Section 2. The distance between grid points (tails of the vectors) in the enclosed plots is the vector length scale for 20 m s^{1} wind speeds. Wind speeds higher than this magnitude cannot be handled by the plotting package, resulting in occasional missing vectors with only a dot at the base. Zero wind speed has no dot. Note that the vector direction follows the oceanographic convention and that north is to the right in each plot.

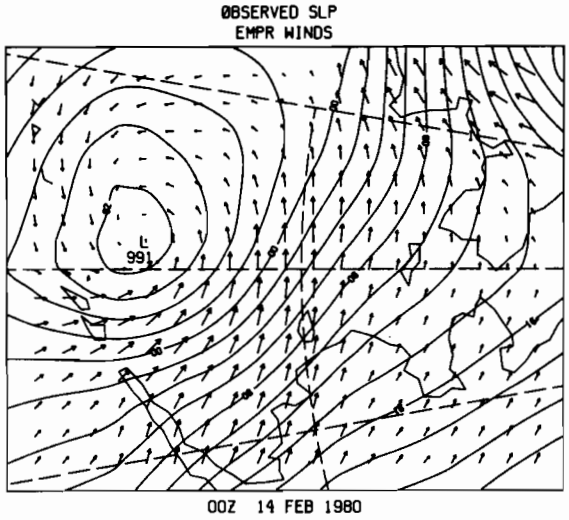

00Z 14 FEB 1980

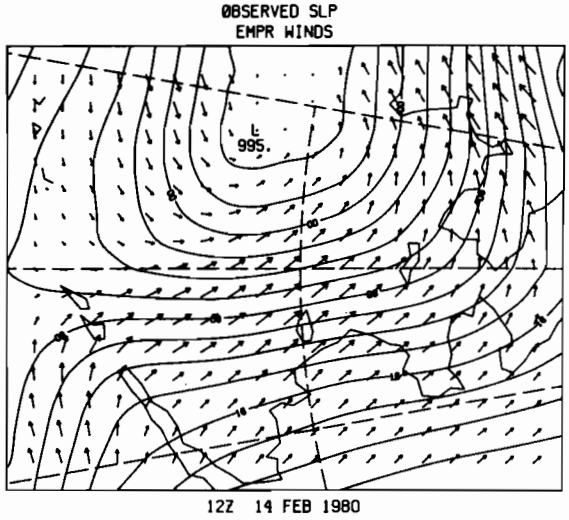

12Z 14 FEB 1980

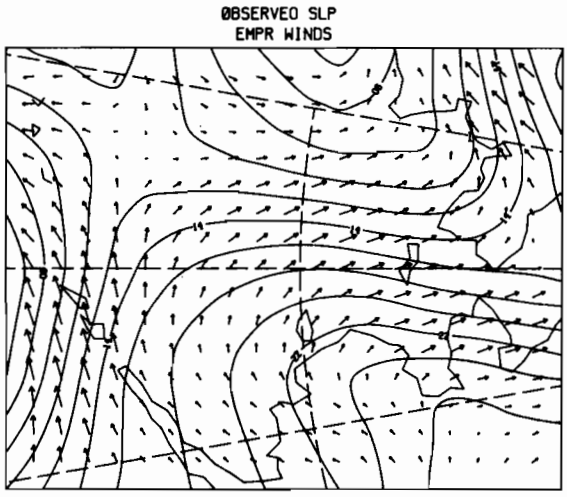

00Z 15 FEB 1980

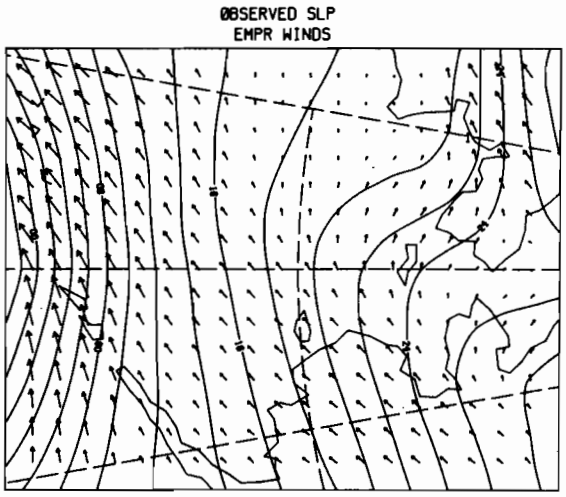

12Z 15 FEB 1980

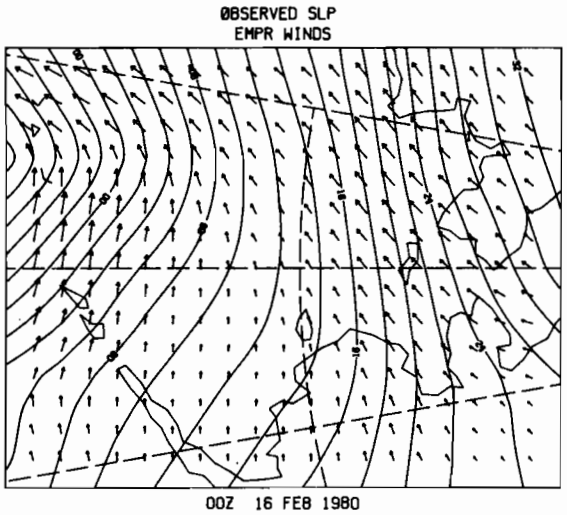

00Z 16 FEB 1980

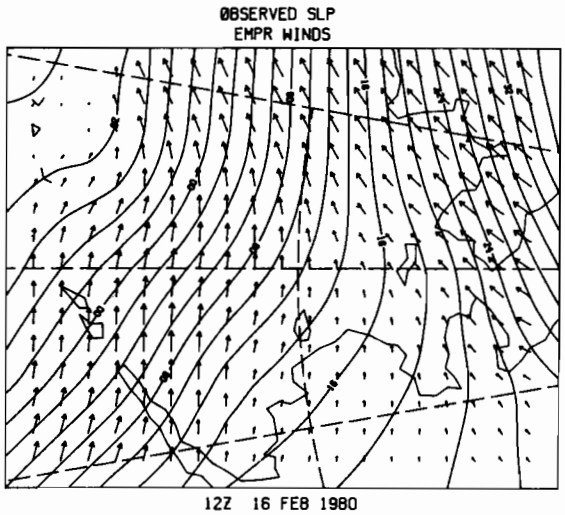

12Z 16 FEB 1980

ØBSERVED SLP
EMPR WINDS

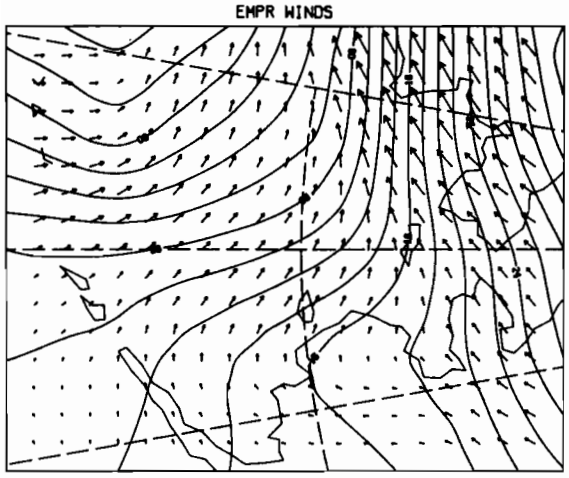

00Z 17 FEB 1980

ØBSERVED SLP
EMPR WINDS

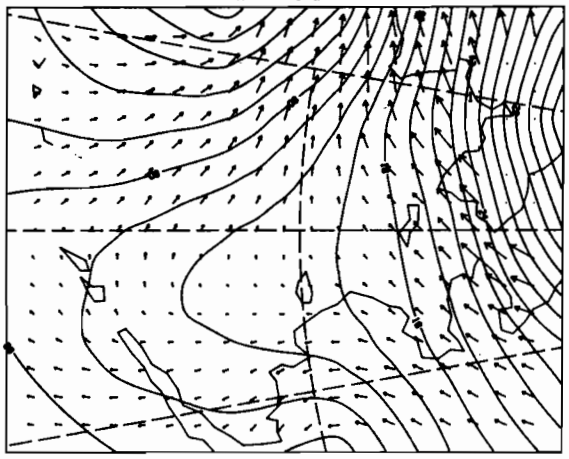

12Z 17 FEB 1980

ØBSERVED SLP
EMPR WINDS

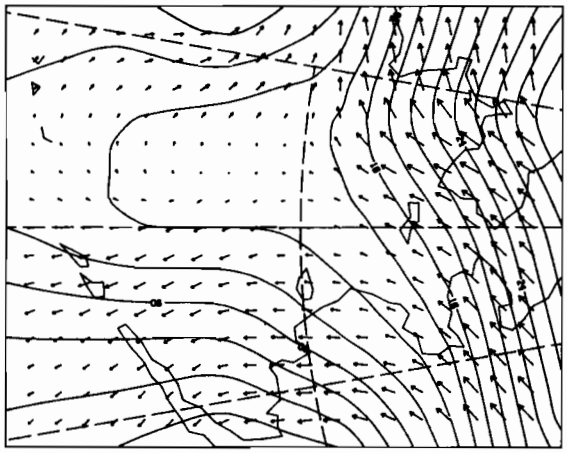

00Z 18 FEB 1980

ØBSERVED SLP
EMPR WINDS

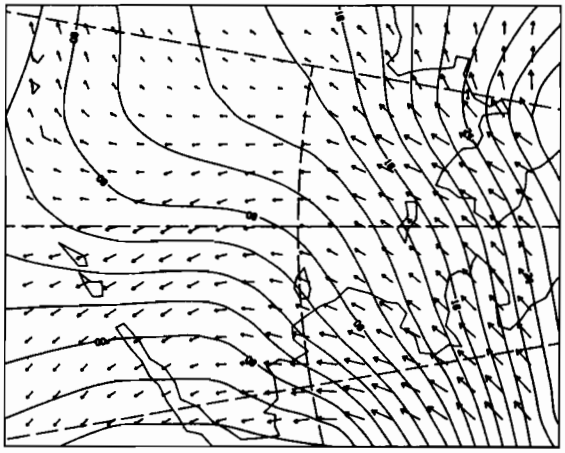

12Z 18 FEB 1980

ØBSERVED SLP
EMPR WINDS

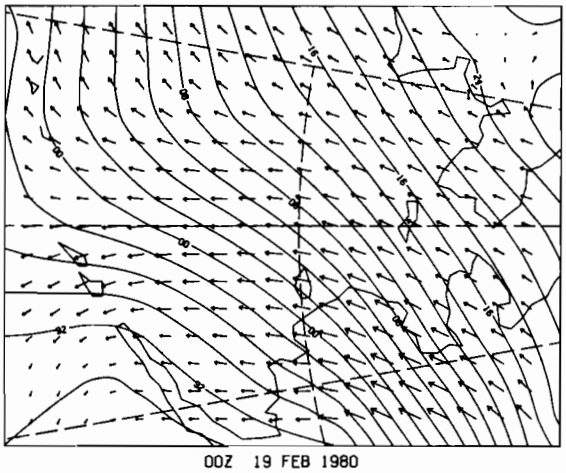

00Z 19 FEB 1980

ØBSERVED SLP
EMPR WINDS

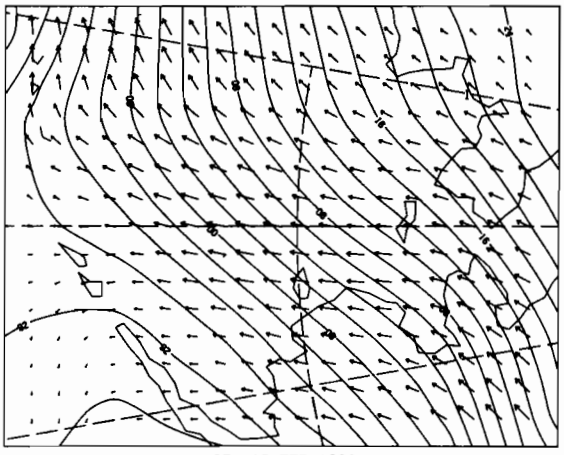

12Z 19 FEB 1980

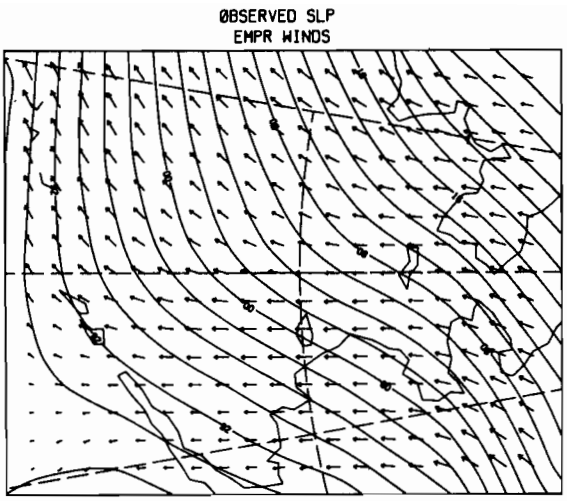

00Z 20 FEB 1980

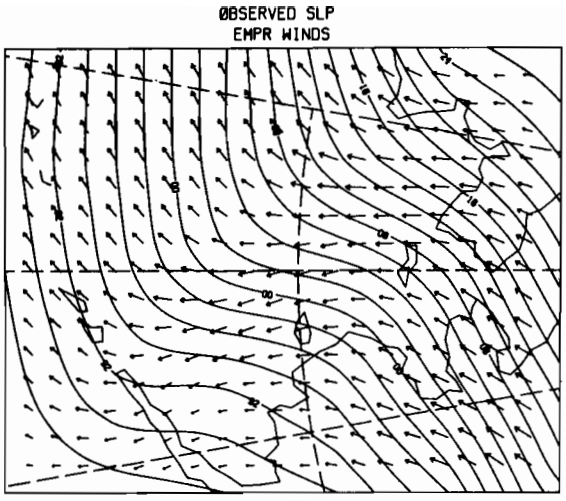

12Z 20 FEB 1980

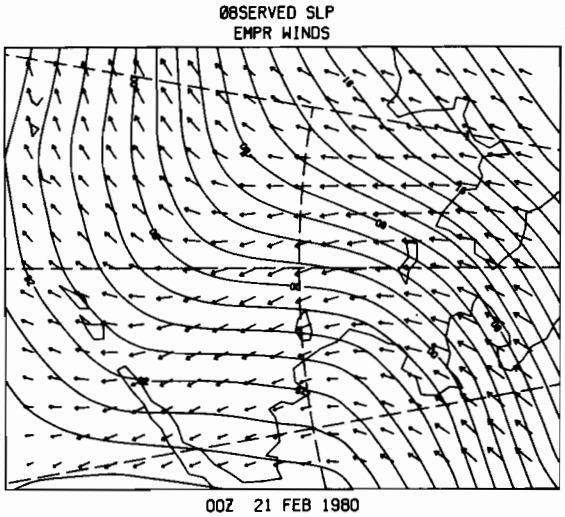

00Z 21 FEB 1980

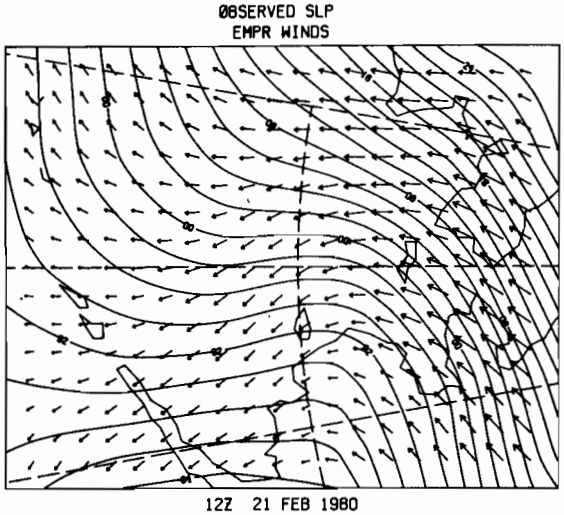

12Z 21 FEB 1980

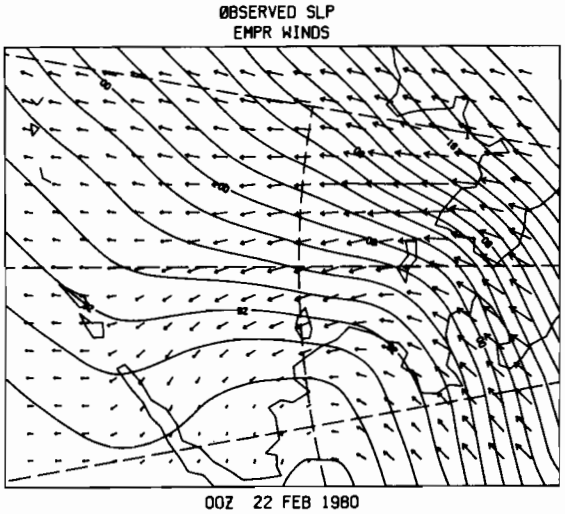

00Z 22 FEB 1980

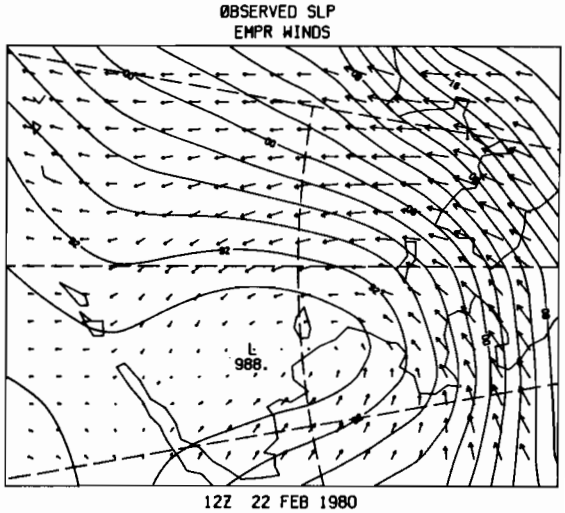

12Z 22 FEB 1980

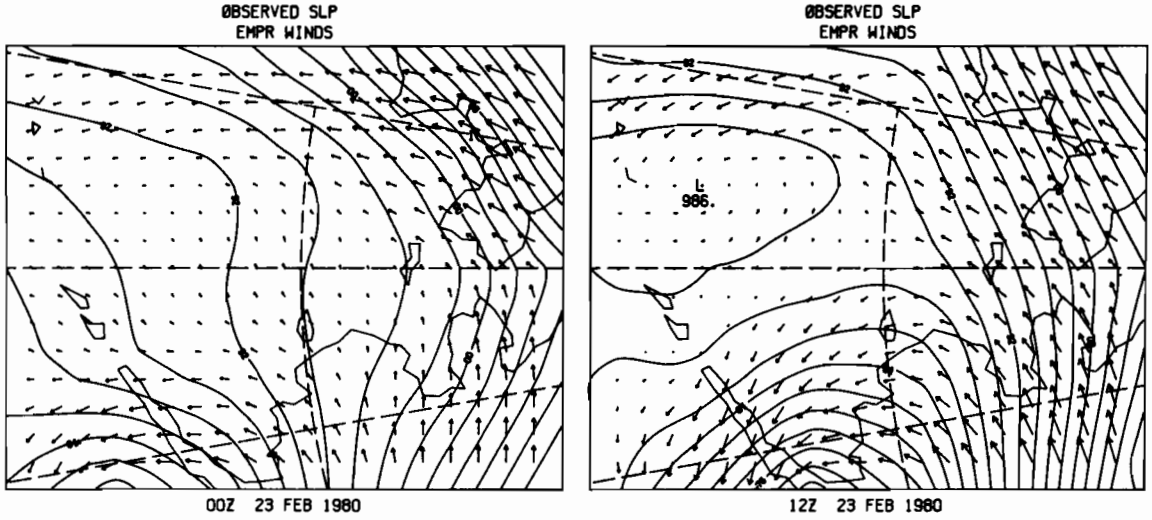

00Z 23 FEB 1980

12Z 23 FEB 1980

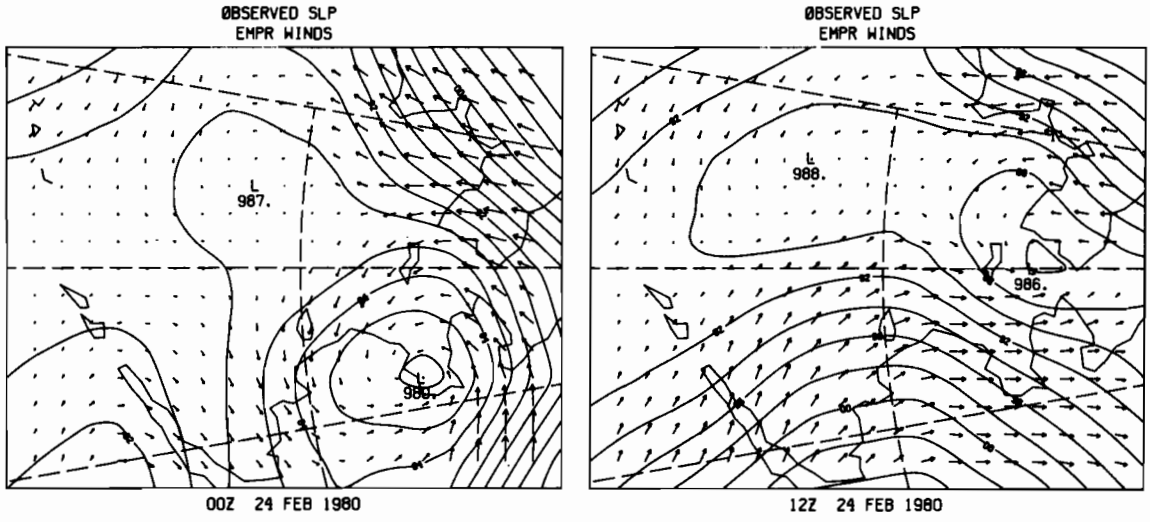

00Z 24 FEB 1980

12Z 24 FEB 1980

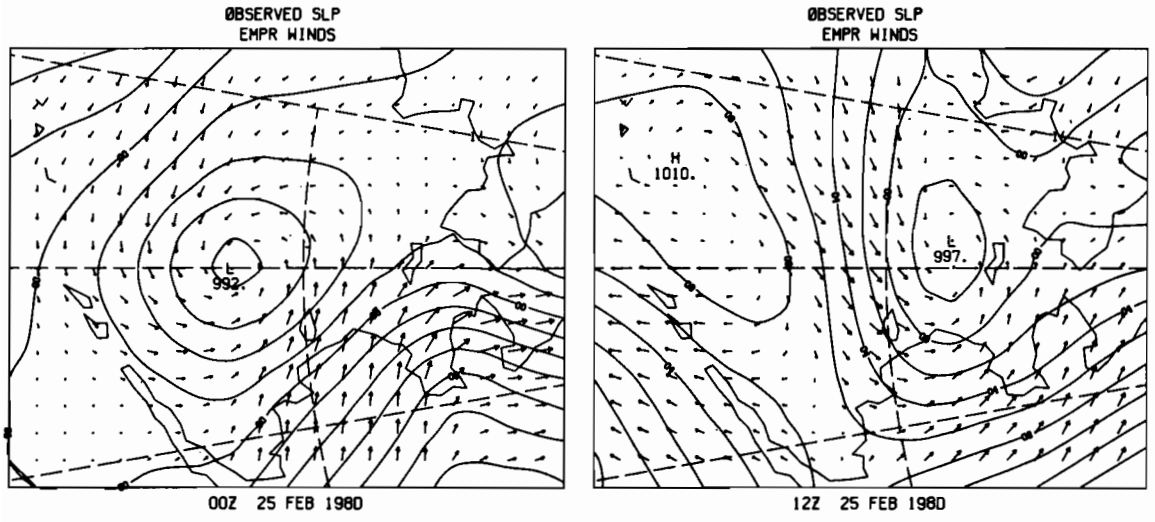

00Z 25 FEB 1980

12Z 25 FEB 1980

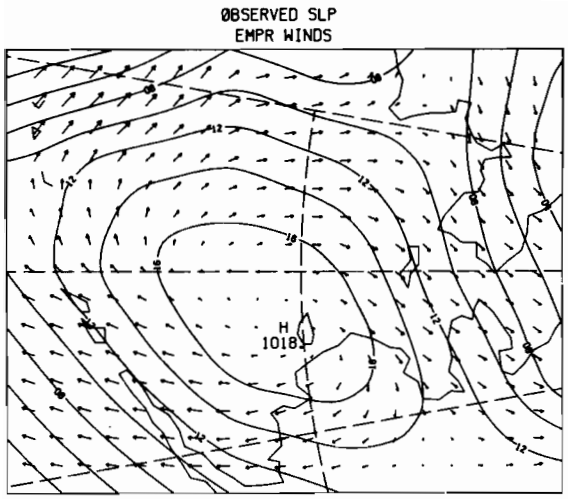

00Z 26 FEB 1980

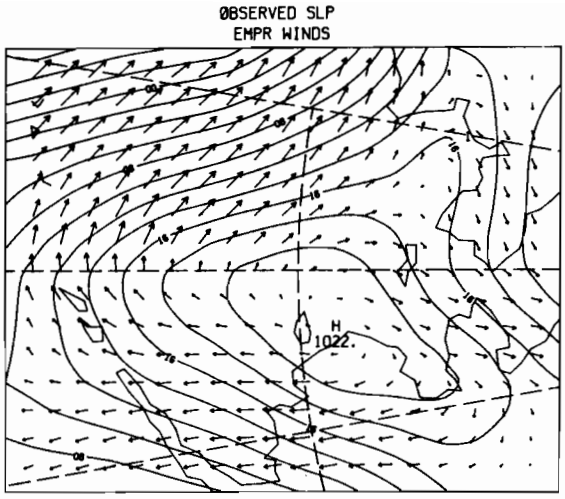

12Z 26 FEB 1980

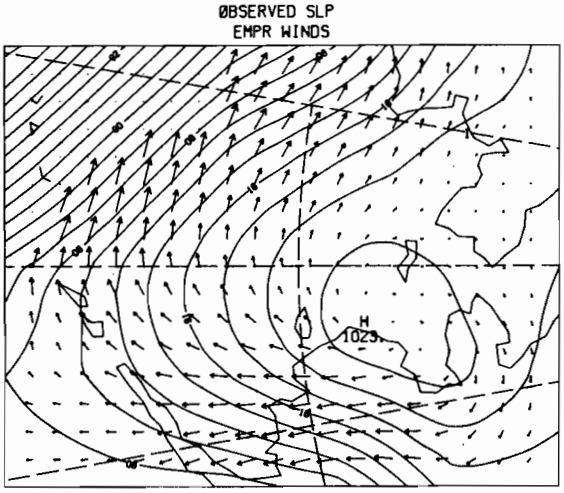

00Z 27 FEB 1980

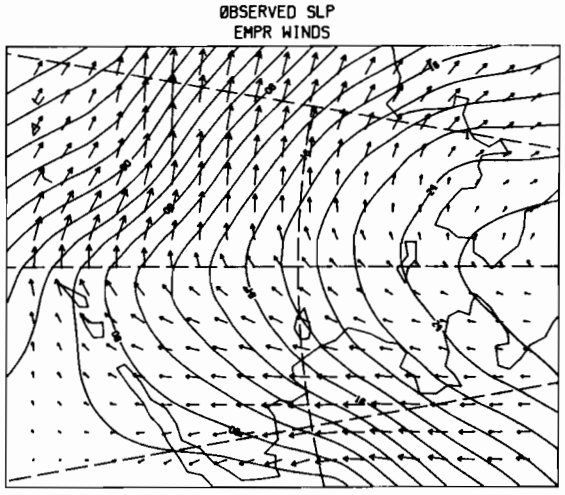

12Z 27 FEB 1980

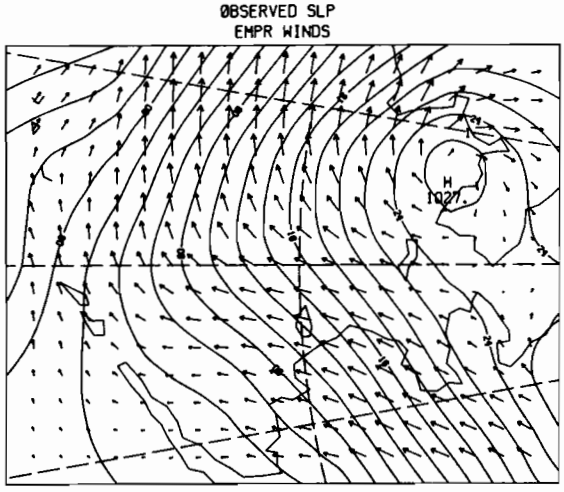

00Z 28 FEB 1980

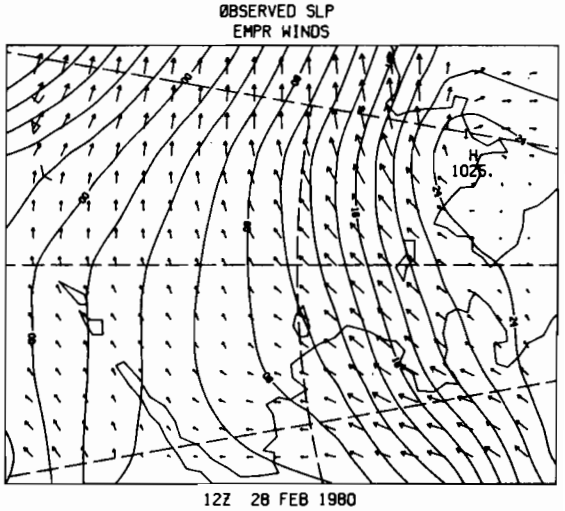

12Z 28 FEB 1980

ØBSERVED SLP
EMPR WINDS

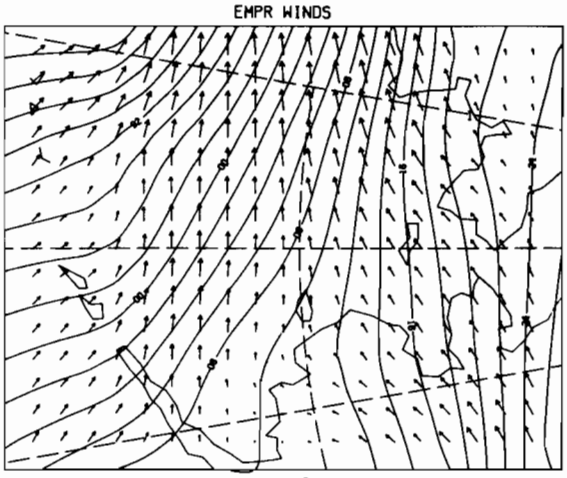

00Z 29 FEB 1980

ØBSERVED SLP
EMPR WINDS

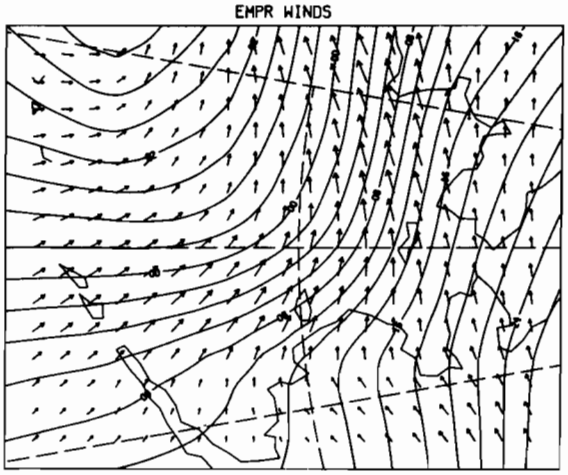

12Z 29 FEB 1980

ØBSERVED SLP
EMPR WINDS

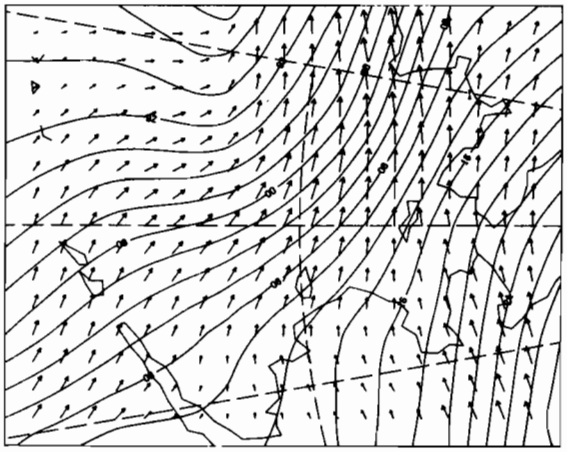

00Z 1 MAR 1980

ØBSERVED SLP
EMPR WINDS

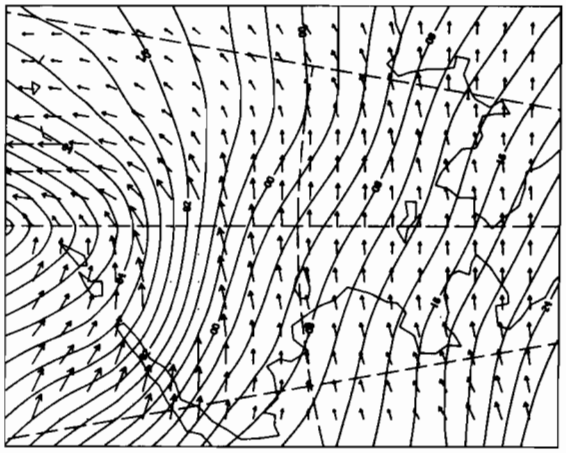

12Z 1 MAR 1980

ØBSERVED SLP
EMPR WINDS

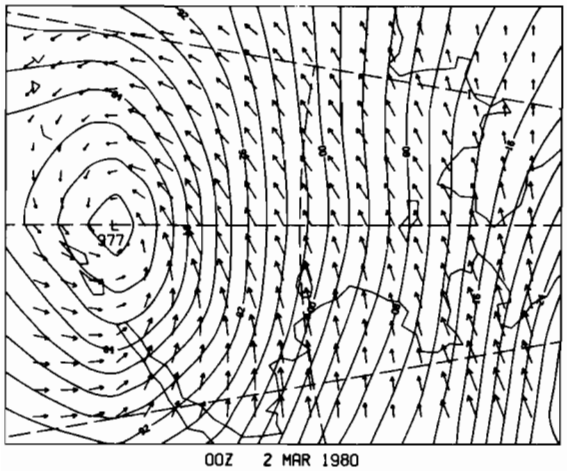

00Z 2 MAR 1980

ØBSERVED SLP
EMPR WINDS

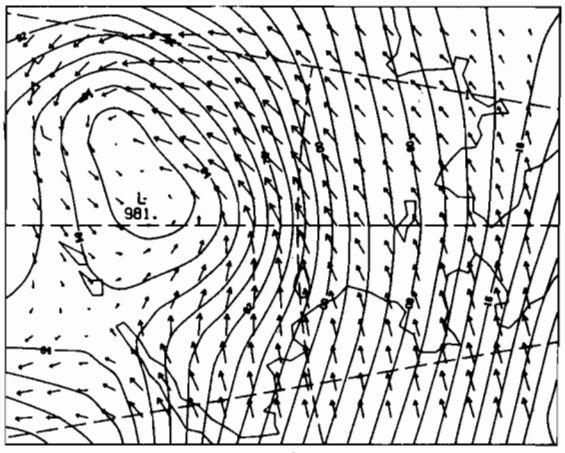

12Z 2 MAR 1980

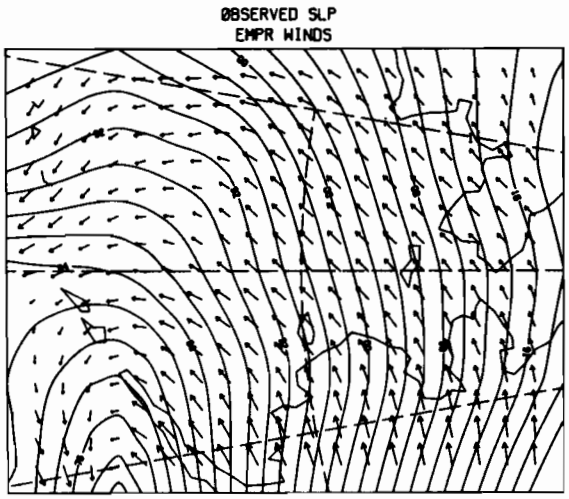

00Z 3 MAR 1980

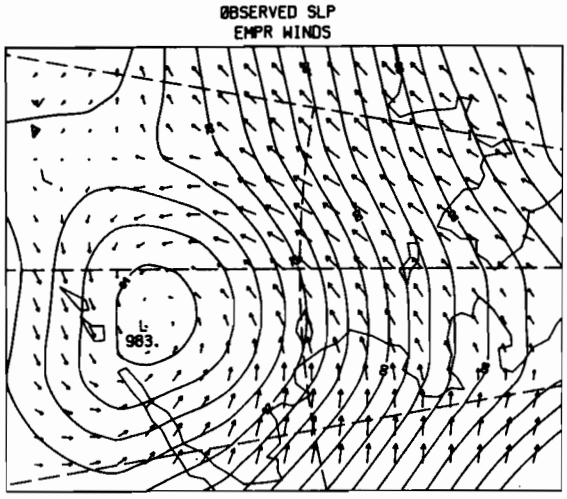

12Z 3 MAR 1980

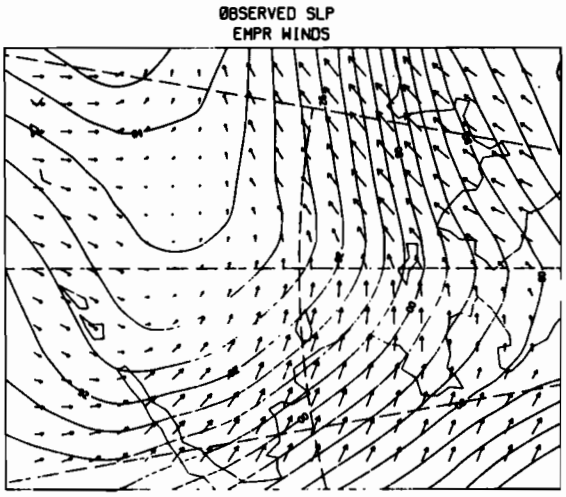

00Z 4 MAR 1980

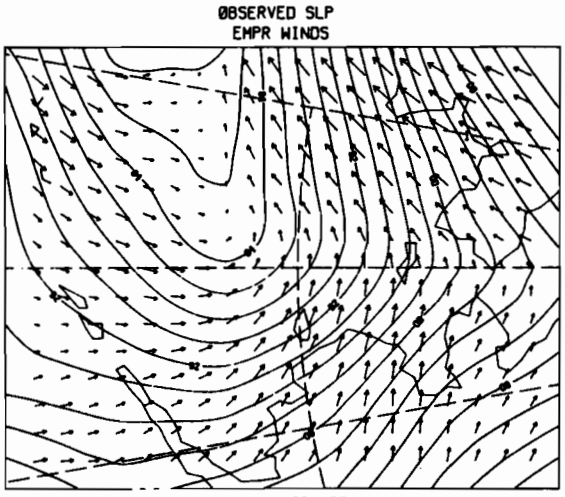

12Z 4 MAR 1980

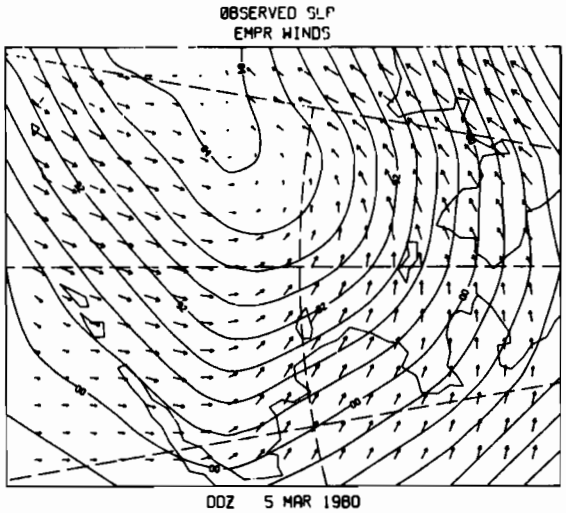

00Z 5 MAR 1980

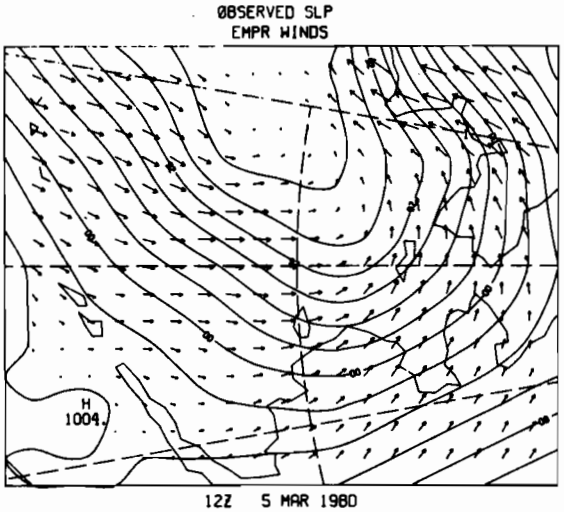

12Z 5 MAR 1980

ØBSERVED SLP
EMPR WINDS

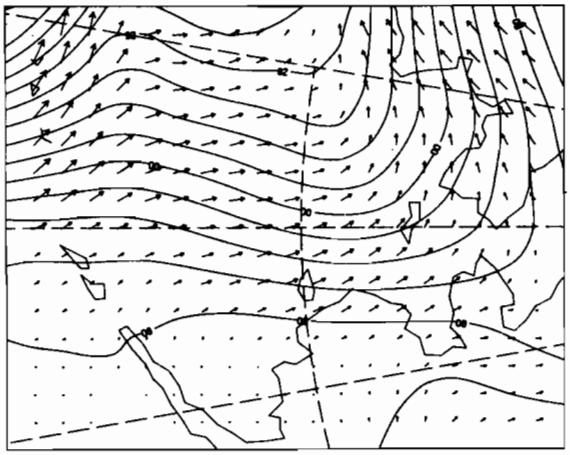

00Z 6 MAR 1980

ØBSERVED SLP
EMPR WINDS

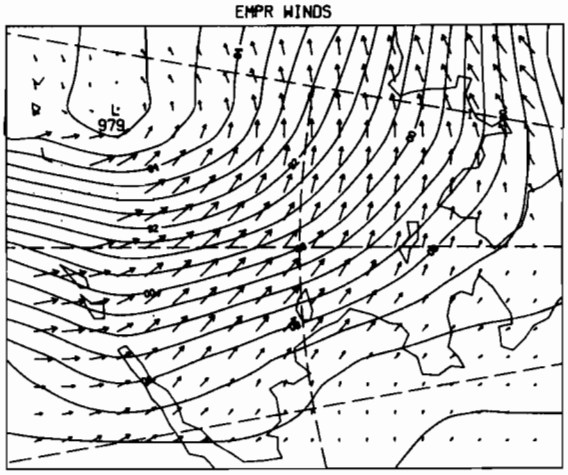

12Z 6 MAR 1980

ØBSERVED SLP
EMPR WINDS

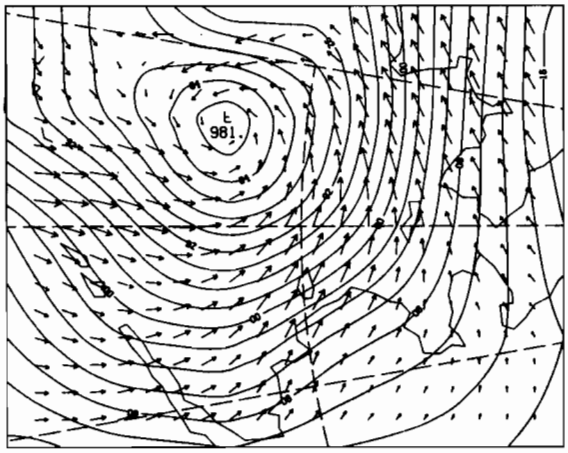

00Z 7 MAR 1980

ØBSERVED SLP
EMPR WINDS

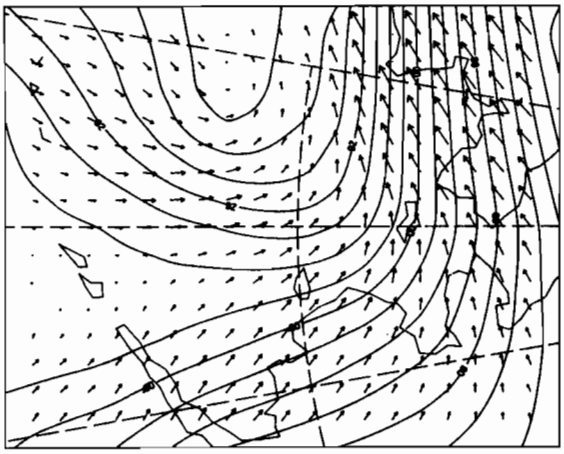

12Z 7 MAR 1980

ØBSERVED SLP
EMPR WINDS

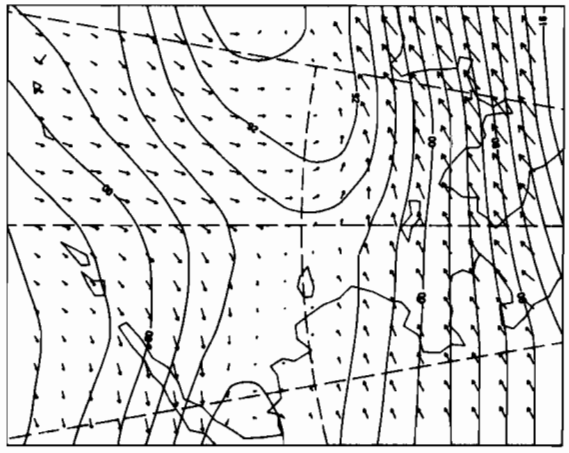

00Z 8 MAR 1980

ØBSERVED SLP
EMPR WINDS

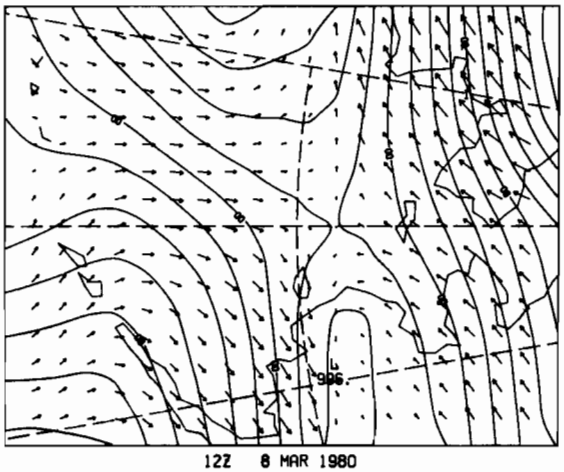

12Z 8 MAR 1980

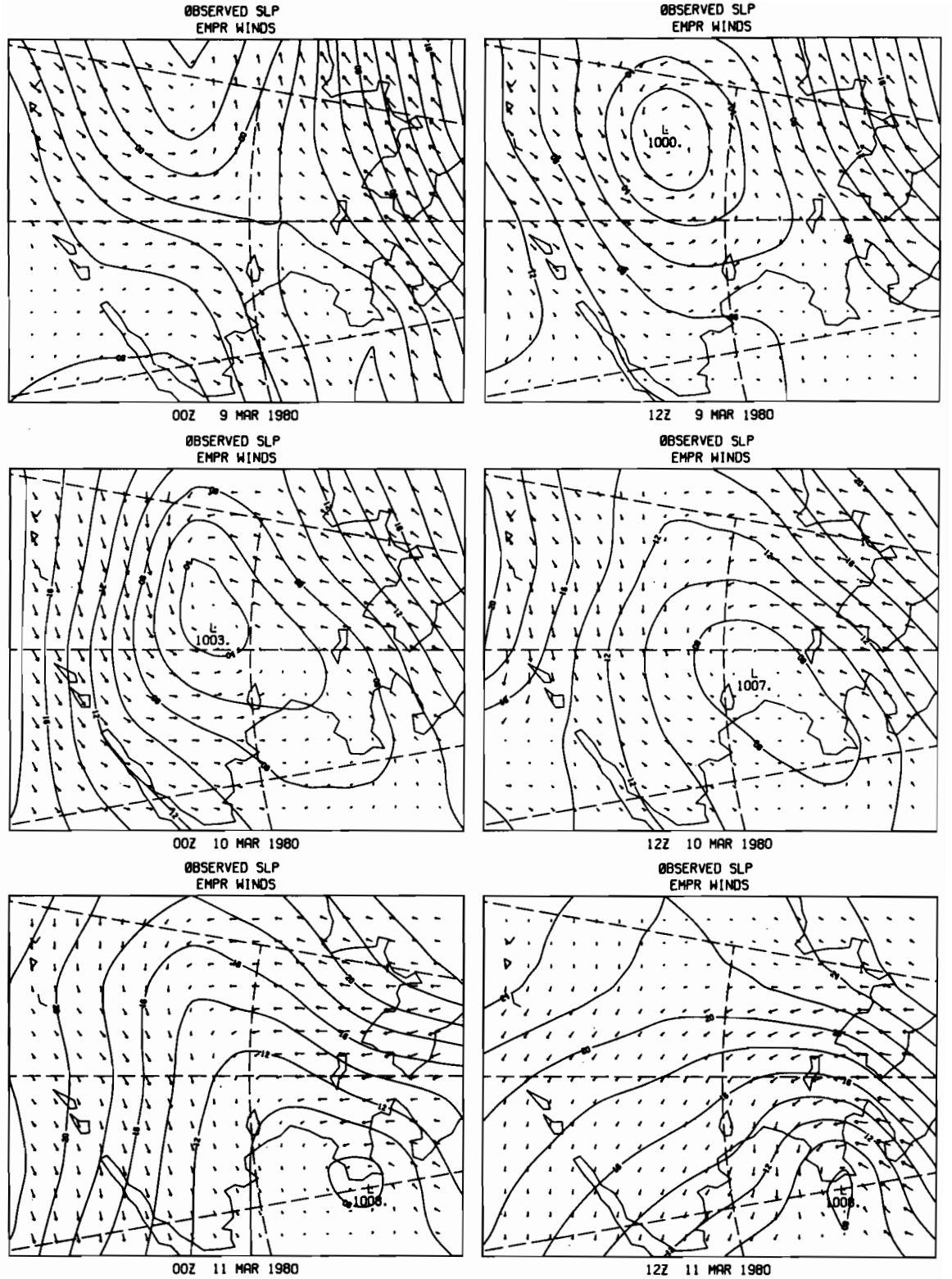
ØBSERVED SLP
EMPR WINDS
00Z 9 MAR 1980
ØBSERVED SLP
EMPR WINDS
1000.
12Z 9 MAR 1980
ØBSERVED SLP
EMPR WINDS
1003.
00Z 10 MAR 1980
ØBSERVED SLP
EMPR WINDS
1007.
12Z 10 MAR 1980
ØBSERVED SLP
EMPR WINDS
1008.
00Z 11 MAR 1980
ØBSERVED SLP
EMPR WINDS
1008.
12Z 11 MAR 1980

ØBSERVED SLP
EMPR WINDS

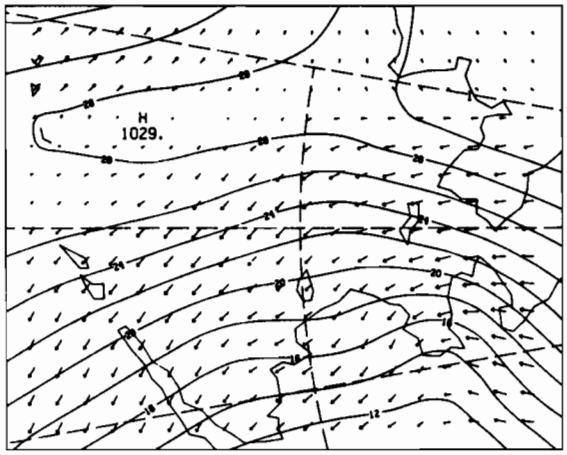

00Z 12 MAR 1980

ØBSERVED SLP
EMPR WINDS

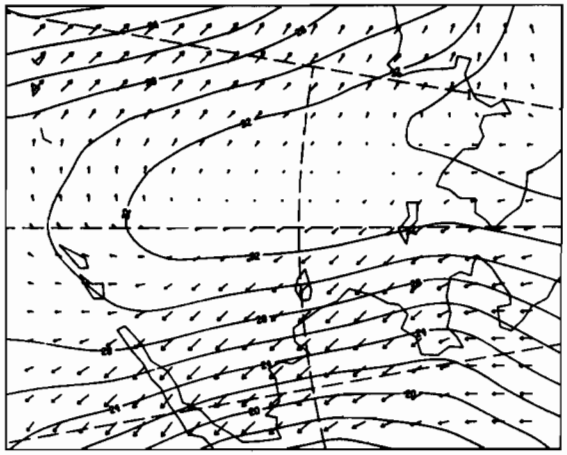

12Z 12 MAR 1980

ØBSERVED SLP
EMPR WINDS

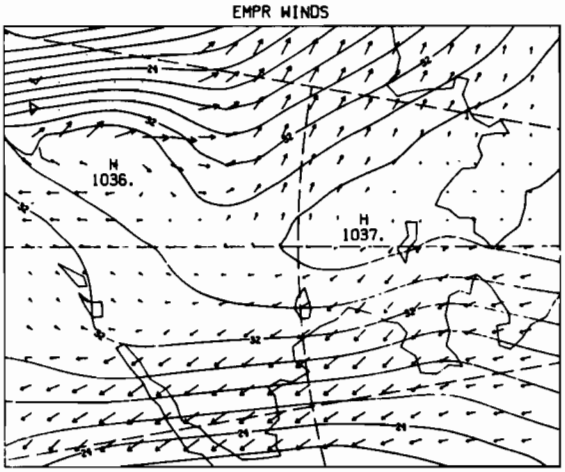

00Z 13 MAR 1980

ØBSERVED SLP
EMPR WINDS

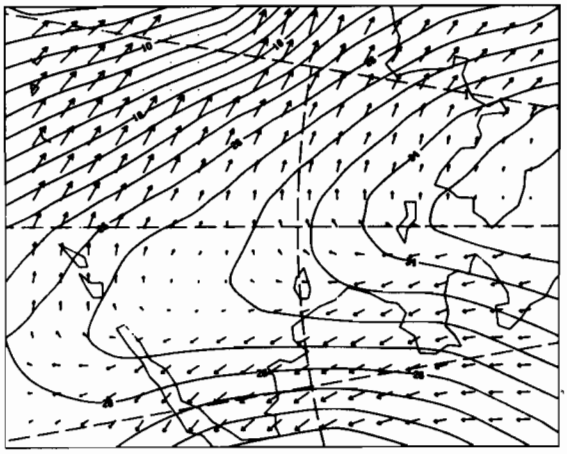

12Z 13 MAR 1980

ØBSERVED SLP
EMPR WINDS

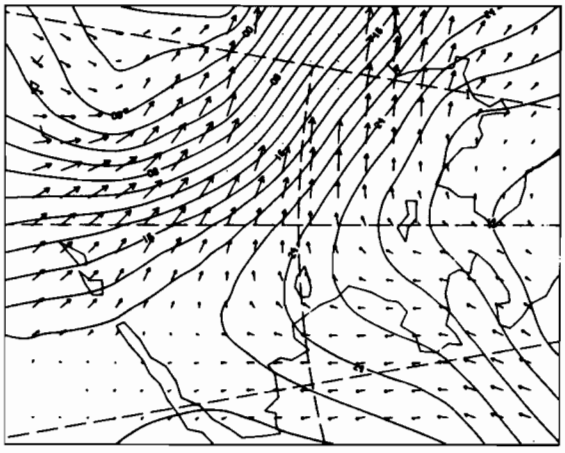

00Z 14 MAR 1980

ØBSERVED SLP
EMPR WINDS

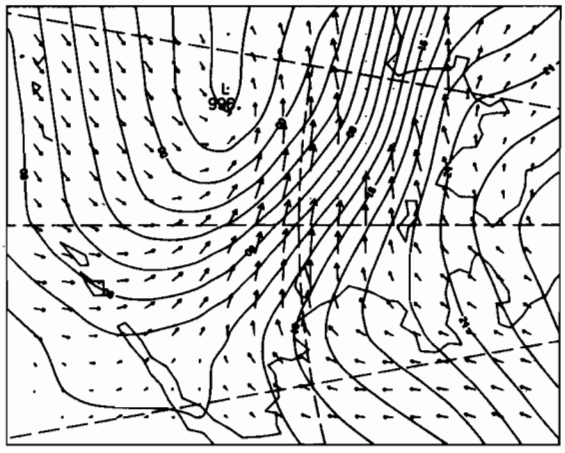

12Z 14 MAR 1980

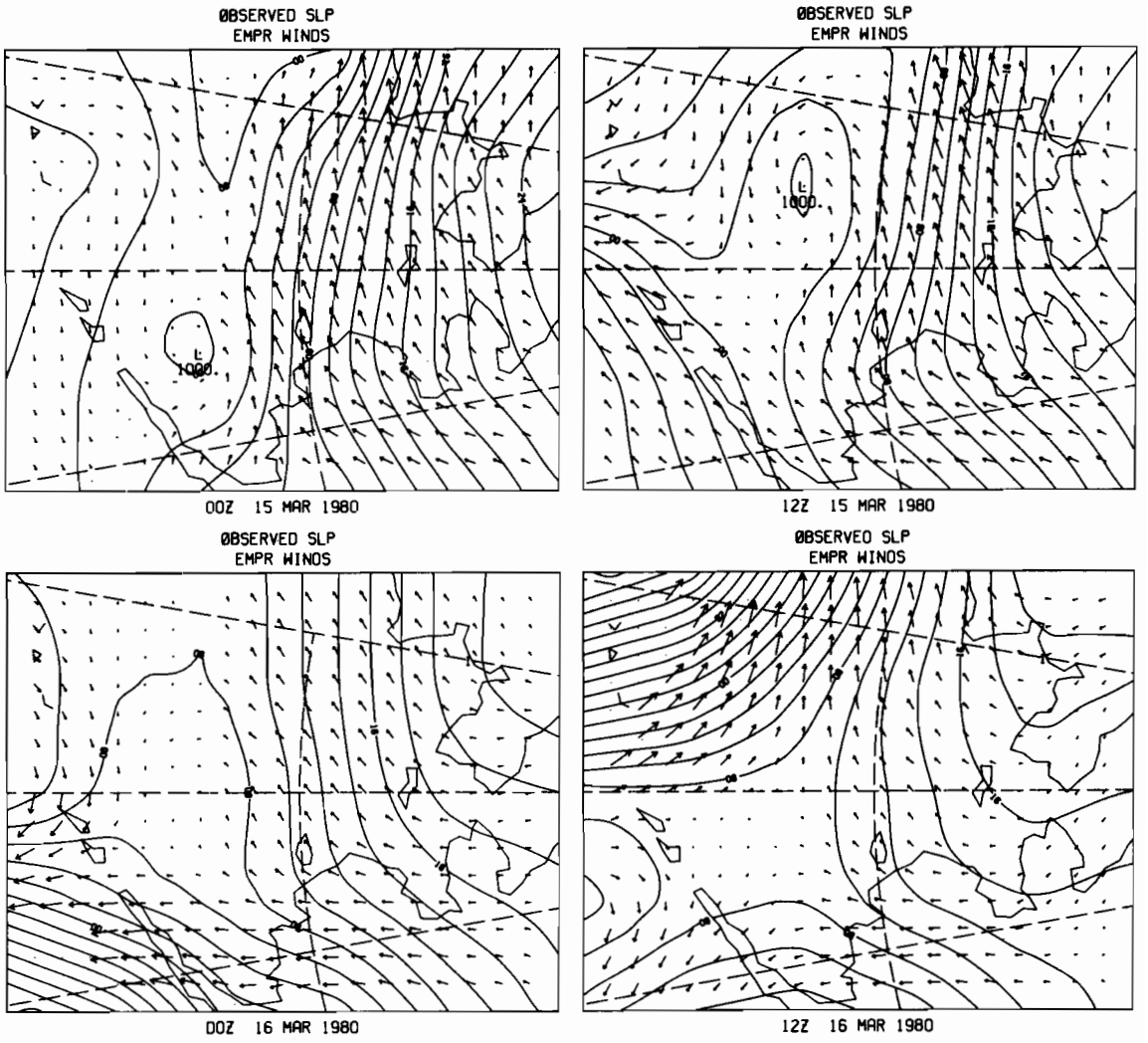
OBSERVED SLP
EMPR WINDS
1000.
00Z 15 MAR 1980
OBSERVED SLP
EMPR WINDS
1000.
12Z 15 MAR 1980
OBSERVED SLP
EMPR WINDS
00Z 16 MAR 1980
OBSERVED SLP
EMPR WINDS
12Z 16 MAR 1980

APPENDIX B

SURFACE ISOTHERMS ANALYZED FROM ALASKA REGION NWS SURFACE AIR TEMPERATURE OBSERVATIONS

As with the wind fields described in Appendix A, an additional source for air temperature data other than direct on-ice measurements is needed for sea ice modelling. One possible source is temperature estimates analyzed from surface air temperature reports. To test the validity of this source we hand analyzed and digitized surface air temperatures from the Alaska Region NWS charts onto the same grid as described for the pressure plots. Similarly METLIB was used to contour and plot the scalar temperature fields for 00 GMT and 12 GMT from 14 February through 16 March 1980. The temperatures are expressed in degrees Kelvin. Note that the freezing point of freshwater is about 273°K and of very salty water is about 271°K. Again north is to the right in each plot.

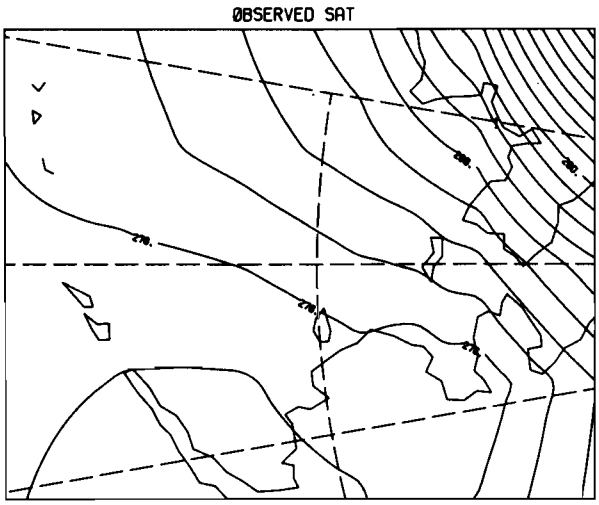

00Z 14 FEB 1980

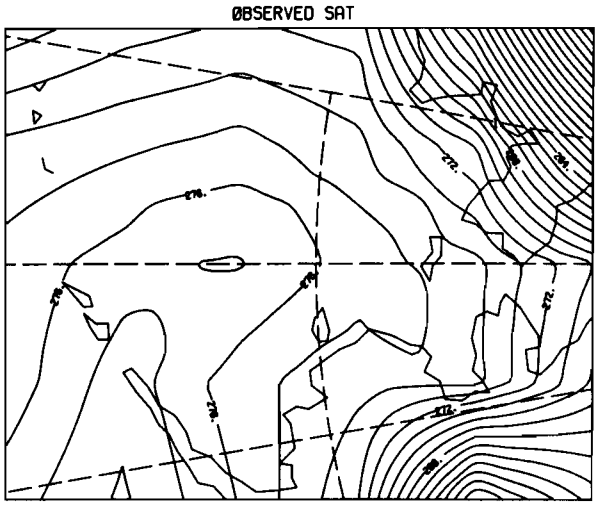

12Z 14 FEB 1980

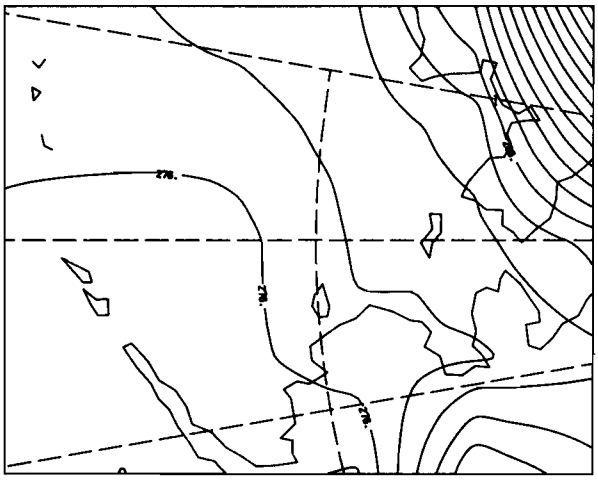

00Z 15 FEB 1980

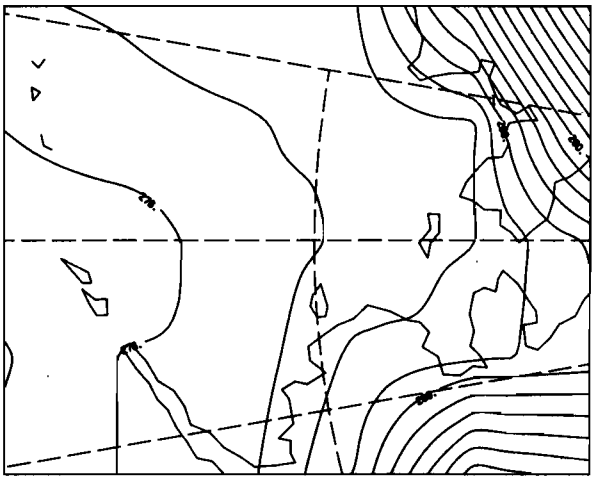

12Z 15 FEB 1980

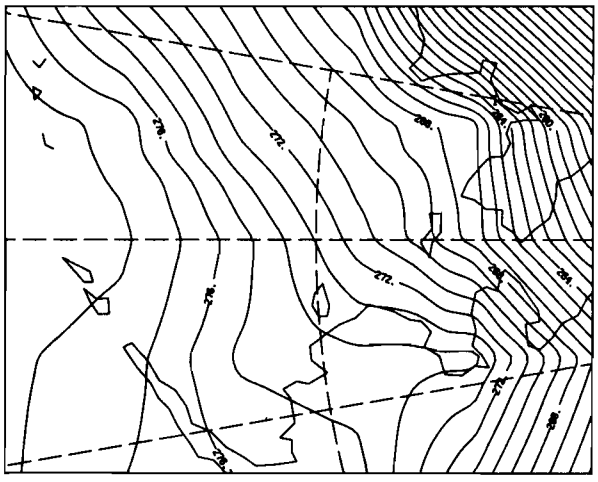

00Z 16 FEB 1980

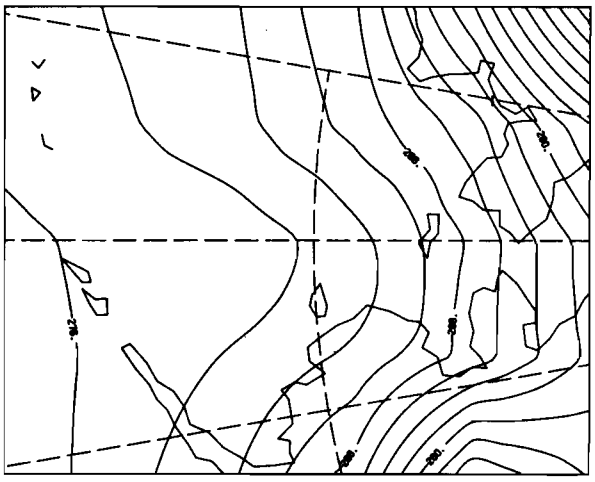

12Z 16 FEB 1980

ØBSERVED SAT

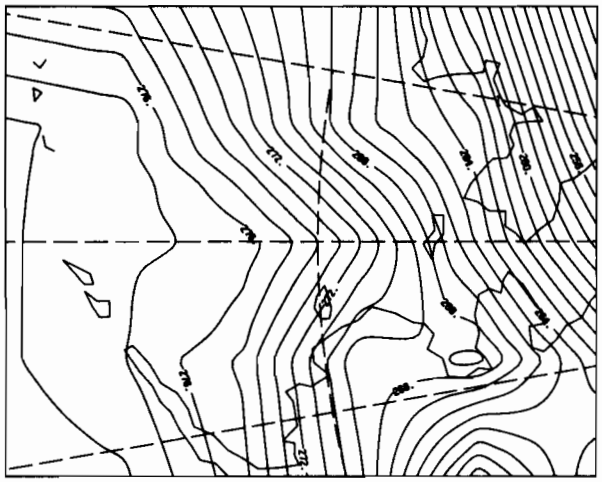

00Z 17 FEB 1980

ØBSERVED SAT

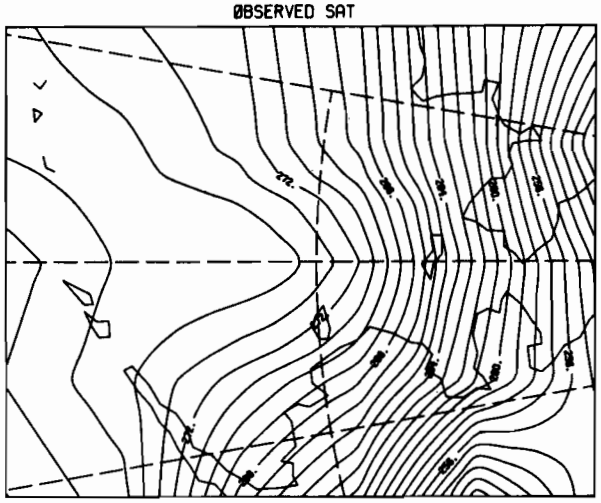

12Z 17 FEB 1980

ØBSERVED SAT

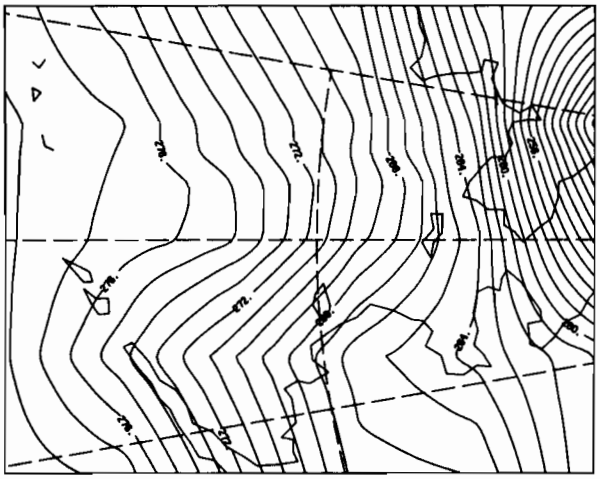

00Z 18 FEB 1980

ØBSERVED SAT

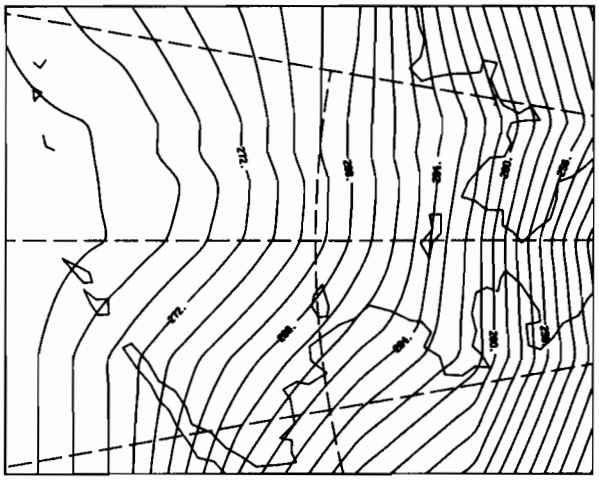

12Z 18 FEB 1980

ØBSERVED SAT

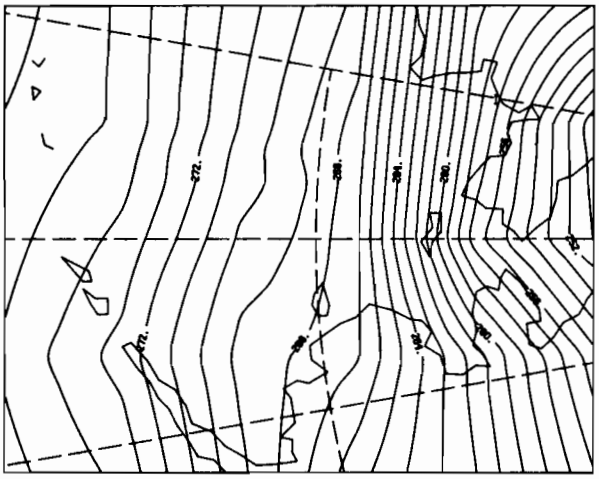

00Z 19 FEB 1980

ØBSERVED SAT

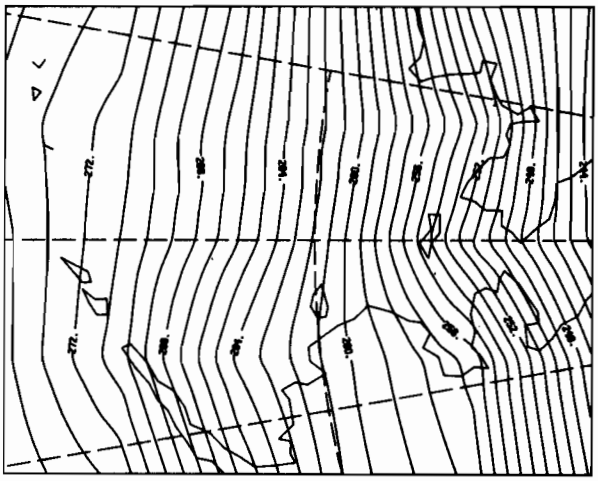

12Z 19 FEB 1980

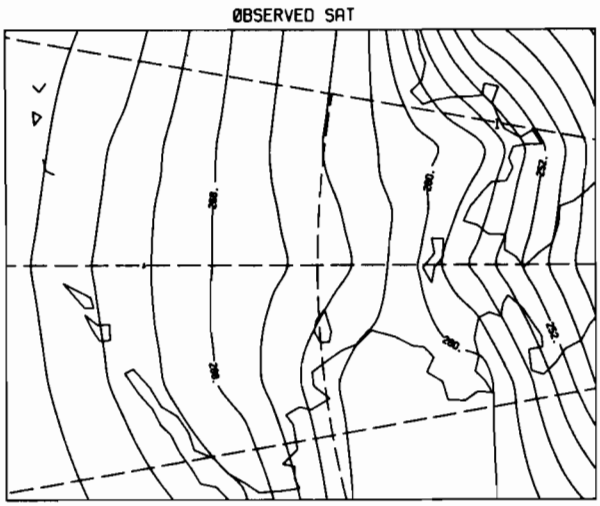

00Z 20 FEB 1980

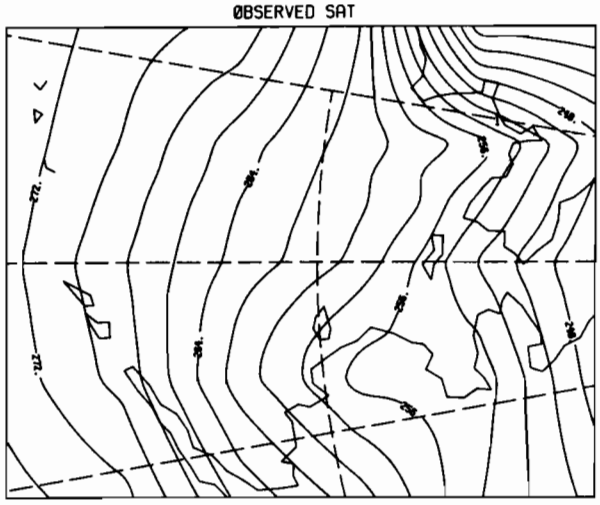

12Z 20 FEB 1980

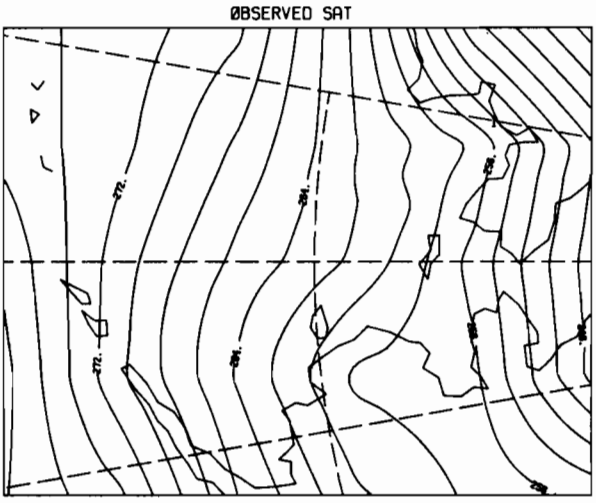

00Z 21 FEB 1980

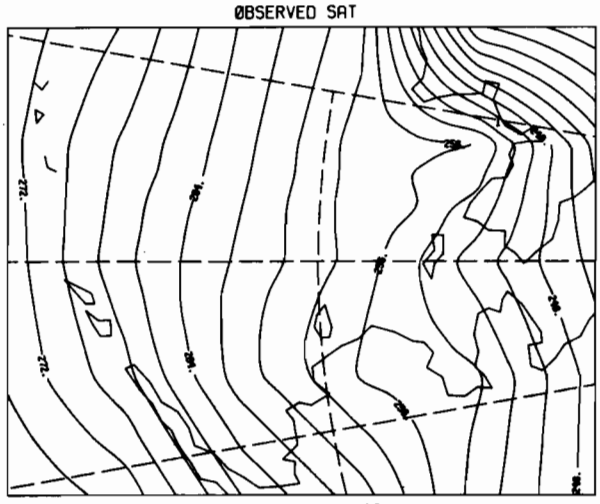

12Z 21 FEB 1980

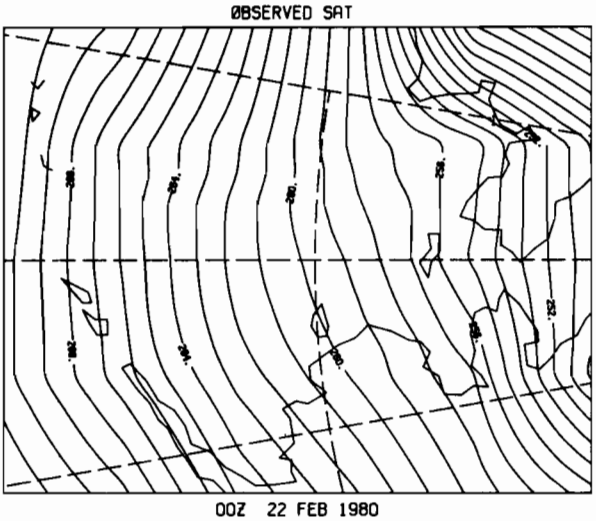

00Z 22 FEB 1980

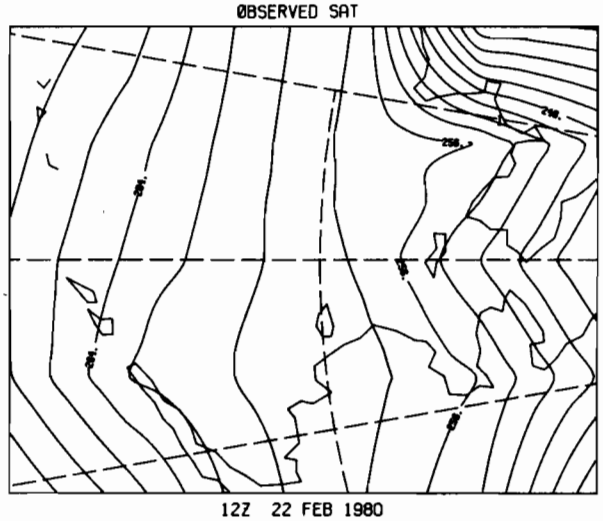

12Z 22 FEB 1980

ØBSERVED SAT

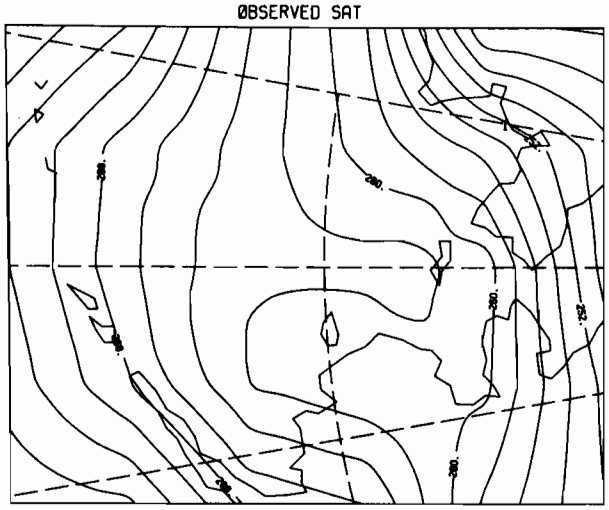

00Z 23 FEB 1980

ØBSERVED SAT

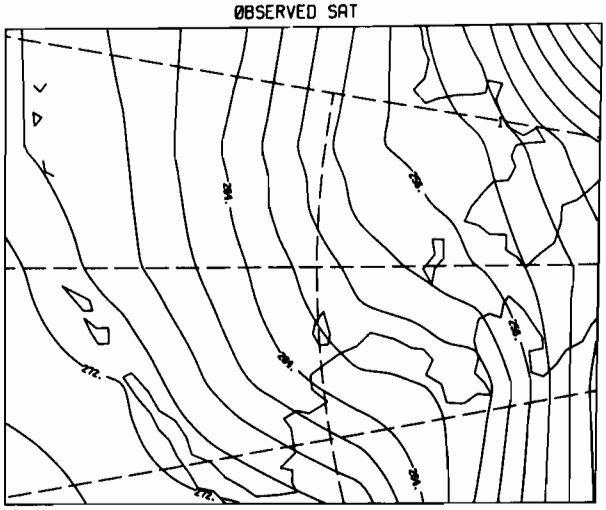

12Z 23 FEB 1980

ØBSERVED SAT

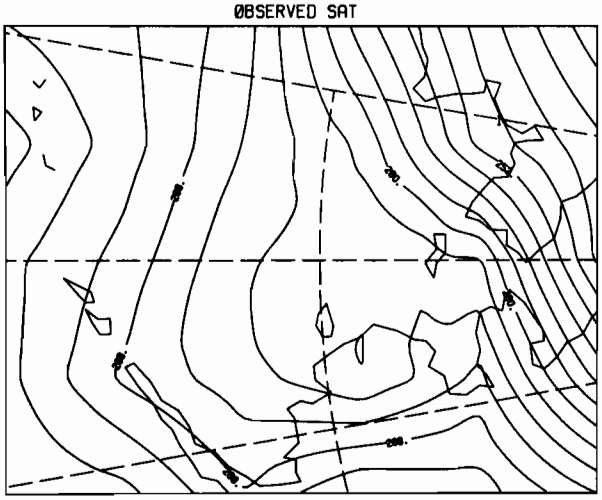

00Z 24 FEB 1980

ØBSERVED SAT

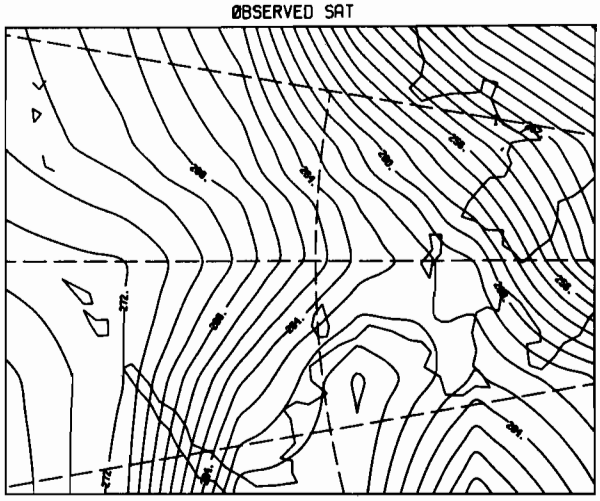

12Z 24 FEB 1980

ØBSERVED SAT

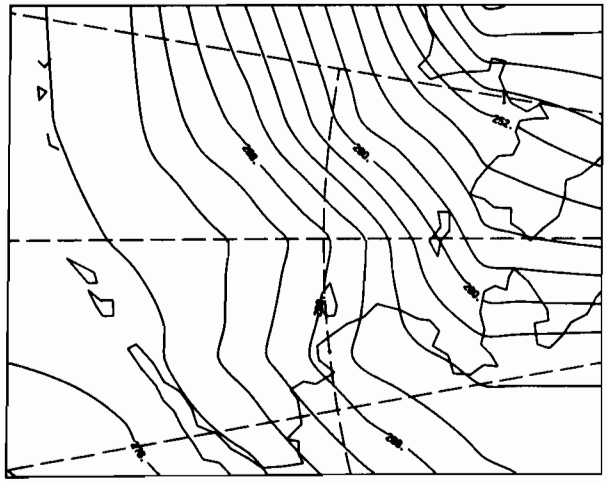

00Z 25 FEB 1980

ØBSERVED SAT

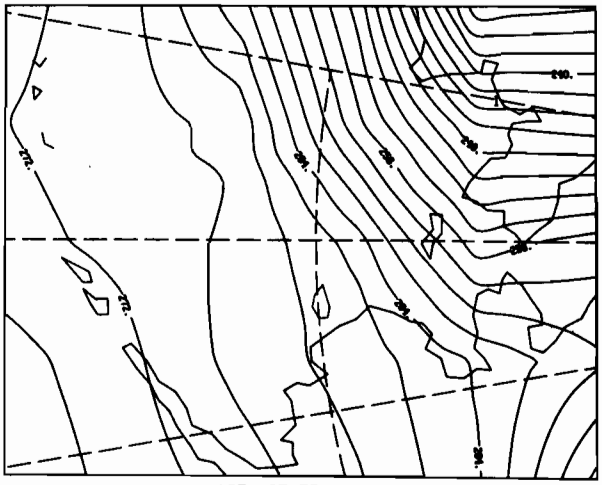

12Z 25 FEB 1980

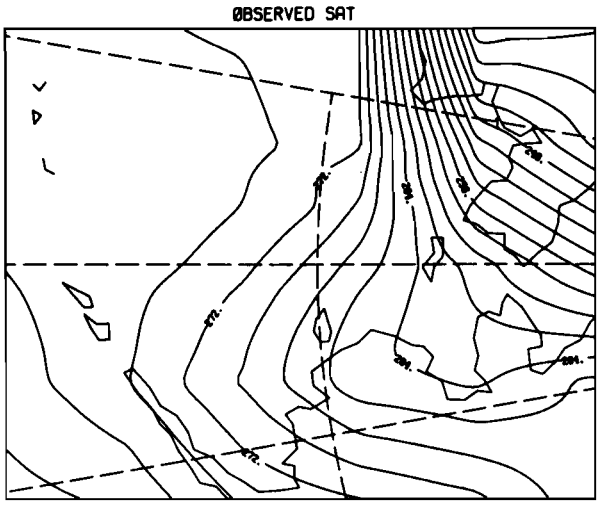

00Z 26 FEB 1980

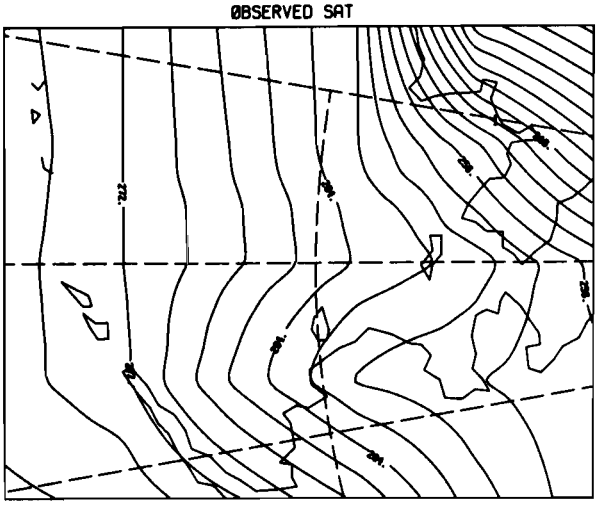

12Z 26 FEB 1980

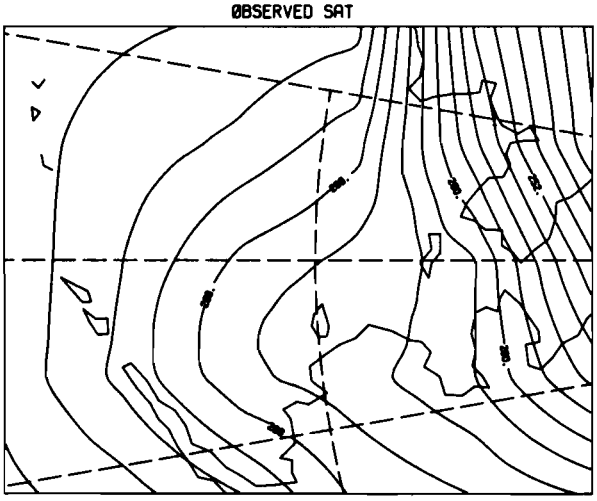

00Z 27 FEB 19 8

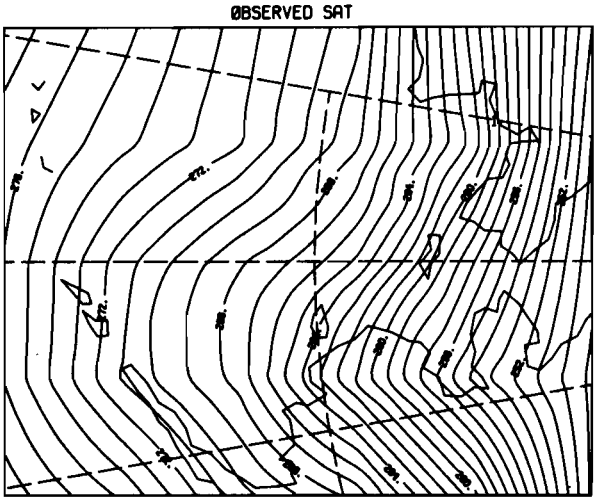

12Z 27 FEB 1980

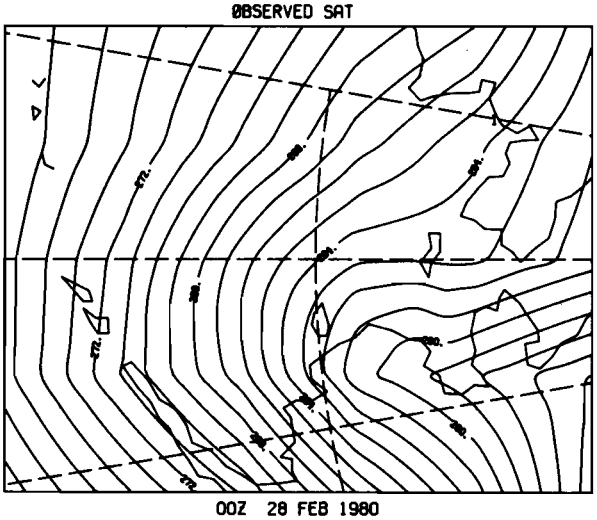

00Z 28 FEB 1980

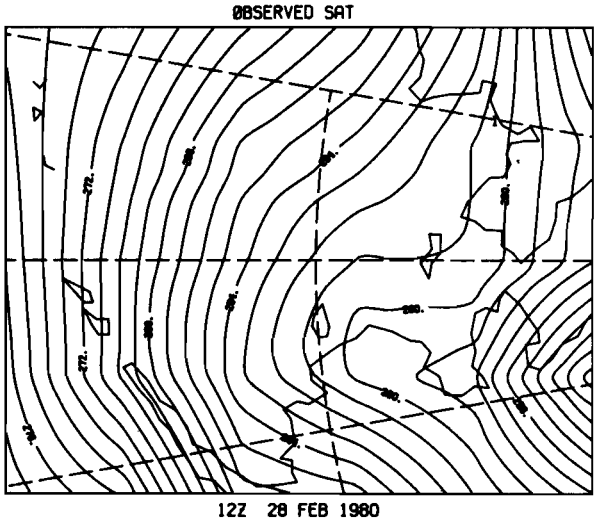

12Z 28 FEB 1980

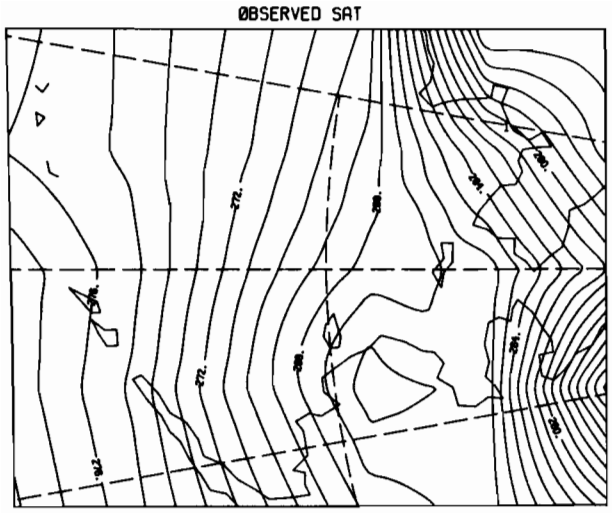

00Z 29 FEB 1980

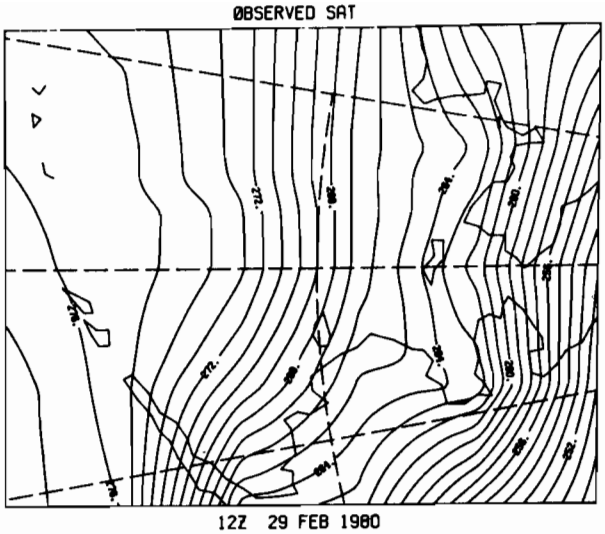

12Z 29 FEB 1980

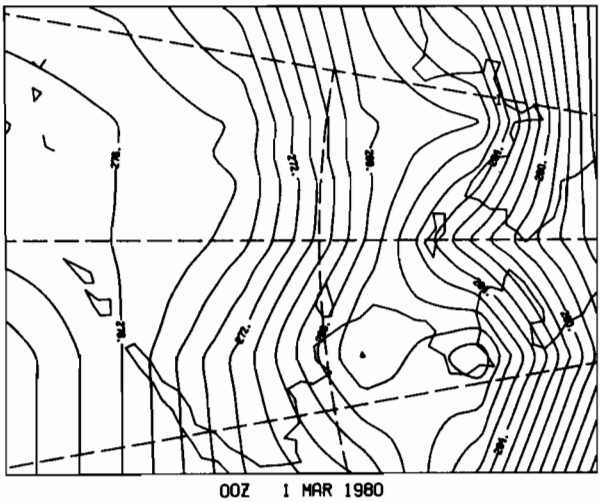

00Z 1 MAR 1980

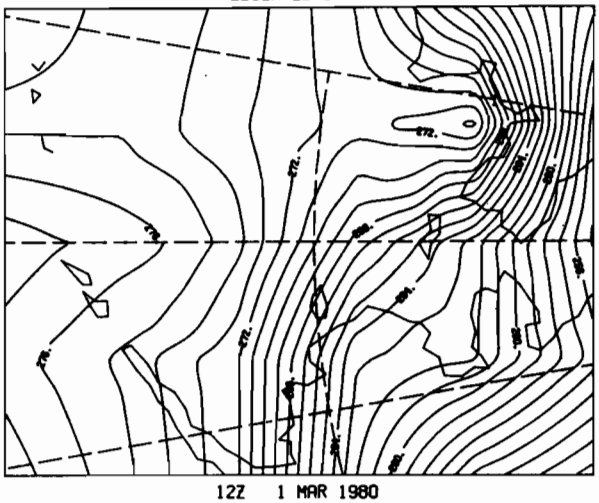

12Z 1 MAR 1980

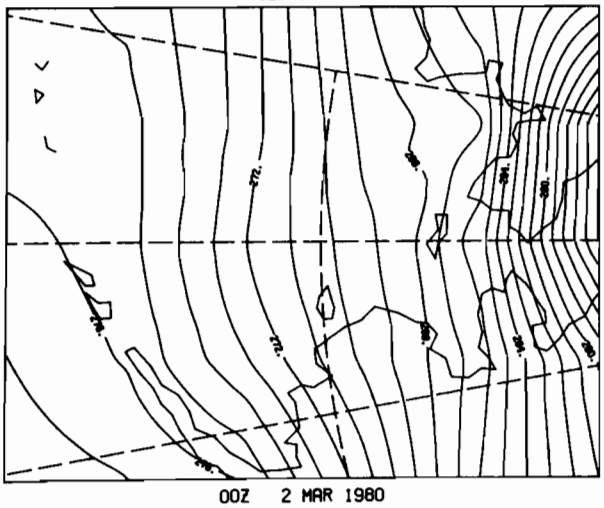

00Z 2 MAR 1980

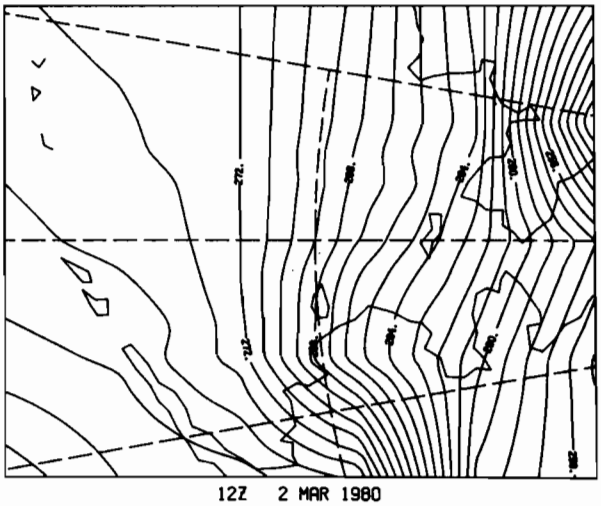

12Z 2 MAR 1980

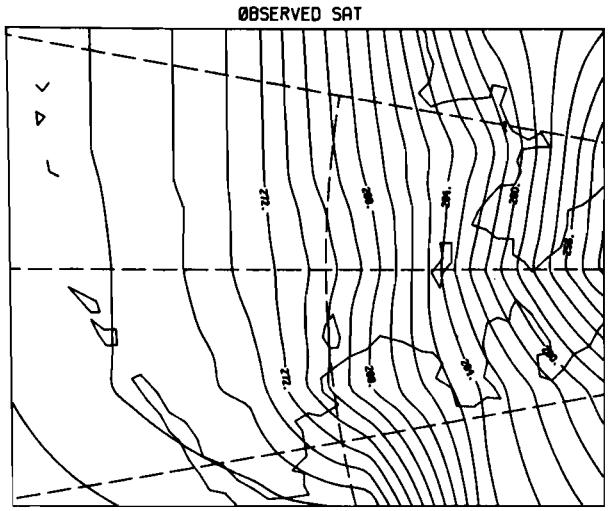

00Z 3 MAR 1980

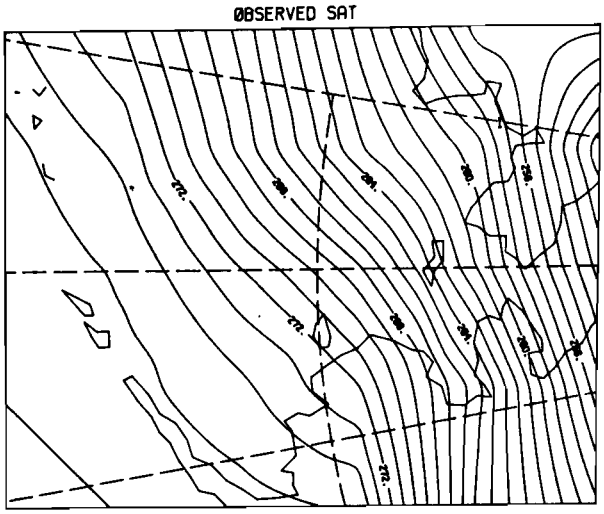

12Z 3 MAR 1980

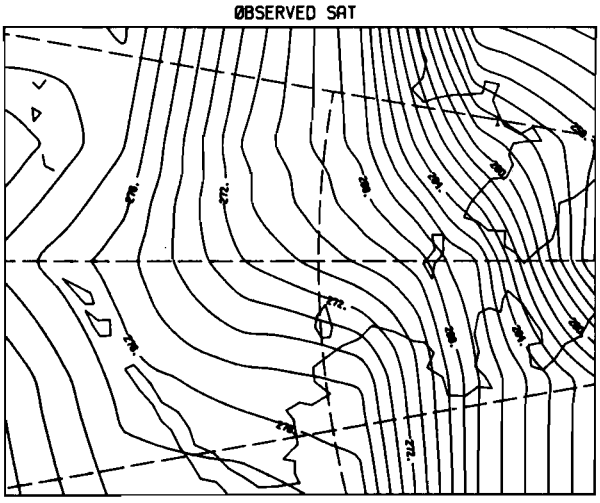

00Z 4 MAR 1980

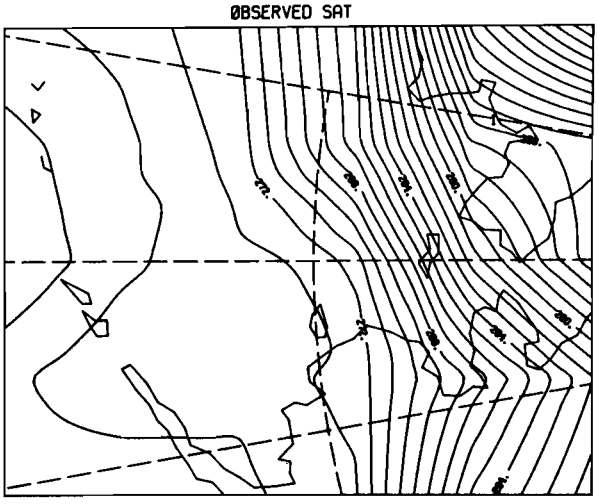

12Z 4 MAR 1980

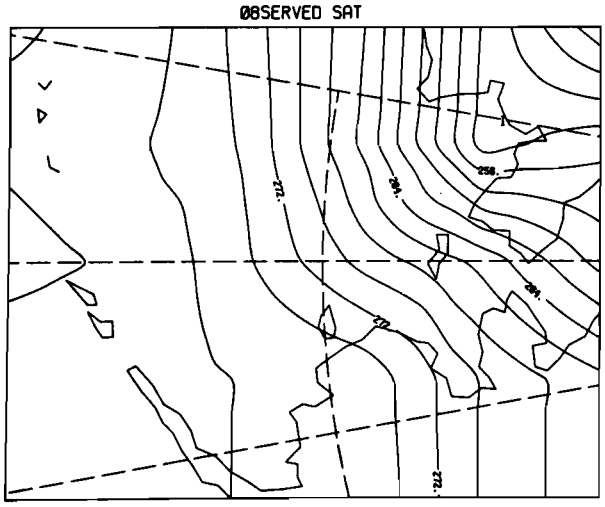

00Z 5 MAR 1980

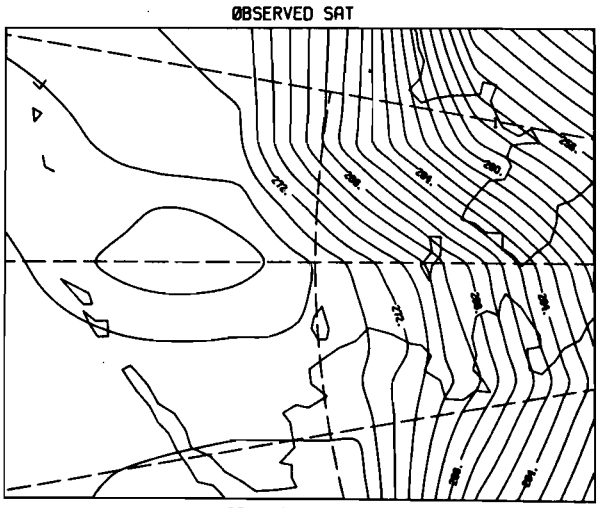

12Z 5 MAR 1980

ØBSERVED SAT

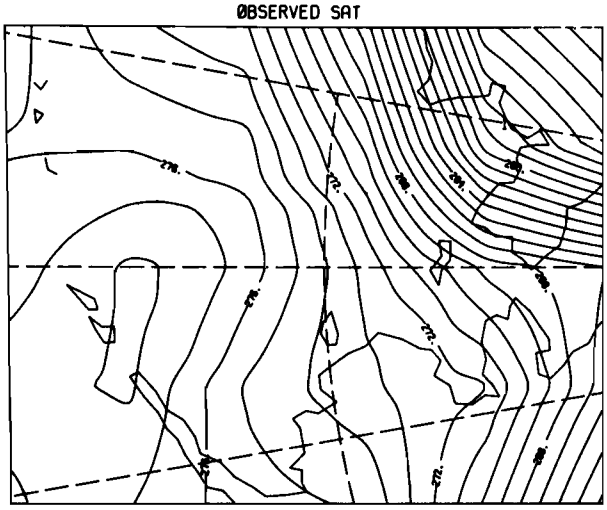

00Z 6 MAR 1980

ØBSERVED SAT

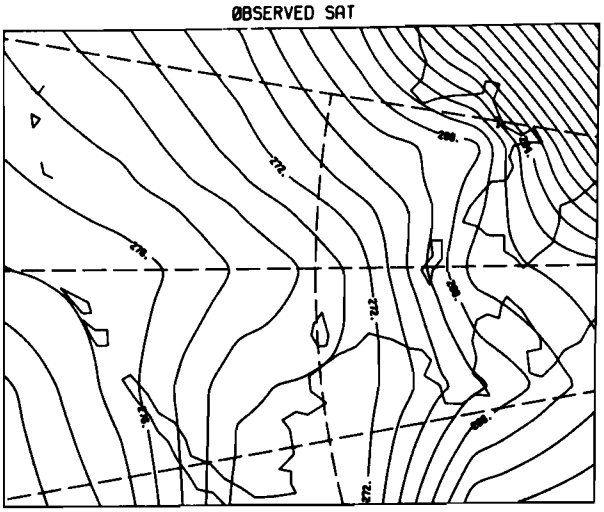

12Z 6 MAR 1980

ØBSERVED SAT

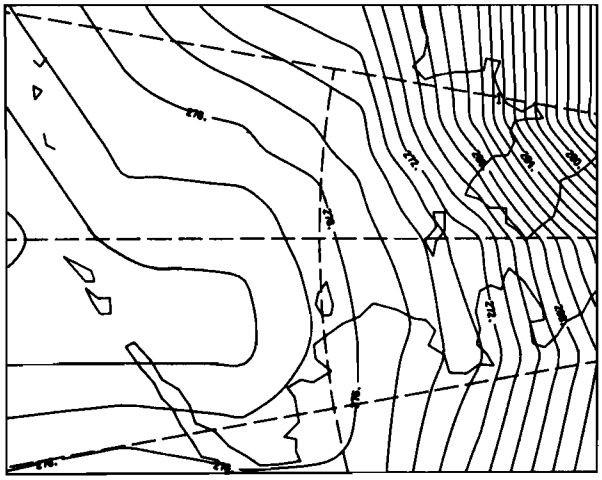

00Z 7 MAR 1980

ØBSERVED SAT

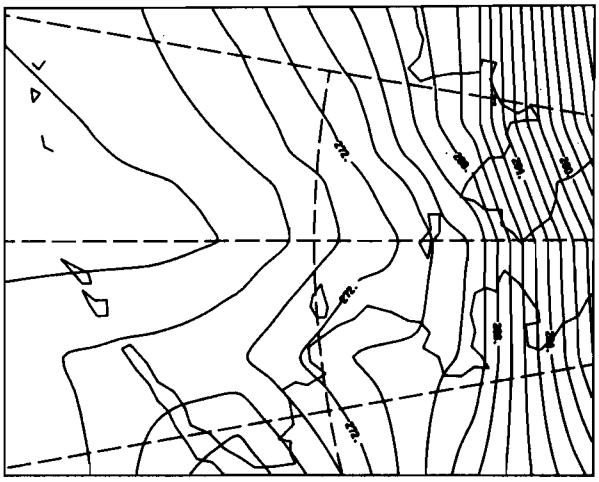

12Z 7 MAR 1980

ØBSERVED SAT

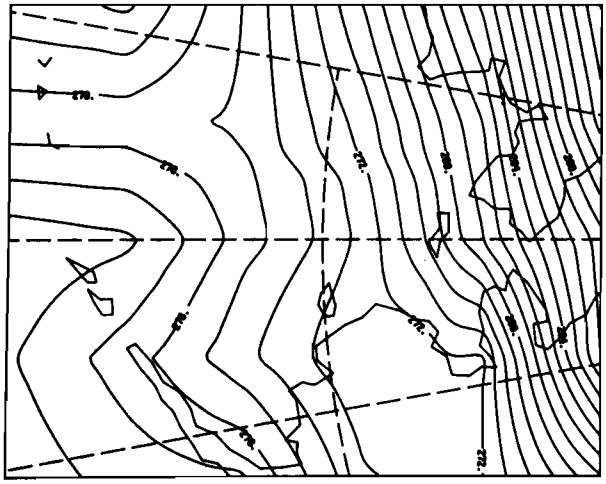

00Z 8 MAR 1980

ØBSERVED SAT

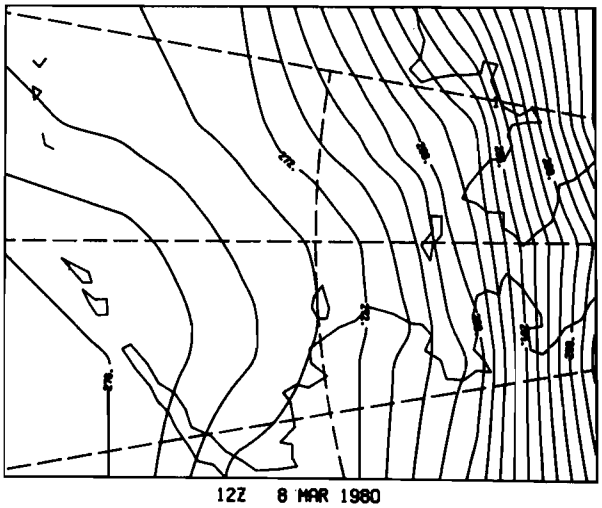

12Z 8 MAR 1980

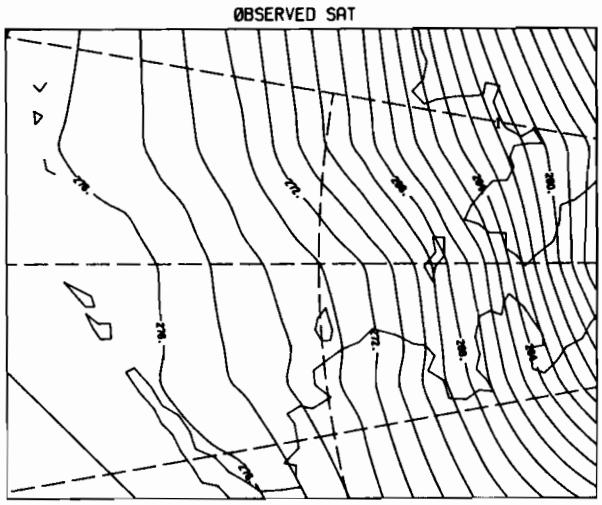

00Z 9 MAR 1980

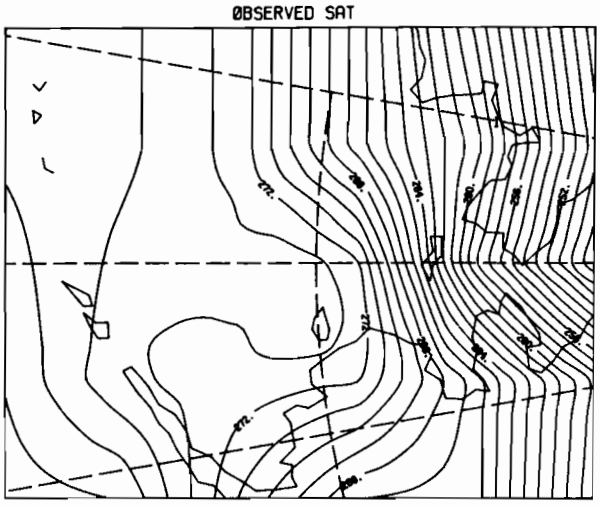

12Z 9 MAR 1980

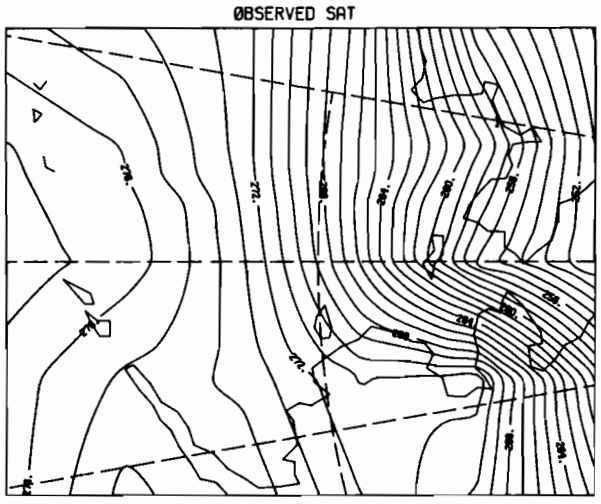

00Z 10 MAR 1980

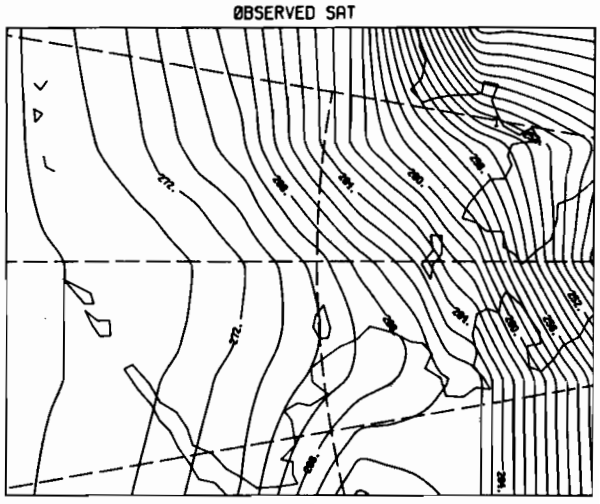

12Z 10 MAR 1980

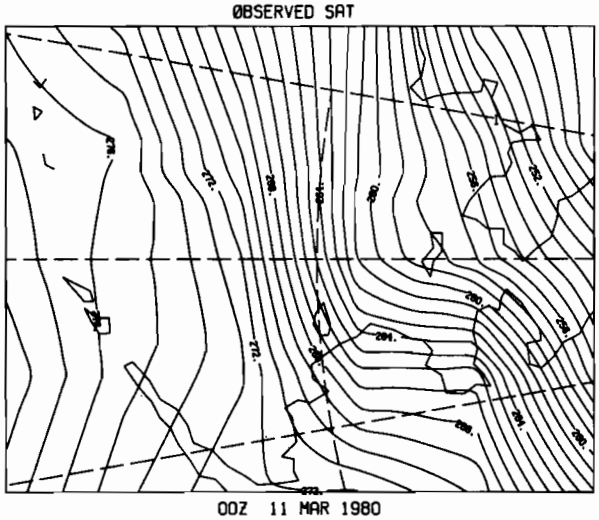

00Z 11 MAR 1980

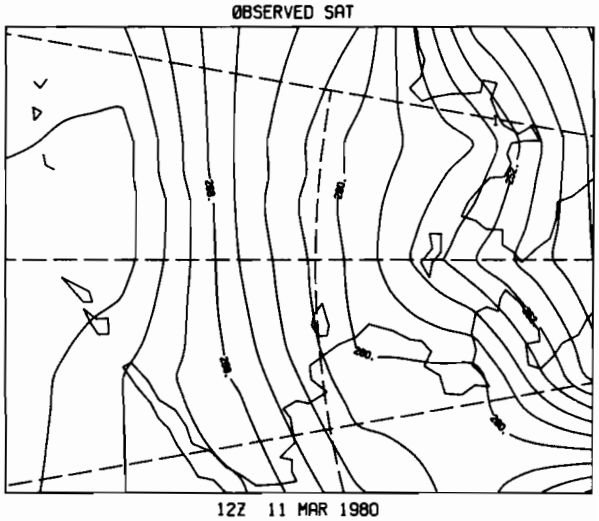

12Z 11 MAR 1980

ØBSERVED SAT

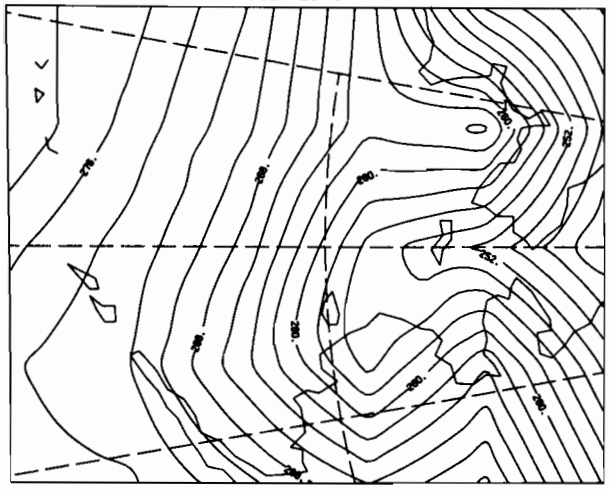

00Z 12 MAR 1980

ØBSERVED SAT

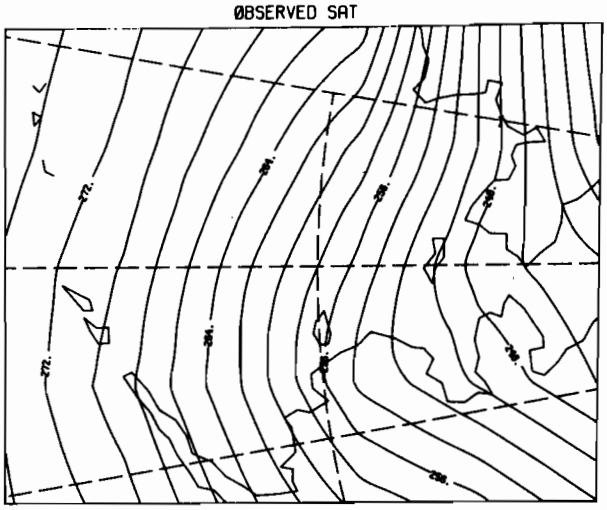

12Z 12 MAR 1980

ØBSERVED SAT

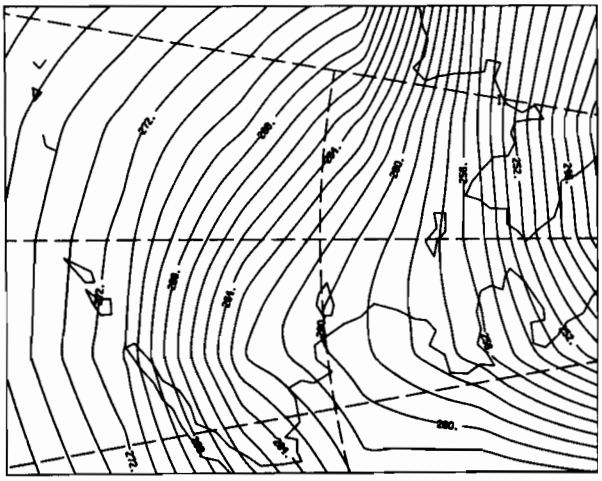

00Z 13 MAR 1980

ØBSERVED SAT

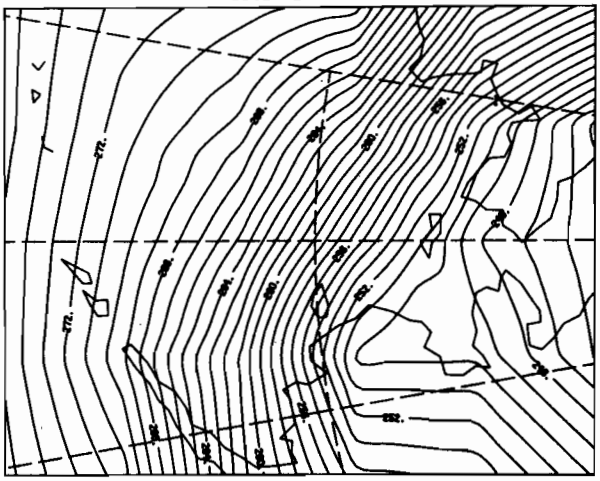

12Z 13 MAR 1980

ØBSERVED SAT

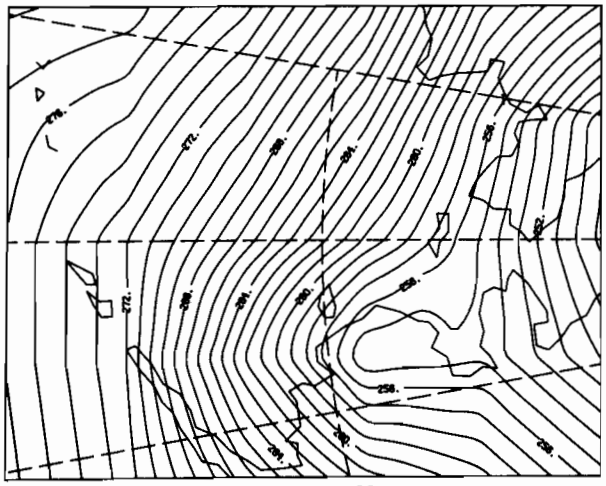

00Z 14 MAR 1980

ØBSERVED SAT

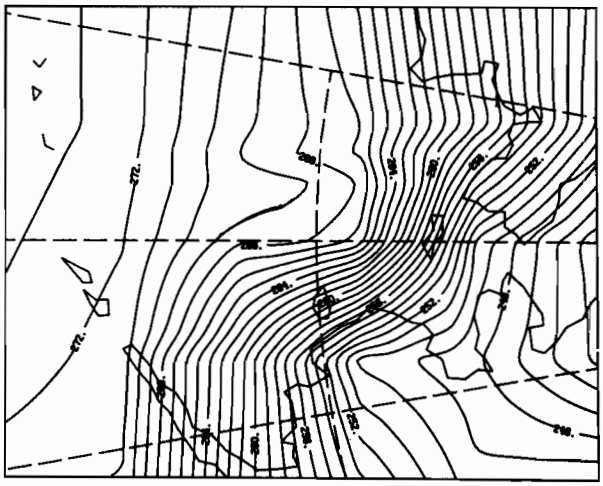

12Z 14 MAR 1980

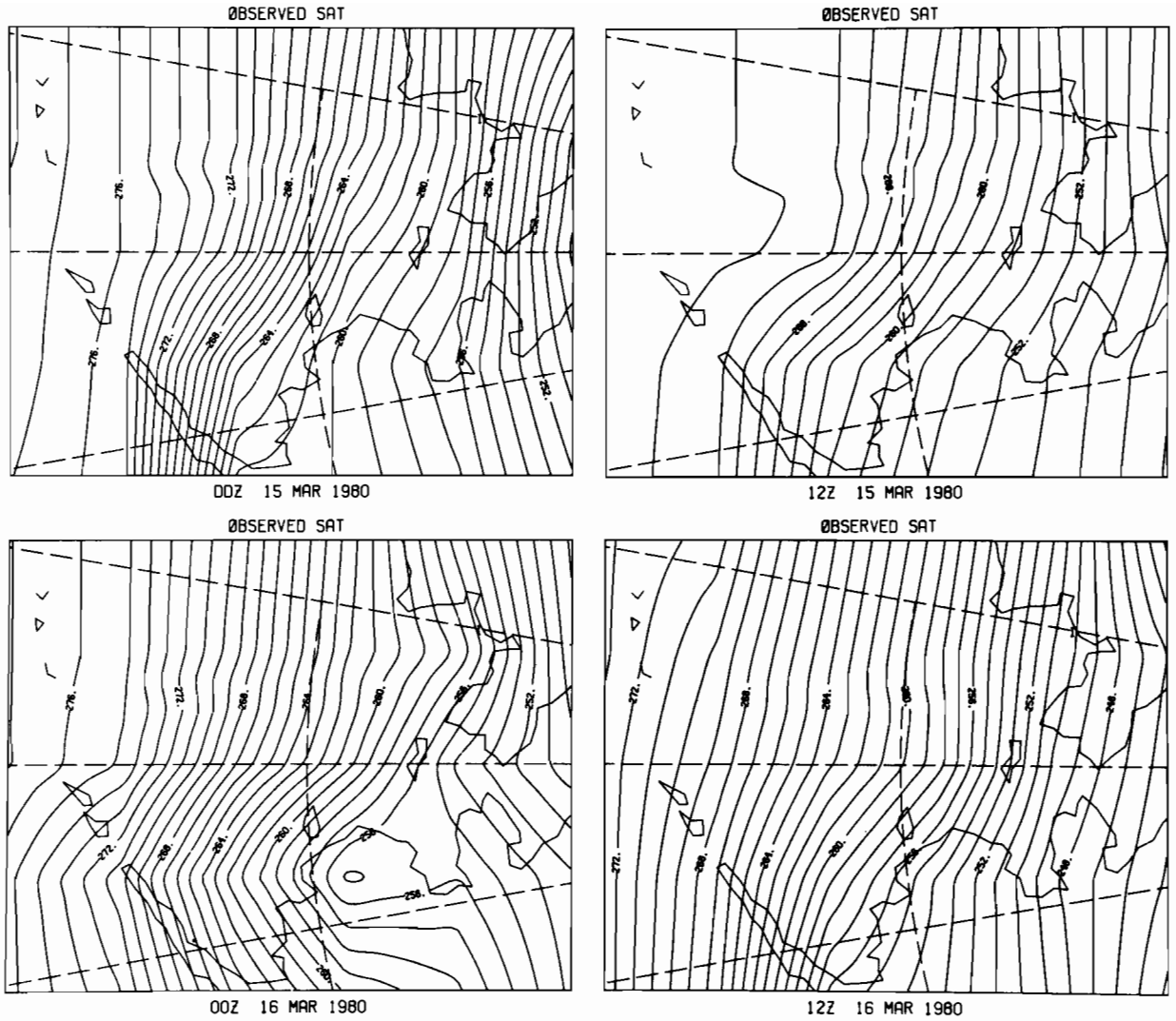
ØBSERVED SAT
00Z 15 MAR 1980
ØBSERVED SAT
12Z 15 MAR 1980
ØBSERVED SAT
00Z 16 MAR 1980
ØBSERVED SAT
12Z 16 MAR 1980

APPENDIX C

GLOSSARY OF WMO SEA-ICE TERMS USED IN THIS REPORT

The following abridged ice nomenclature is taken from a list adopted and published by the World Meteorological Organization (1970).

Brash ice: Accumulations of *floating ice* made up of fragments not more than 2 m across, the wreckage of other forms of ice.

Compacting: Pieces of *floating ice* are said to be compacting when they are subjected to a converging motion, which increases ice *concentration* and/or produces stresses which may result in ice deformation.

Concentration: The ratio in tenths of the sea surface actually covered by ice to the total area of sea surface, both icecovered and *ice-free*, at a specific location or over a defined area.

Diverging: *Ice fields or floes* in an area are subjected to diverging or dispersive motion, thus reducing ice *concentration* and/or relieving stresses in the ice.

Fast ice: *Sea ice* which forms and remains fast along the coast, where it is attached to the shore. Vertical fluctuations may be observed during changes of sea level. Fast ice may be formed *in situ* from sea water or by freezing of *pack ice* of any age to the shore, and it may extend a few metres or several hundred kilometres from the coast.

Finger rafting: Type of rafting whereby interlocking thrusts are formed, each floe thrusting "fingers" alternately over and under the other. Common in *nilas* and *grey ice*.

Firn: Old snow which has recrystallized into a dense material. Unlike snow, the particles are to some extent joined together; but, unlike ice, the air spaces in it still connect with each other.

First-year ice: *Sea ice* of not more than one winter's growth, developing from *young ice*; thickness 30 cm - 2 m. May be subdivided into *thin first-year ice*/white ice, *medium first-year ice* and *thick first-year ice*.

Flaw: A narrow separation zone between *pack ice* and *fast ice*, where the pieces of ice are in chaotic state; it forms when pack ice shears under the effect of a strong wind or current along the *fast ice boundary*.

Floe: Any relatively flat piece of *sea ice* 20 m or more across. Floes are subdivided according to horizontal extent as follows:

GIANT: Over 10 km across.
VAST: 2-10 km across.
BIG: 500-2,000 m across.
MEDIUM: 100-500 m across.
SMALL: 20-100 m across.

Flooded ice: *Sea ice* which has been flooded by meltwater or river water and is heavily loaded by water and wet snow.

Ice boundary: The demarcation at any given time between *fast ice* and *pack ice* or between areas of *pack ice* of different *concentrations*.

Ice breccia: Ice pieces of different age frozen together.

Lead: Any *fracture* or passage-way through *sea ice* which is navigable by surface vessels. [Author's note: More typically taken to mean long linear opening of water between floes or groups of floes of 1 m to 100 m across and 100 m to a few kms long.]

New ice: A general term for recently formed ice which includes *frazil ice, grease ice, slush*, and *shuga*. These types of ice are composed of ice crystals which are only weakly frozen together (if at all) and have a definite form only while they are afloat.

Nilas: A thin elastic crust of ice, easily bending on waves and swell and under pressure, thrusting in a pattern of interlocking "fingers" (*finger rafting*). Has a matt surface and is up to 10 cm in thickness. May be subdivided into *dark nilas* and *light nilas*.

Open water: A large area of freely navigable water in which *sea ice* is present in *concentrations* of less that 1/10 (1/8). When there is no sea ice present, the area should be termed *ice-free*.

Pack ice: Term used in a wide sense to include any areas of *sea ice*, other than *fast ice*, no matter what form it takes or how it is disposed.

Polynya: Any nonlinear shaped opening enclosed in ice. Polynyas may contain *brash ice* and/or be covered with *new ice, nilas,* or *young ice*. Sometimes a polynya is limited on one side by the coast and is called a *shore polynya* or by *fast ice* and is called a *flaw polynya*. If it recurs in the same position every year, it is called a *recurring polynya*.

Rafting: Pressure processes whereby one piece of ice overrides another. Most common in *new* and *young ice*.

Ridging: The pressure process by which *sea ice* is forced into *ridges*.

Sastrugi: Sharp irregular ridges formed on a snow surface by wind erosion and deposition.

Sea ice: Any form of ice found at sea which has originated from the freezing of sea water.

Shearing: An area of *pack ice* is subject to shear when the ice motion varies significantly in the direction normal to the motion, subjecting the ice to rotational forces. These forces may result in phenomena similar to a *flaw*.

Slush: Snow which is saturated and mixed with water on land or ice surfaces, or as a viscous floating mass in water after a heavy snowfall.

Snowdrift: An accumulation of wind-blown snow deposited in the lee of obstructions or heaped by wind eddies.

Young ice: Ice in the transition stage between ***nilas*** and ***first-year ice***, 10-30 cm in thickness. May be subdivided into ***grey ice*** and ***grey-white ice***.

GPO 833-849